



**Università
degli Studi
di Ferrara**

**DOCTORAL COURSE IN
"MOLECULAR MEDICINE AND PHARMACOLOGY"**

CYCLE XXXII

DIRECTOR Prof. Di Virgilio Francesco

**Role of the P2X7 receptor in radiation therapy
response and resistance in glioblastoma multiforme**

Scientific/Disciplinary Sector (SDS) Med/05

Candidate

Dott. Zanoni Michele

Supervisor

Prof. Di Virgilio Francesco

Years 2016/2019

Contents

Introduction	1
Glioblastoma Multiforme	1
Epidemiology.....	1
Classification.....	2
Therapeutical strategies.....	4
Mechanisms of treatment response and resistance	5
GBM intra- and inter-tumor heterogeneity	6
BBB as main obstacle to drug delivery in brain	7
GBM tumor microenvironment	8
Radiotherapy	10
General aspects	10
Radiotherapy affects tumor microenvironment (TME)	12
Purinergic signaling in cancer	14
ATP is an important constituent of the TME.....	14
P2 receptors in cancer	16
P2X7 receptor	17
P2X7R variants	18
P2X7R role in cancer	18
P2X7R as therapeutic target.....	19
Aims of the study	22
Materials and methods	23
Cell culture.....	23
Irradiation treatment.....	23
RNA extraction and Real-Time Quantitative Polymerase Chain Reaction	23
<i>In vitro</i> measure of extracellular ATP levels	24
Cytosolic free calcium concentration measurements.....	24
Etidium bromide uptake.....	24
Soft agar assay	25
Western Blot	25
β -galactosidase assay	25
<i>In vitro</i> measure of lactate dehydrogenase (LDH) release.....	26
Total cholesterol assay	26
Inflammasome Caspase-1 activity assay.....	26
Digital PCR.....	27
Cell cycle distribution	27
Immunophenotypic analysis	27
Alkaline Comet Assay	28

Comet Analyser Software	28
Results	30
P2X7R is expressed in patients-derived GBM stem-like cells	30
P2X7R is functional in GBM stem-like cells.....	31
Radiation induces cell death and ATP release during time in patients-derived GBM stem-like cells	35
Radiation-resistant GBM cells display a senescent phenotype.....	40
Radiation dynamically modifies P2X7R signaling in GBM cells during recovery from treatment.....	43
Discussion.....	47
Bibliography	51

Introduction

1. Glioblastoma multiforme

1.1 Epidemiology

Glioblastoma multiforme (GBM) is the most aggressive and malignant primary brain tumor [1].

The annual average age-adjusted incidence of GBM is approximately 3.20 cases per 100,000 people, with more than 11,000 new cases diagnosed each year in the United States [2]. GBM has the highest incidence among malignant primary brain tumors; representing the most common malignancy that affects the brain and the central nervous system (CNS).

GBM accounts the 47.1% of the malignant brain tumors, the 14.9% of all primary brain and CNS tumors and the 56.1% of all gliomas [2].

GBM is primarily diagnosed in elderly people with a median age of 64 at diagnosis [2]. The incidence increases with age with a peak between 75 and 84 years (15.28 cases per 100,000) and a drop down after 85 years (9.16 cases per 100,000) [2]. GBM is rare in children and adolescents (0-19.0 years) accounting only the 2.9% of all primary brain and CNS tumors [2]. The incidence is higher in male than in female (3.99 vs 2.52 cases per 100,00 people) [2].

From the race/ethnicity point of view, whites have the highest incidence rates (3.46 cases per 100,000), followed by blacks (1.79 cases per 100,000), Asian/Pacific Islander (1.61 cases per 100,000) and American Indian/Alaskan Native (1.47 cases per 100,000) [2].

GBM is mainly located in the supratentorial region in particular in the subcortical white matter and in the deeper grey matter of the cerebral hemispheres (95% of all GBM cases) [3]. The sites with the highest rate are the temporal lobe (31% of the cases), followed by the parietal lobe (24% of the cases), the frontal lobe (23% of the cases) and finally the occipital lobe (16% of the cases) [1,4]. GBM that occurs in subcortical regions often infiltrates the adjacent cortex, reaching the corpus callosum and then the contralateral hemisphere [5]. GBM rarely arises in the brain stem, into the cerebellum and in the spinal cord [3,6]. Patients with cerebellar GBM are younger when compared with those with GBM in supratentorial location (median of 50.3 vs 64 years) [7] and the tumor displays distinct features such as immunohistochemical characteristics [8], less perilesional edema [9], and increased rates of multifocality [10]. Spinal cord GBM arises predominantly in young male patients with a mean age of 27 years [11].

The incidence of these tumors has slightly increased over the last two decades, especially in elderly people, mainly as results of improved diagnostic imaging systems [12].

A series of environmental and genetic factors have been investigated for GBM but, to date, the only validated risk factor remains the exposure to ionizing radiation [13]. Gene polymorphisms affecting some main cellular processes as DNA repair, cell-cycle regulation and detoxification have been involved in GBM development [13]. Only the 5% of GBM patients shows a family history for gliomas and this seems to be related to some rare genetic syndromes such as neurofibromatosis, Li-Fraumeni syndrome and Turcot's syndrome [14].

GBM remains a lethal and incurable tumor with a median survival for patients of 12-18 months, as the majority of them dies within two years [12].

1.2 Classification

WHO 2016-updated classification of CNS tumors reports GBM as an histologically classified grade IV malignancy [1]. GBM new classification is based not only on histological features and on growth pattern but also on the genetic status of isocitrate dehydrogenase genes *IDH1* and *IDH2* [1]. Phenotype and genotype allow to group tumors sharing the same prognostic markers and those probably responding to treatments in a similar way. Mutations of *IDH1* and *IDH2* genes are hallmarks of low-grade gliomas, suggesting that this type of GBM has been developed from lower grade lesions. GBM that slowly develops from low-grade gliomas, low-grade diffuse astrocytoma (WHO grade II) or anaplastic astrocytoma (WHO grade III) are usually termed "secondary GBMs IDH mutant" and represents only the 10% of the cases. Approximately the 90% of the GBM cases is called "primary GBM IDH wild-type" as it arises *de novo*, after a short clinical history, without any recognizable sign of lower-grade prior lesions [15-16]. Primary GBM, typically affecting adults (mean age at diagnosis 62 years), is a more common and malignant type of GBM, than secondary GBM (mean age at diagnosis 45 years) [17-18].

From the clinical point of view GBMs has a rapid evolution. Symptoms depend on tumor size and location in the brain parenchyma, but usually occur as neurological deficits (e.g. aphasia), behavioural and neurocognitive alterations (e.g. persistent headache, nausea, etc.) and an increase in intracranial pressure due to the tumor-associated edema [12,19-20], especially in patients with more rapid primary GBM. IDH mutant GBM patients have a longer clinical history (16.8 months) than patients with IDH wild-type GBM (6.3 months) [15,19-20]. Differences in imaging features are described for primary and secondary GBMs: IDH wild-type GBMs display an irregular shape with a large central necrotic area surrounded by an enhanced contrast ring-shaped zone. IDH mutant GBMs usually do not show necrotic areas, are larger in size but with less enhancing contrast elements and less edema [21-22]. Extensive haemorrhagic foci are present, causing stroke-like symptoms, sometimes the first clinical sign of the tumor. The histological features of both IDH

wild-type and IDH mutant GBMs are similar and are essential for the diagnosis; usually GBM is an high cellularized tissue composed by poorly differentiated astrocytic cells with nuclear atypia and active proliferating cells. Another indispensable feature is the presence of microvascular proliferation and/or necrosis. Due to the high heterogeneity of this tumor, the distribution of these key histopathological features is extremely variable making difficult the diagnosis using specimens obtained by needle biopsies [23].

Molecular and genetic features of GBM are useful additional tools to both diagnosis and treatment guidance, showing an increasing importance in daily practice and helping in classify brain tumors. Among astrocytic neoplasms, GBM contains the greatest number of genetic and epigenetic alterations. Imbalances in chromosomes, such as gain of chromosome 7, or loss of chromosome 9, 10, and 13, are one of the most common genetic alterations in primary GBM [1,24]. In particular Epidermal growth factor receptor gene (*EGFR*), located in chromosome 7, is the most frequently amplified gene in GBM [24-25]. *EGFR* amplification is often associated with overexpression of the gene (in the 70-90% cases) and with the truncation of the amplified genes, resulting in various truncations forms within different regions of the same tumor [26]. The most common truncated *EGFR* form expressed in GBM is *EGFRvIII* where the receptor is constitutively activated in a ligand- independent manner [27-28]. In addition to *EGFR*, other receptor tyrosine kinase signaling pathways are altered in GBM: *PDGFRA* amplification (in 15% of the cases) and *MET* amplification (in 55% of the cases) [24].

Mutations and amplification of *PI3K* are less common (< of 10% of the cases) [29-30], indeed mutations in the tumor-suppressor genes *PTEN* and *NFI* occur in the 15-40% [31] and in the 20% [32] of primary GBMs respectively.

Alterations in p53 pathways occurs in more than 90% of the GBMs [32]. *TP53* mutations are more common in secondary GBM (67% of the cases), rather than primary GBM (11% of the cases) [33]. *MDM2* overexpression or amplification is also an alternative mechanism used by GBM cells to avoid p53 regulation of cell cycle and cell proliferation in particular in primary GBM (more than 50% of the cases) than secondary GBM (11% of the cases) [34]. *RB1* and *CDKN2A* are also important pathways altered in GBM [35]. *CDKN2A* deletion and *RBI* alterations are mutually exclusive in GBM [36]. *CDKN2A* deletions are showed in the 76% of GBMs, both primary and secondary [37]. *RBI* mutations are not common, whilst alteration in methylation of its promoter is more present in secondary GBM (43% of the cases) than primary GBM (14% of the cases) [38].

TERT promoter region mutations are also found in more than 80% of GBMs [39]. These alterations lead to aberrant *TERT* expression and telomeres maintenance especially in primary GBMs [40]; secondary GBMs activate alternative pathways (e.g. *ATRX* mutations) to elongates telomeres.

Mutation in genes involved in epigenetic regulation and chromatin remodeling are common in GBMs [41]. In general, molecular mechanisms defining chromatin structure status are altered in GBM. These processes modulate gene expression, regulating several pathway relevant to GBM cells as stemness, invasion, senescence and resistance to therapy [16,42]. Gene silencing by methylation of promoters is another common mechanism activated by cancer cells to inactivate specific genes with tumor suppressor function [43]. In GBM but also in other cancers *MGMT* is the most common methylated gene. *MGMT* codify for a DNA-methyltransferase protein crucial for genome stability as it removes alkyl groups from guanosine in position N7, a typical modification induced by the treatment with alkylating agents [44]. *MGMT* methylation, that occurs in 40-50% of GBM patients, is a predictive marker of the response to therapy with alkylating agents, as temozolomide (TMZ), suggesting a partial inability of the tumor to repair the DNA damages induced by such chemotherapeutic drugs [45].

Coupling genetic data and expression profile data, it has been possible to cluster GBM in categories those correlates with histology and grading, better reflecting the clinical outcome of these patients. Four categories correlated with the most common GBM genetic alterations (EGFR amplification/mutation, *TP53* mutations, *PDGFRA* alterations and *NF1* mutation/deletion) has been individuated: proneural, neural, classical and mesenchymal subtypes [24]. Regardless of the above-mentioned classification, GBM is characterized by high heterogeneity and it has been shown that individual cells with different subtype profiles co-exist in the same tumor specimens [46-48]. Because of GBM complexity, a better understanding of the sources of such heterogeneity (genetic, epigenetic, microenvironmental) still remain a critical goal and a great challenge that still must be addressed [49].

1.3 Therapeutical strategies

Therapeutic plan for GBM-patients should be evaluated by a multidisciplinary team of experts such as neuropatologists, neurosurgeons, neuroradiologists and medical and radiation oncologists [50]. Surgery, when possible, is the first therapeutic option used to reduce tumor dimension and to obtain tissue for diagnosis. Complete surgical resection is difficult due to the infiltrative nature of this tumor but, since resection is a favorable prognostic marker, patients should undergo to maximal resection possible without compromise neurological functions [51]. When surgery is not possible, because of the critical location of the tumor or the impaired clinical condition of the patient, a biopsy should be done for molecular and histopathological diagnostic purpose [52]. Improvements in surgery as intraoperative MRI and fluorescence guided surgery (tumor is fluorescently-labeled

using 5-amino-laevulinic acid) have increased safety, progression free survival (PFS) and the extent of resection rate [53].

Radiotherapy is the most important and effective treatment for GBM. Conventional fractionated radiotherapy (60Gy in 30 fractions of 2Gy each) is the standard treatment after surgical resection [54]. Hypofractionation of radiation dose is actually under study and should be a possibility especially in relapsing patients. It consists in accelerating treatment time increasing the doses of radiation of each fraction. Accelerated hypofractionation can potentially improve the treatment outcome of the patients but also their quality of life, reducing the total treatment duration. In addition this approach might reduce costs of the treatments. Studies have demonstrated the feasibility and tolerance of the treatment, especially in elder patients (>70 years) where the hypofractionated treatment is slightly superior to the conventional one in terms of overall-survival (OS) [55]. Further investigations have to be done in order to better define the optimal fraction and dose of radiotherapy also in younger patients with good prognostic factors where no differences have been found between the conventional and the hypofractionated radiotherapy[55-56]. Concomitant and adjuvant treatment with TMZ in addition to radiotherapy is actually the standard of care treatment since it was demonstrated a significant increase in the median survival, compared with radiotherapy alone (14.6 months vs 12.1 months) [57] and in the 2- and 5- years survival rate in patients who used these treatment [58]. TMZ is a potent alkylating drug able to cross the blood-brain barrier (BBB) [59]. TMZ is a pro-drug activated by hydrolytic reaction in the activated intermediate MTIC which methylates DNA [60]. Combination treatment of TMZ plus radiotherapy gives the best performance in patients carrying methylated *MGMT* promoter, but the lack of valid alternatives for the unmethylated counterpart makes this treatment applicable to almost all GBM patients [61]. Supportive treatment to manage clinical symptoms of the tumor should have to be considered based on the performance status and neurological condition of the patient [50]. Treatment with corticosteroids (e.g. dexamethasone) is used to reduce tumor-associated edema and the correlated clinical symptoms. Anti-epileptic treatment is recommended in patients with seizures however this treatment has to be interrupted after tumor resection and re-introduced only if seizures appears again, in order to avoid a strong activation of hepatic metabolism that could interfere with the chemotherapeutic agents [62].

1.4 Mechanisms of treatment response and resistance

Despite many tumors respond to standard treatment at the beginning, almost all the patients with GBM relapse; indeed the median time to progression is 6.9 months [57]. GBM is highly resistant to therapy and usually recurs locally, spreading from the surgical cavity, without the colonization of

other organs [63] despite a few evidences of extracranial dissemination [64,65]. In the last decades several clinical trials have failed, achieving only very limited therapeutic success. This is mainly due onto the tumor cells those survive the initial therapy. Survival of these cells depends by multiple factors as the high intra- and inter-tumor heterogeneity, the presence of BBB that made difficult the delivery of drugs and the stromal and immune microenvironment.

1.4.1 GBM intra- and inter-tumor heterogeneity

A better understanding of the different sources of tumor heterogeneity and of their relationship with treatment response and resistance is one of the main goal for neuro-oncology [49]. Recent papers elucidated the complex genomic landscape of GBM [24,47-49]. Each tumor is unique and such diversity derives from the contribution of genetic, epigenetic and microenvironmental factors. Differences in the original cells those give rise to GBM are a possible source of such inter-tumor heterogeneity. Several CNS progenitor cells as well as mature astrocytes and neurons have been considered as cells of origin of GBM [66-70]. Besides inter-tumor heterogeneity, recent genomic analysis on different regions of the same tumor have demonstrated that multiple clones, harboring different genetic alterations, coexist within the same tumor [46-48]. In addition differences in transcriptional profile affecting many cellular processes as cell cycle, immune response and hypoxia, have been found also in single cells sharing the same genetic alterations [47]. Such intra-tumor heterogeneity contributes to the definition of a hierarchical organization of the tumor cells characterized by a different degree of differentiation and stemness. GBM stem cells (GSCs) are subpopulations of cells displaying higher chemo- and radio- resistance than more differentiated tumor populations. GSCs have specific properties, such as high tumorigenic ability, theoretically unlimited self-renewal and the ability to differentiate in multiple lineage progeny [71]. Identifying GSCs is anything but simple since the most common GSCs markers such as CD133, CD44, CD15/SSEA-1 are useful to enrich populations of stem cells from the bulk of tumor cells but fails to discriminate all the tumor cells with self-renewal and tumor initiating ability [71]. Such cells are extremely plastic and can overcome damages induced by chemo- and radiotherapy-induced adaptive resistance pathways [68,72]. Among these, stemness state is maintained trough the activation of the Wnt/ β -catenin [73-74], Notch [75], NF- κ B [76], JAK/STAT [77] pathways and through the expression of several transcription factors as OLIG2 [78], NANOG [79], SOX2 [80], OCT4 [81] and ID1 [82] those affect cell proliferation and survival, self-renewal and metabolism. Activation of DNA damage repair mechanisms is another important determinant in chemo- and radio- resistance in GSCs. These cells display an increased expression of checkpoint kinases Chk1

and Chk2 and of ataxia telangiectasia mutated (ATM), overcoming radiation-induced apoptosis and increasing repair of damaged DNA [83].

1.4.2 BBB as main obstacle to drug delivery in brain

BBB is a complex and dynamic vascular network with selective permeability for several types of cells, molecules and drugs [84], representing a real physical and biochemical barrier that normally protects the brain from infectious agents and neurotoxicant [85]. BBB is mainly composed by endothelial cells closely connected each other by tight junctions; pericytes and perivascular macrophages that literally embrace the endothelium, laying on the basal membrane of the endothelial cells and helping in maintain rigidity; and finally by astrocytic end-foot processes that are interconnected both with pericytes and endothelial cells [86]. Despite the presence of these different cell types, the most important cellular component that mainly regulate BBB permeability is the endothelium. Endothelial cells in BBB are unique in organization, resulting in a continuous layer that lacks fenestrations [87]. This anatomical organization coupled with the high expression of ABC transporters P-glycoproteins that pumps back to the bloodstream some molecules are the main obstacle to deliver drugs into the brain [88]. Other physiochemical properties as charge, molecular weight, and lipophilicity affect the ability to pass the endothelial layer of BBB [89]. Highly charged, hydrophilic and $> 400\text{--}600$ Da molecules hardly pass the BBB and the design of permeable but effective drugs is difficult. In addition, the anisotropic brain extracellular space, composed by a dense extracellular matrix (ECM), and the presence of the lymphatic system are additional barriers to the penetration and retention of drugs [90-91]. Many strategies are currently under study to improve BBB penetration and to increase drug delivery without compromising the integrity of brain parenchyma. Convection-enhanced delivery (CED) was used to infuse TMZ in GBM patients but, compared to standard treatment schedule no significantly increase survival was observed [92] while potential tissue damage due to infusate reflux can occur. Focused ultrasound (FUS) can be used to temporally and locally disrupt BBB in order to improve drug penetration. Preclinical models or GBM in rat have demonstrate that FUS can make BBB permeable to chemotherapy including TMZ [93]; clinical trials are currently ongoing in patients with malignant gliomas.

Vasoactive peptides as bradykinin and its analog RMP-7 have demonstrated an increased vascular permeability widening the tight junctions between endothelial cells [94]. Despite these encouraging preclinical results further phase II clinical trials fail to demonstrate an increase in efficacy of the drugs used (carboplatin) in combination rather than drugs alone and for this reason phase III clinical trial was discontinued [95].

Nanoparticles with different composition were proposed to carry drugs across BBB. Polymeric nanoparticles of poly (D,Lactide-co-glycolate, PLGA), liposomes and metallic nanoparticles were all tested systems in preclinical model [96-98]. The main problem of these systems is that they are recognized by the mononuclear phagocytes and eliminated before reaching the target. For this reason the use of exosomes [99] or the functionalization of these nanoparticles with peptides, antibodies or ligands activating the endocytic processes in endothelium have provided some promising preliminary results [100].

1.4.3 GBM tumor microenvironment

GBM tumor microenvironment is very complex [101], being composed by distinct phenotypic cellular components including heterogeneous tumor cells, reactive astrocytes [102], infiltrating immune cells [103], microglia [104], abnormal vasculature [105], extensive hypoxic zones [106] as well as different soluble mediators [107]. Taken together, these components are responsible for GBM aggressive behavior and invasiveness and represent a key obstacle for the treatment of this tumor. The majority of immune cells into GBM (constituting more than 30% of the tumor mass) is represented by both tissue-resident microglia and bone marrow-derived macrophages (BMDMs) [108-109]. An accurate distinction between these populations is difficult since only recently new more appropriate surface markers have emerged such as TMEM119, expressed by microglia but not by BMDMs, and CD49D/ITGA4, a specific BMDM marker [109-110]. Tumor-associated macrophages/microglia (TAM) in GBM seem to be more pro-tumorigenic and their amount is increased with higher tumor grade [108,111]. TAM display alternative activation phenotype, producing anti-inflammatory cytokines and tissue remodeling molecules. Presence of these immune population increase GBM growth and invasion developing an intricate crosstalk. GBM cells recruit TAM by CSF-1 and CCL2 release, activating and educating them to a pro-tumorigenic phenotype that in turn fuels GBM cells, promoting invasiveness through IL-6, EGF and TGF- β [112-114]. In addition TAM have been implicated in angiogenesis by modulating vessel integrity and function, and affecting the response to anti-angiogenic therapies [115-116]. The lymphoid component of the immune system composed by T cells, B cells and Natural-Killer (NK) cells are less represented in GBM. Some studies on GBM tissue composition have shown that more than 3.2% of cells composing the tumor express the T cell marker CD3 [117]. These lymphocytes do not display any effector functions, and despite they seem to be tumor-antigen specific, they have been rendered silent by tumor cells. Soluble factors as IL-10, TGF- β , prostaglandin E2 (PGE2) and exosomes deeply affect immune functions [118]. PGE2 impacts on T cell activation, proliferation and differentiation suppressing also NK cells and inducing the expression of FoxP3 and the production

of IL-10 shifting the immune composition to a regulatory T cells (T_{reg}) phenotype [119]. TGF- β inhibits T cell and B cell proliferation and activation. In particular it affects cytotoxic lymphocytes blocking the production of cytotoxic molecules as perforin, granzymes and Fas ligand [120-121]. To overcome such immunosuppressive microenvironment, reprogramming T cell subsets enhancing anti-tumor activity through the use also of checkpoint inhibitors is currently under investigations in patients with GBM [122].

Astrocytes in normal brain tissue provide structural support, are involved in homeostasis and communicative functions as well as being providers of energy fuel to the neurons [123]. In the context of brain tumor, reactive astrocytes play an important role in GBM biology, being involved in GBM cell invasiveness, especially through the activation of MMP2 [124]. Reactive astrocytes are known also as cells those secrete high levels of tumor necrosis factor- α (TNF- α), TGF- β , IL-6, and insulin growth factor-1 (IGF1), factors that increase the proliferation of GBM cells [125]. Astrocytes are also able to protect GBM cells from chemotherapy-induced apoptosis when they directly interact with the tumor cells [126]. Gap junctions allow the transfer of cGAMP from GBM cells to surrounding astrocytes promoting the release of inflammatory cytokines in the tumor microenvironment that, in turn, activates the STAT-1 and NF-K β pathways in GBM cells promoting invasion and resistance to therapeutics [127]. Beside the singular role of each microenvironmental component the structural architecture of the GBM tumor *in se* deeply affects tumor response and resistance to therapy. Once penetrated into the brain, the drugs meet more challenges when arrive at the tumor site. GBM is characterized by a highly cellular-dense central area, poor of functional vascular system, and by an external invasive area localized at the rim of the tumor. Such compactness and cellular density increase the interstitial fluid pressure (IFP), limiting the penetration of the drugs into the tumor mass and inducing the selection of potentially resistant subclones derived by the exposure to sub-lethal doses of drugs [128-129]. GBM is also an highly hypoxic tumor where cells located in the deepest regions are subjected to severe conditions and activate several pathways through the transcription factor hypoxia inducible factor 1 (HIF-1), in order to survive. The HIF-1 induced transcriptional program comprise angiogenesis, macroautophagy and increase glycolysis to obtain energy [130]. Lactate accumulation due to abnormal glycolysis leads to acidification of the tumor microenvironment. Acidification affects multiple cellular processes including invasion, immune response, angiogenesis and resistance to therapy [131-132]. In addition, at low pH, some drugs are protonated and in this form display a significant reduction in cellular uptake [128,133]. The role of tumor microenvironment is fundamental in cancer progression and therapeutic efficacy. Still a lot of work have to be done in order to fully dissect and understand the complex network created by all these components.

2. Radiotherapy

2.1 General aspects

More than 50% of total cancer patients are treated with radiation, making radiotherapy a pivotal strategy in cancer management [134]. Radiotherapy is used both to cure cancer and as a palliative treatment, usually in combination with other treatment modalities as surgery, chemotherapy and immunotherapy [135]. Ionizing radiation is a physical agent used to kill cancer cells or to control their growth. Ionizing radiation mainly induces damages on DNA of cells, affecting principally cancer cells rather than normal cells, providing treatment benefits in different types of cancer. Since radiation affects also tumor-surrounding healthy tissues, the amount of radiation dose has to be precisely calculated and its delivery has to be done in order to maximize radiation exposure to tumor cells while minimizing the exposure of normal cells. Radiation can be delivered in three ways: by an external beam of high-energy rays from outside the body (called external beam radiation therapy), by the insertion of radiation-emitting source directly into the tumor tissue (called brachytherapy) and by the systemic injection of radioisotopes designed to target the disease (called radioisotopes therapy). External beam radiotherapy is the most common approach in clinical setting and several modalities have been developed during times to optimize this system. Technology advances, in terms of new imaging modalities, more powerful software and new delivery system have improved the efficacy and safety of this radiotherapy modality. Actually with the use of the 3D radiotherapy based on CT scan imaging, tumor localization and organ structures are accurately defined, allowing a better radiation delivery [136]. In addition, the intensity modulated radiation therapy (IMRT) system allows to create irregular shaped radiation doses that fits with the target tumor mass, saving healthy tissue and hitting the tumor with high doses [137]. Finally delivering radiation with a fractionated regimen preserves normal tissue over cancer cells. Indeed normal cells usually proliferate with a slower rate than cancer cells and have more time to repair DNA damage. Common fractionated radiotherapy regimen consists now of a low daily radiation dose (1.5-3.0 Gy) for several weeks [138]. In order to identify the optimal dose per fraction, the linear quadratic formula model is used to define the relationship between cell survival and delivered dose. This important radiobiological model takes into account the type of tissue irradiated and in particular its proliferation rate. The initial slope of a cell survival curve (alpha or α) is the mathematical meaning of the intrinsic radiosensitivity of the irradiated cell that depends linearly on dose. The curvature of a cell survival curve (beta or β) means that the damage is repairable with time, and is the factor on which depends the dose-per-fraction and dose-rate variation in radiobiology. The overall radiosensitivity of any irradiated cell is calculated by the sum of the effects of these two factors.

Taking this into account, tissues with a slow cell proliferation rate have enough time to repair damages before successive fractions, displaying a low α/β ratio. By contrast, tissues with highly proliferative rate have less time to repair radiation induced damages showing an high α/β ratio. α/β is also used to determine the size of fractions since tissues with high α/β ratio are less sensitive to alterations in size fractions than low α/β ratio ones. For gliomas, an intermediate α/β ratio was found (5-10 Gy), probably due to the different histology of tumors in the CNS [139]. From a biological point of view, radiation can act directly or indirectly to kill cancer cells, mainly damaging their DNA. The effect of ionizing radiation can be direct (through the energy transfer of the radiation) or mediated by the production of oxygen-free radicals, reactive oxygen species (ROS) or reactive nitrogen species (RNS) derived mainly by the ionization of water and of other molecules in the cells [140]. These together induce DNA, protein and lipid damage disrupting and/or altering their molecular structure and leading to cell injury and eventually death [141]. Based on the energy delivered, ionizing radiation induces different types of DNA damages, but DNA double-strand breaks (DSBs) represent the major lethal DNA lesions. DSBs activate an intricate signaling network, resulting in amplification of damage signal and in the recruitment of the components of the DNA damage response mechanisms [142-143]. Depending on the amount of DNA damage and cellular DNA repair abilities, tumor cells may completely repair the lesions before returning to the proliferative status, or permanently arrest cell cycle and undergo to cell death through senescence, apoptosis or necrosis [144-145]. Radiation mainly induces the intrinsic apoptotic pathways, causing mitochondrial release of cytochrome c, the apoptosome and caspase cascade [146]. Alternative to induction of apoptosis, activation of p53 by radiation treatment and the following p21 expression lead to senescence, arresting the cells principally in G1 phase [147-148]. Usually senescent cells are in a permanent not proliferative state, no longer able to replicate, but still viable, metabolically active and able to secrete pro-inflammatory cytokines, growth factors and metalloproteases involved in tumor progression and invasion [149]. An interesting hypothesis is that senescence in tumor cells may not be irreversible but only temporarily used to escape the radiation-induced cell death [150]. In addition tumor cells those revert from senescence exhibit an altered gene expression profile and an increased invasiveness [151]. Mitotic catastrophe is the main form of cell death induced by ionizing radiation, resulting in premature mitosis before the completing S and G2 phases [152]. Cells overduplicate chromosomes with consequent aberrant cell division and formation of giant cells, with multiple nuclei and several micronuclei [152]. Cell death usually occurs after the first post-radiation cell division.

2.2 Radiotherapy affects tumor microenvironment (TME)

For decades, the role of TME was not at all considered in studies concerning the radiation treatment outcome, as the all attention was focused on cancer cells; it was lately demonstrated, anyway, that TME plays a crucial role in the success or failure of the treatment [153]. The cellular and biochemical composition of the TME deeply varies after radiation treatment, affecting several important tumor functions like metabolism, motility or proliferation and creating alternatively an immunosuppressive milieu or an antitumor immune response [154-155]. The biochemical composition of the TME after radiation treatment depends on the activity of both tumor and stromal cells. After radiotherapy inflammatory signals increase through the activation of survival pathways and the stimulation of the innate immune system [153]. The resulting cellular stress and death induces the release of metabolites, cytokines, growth factors, cytotoxic molecules and damage-associated molecular patterns (DAMPs) those accumulate in TME, affecting both tumors and stromal components [156]. DAMPs might be recognized by their corresponding pattern recognition receptors (PRRs), triggering on immune cells an effective antitumor response that leads to the immunogenic cell death (ICD) of cancer cells [157]. DAMPs can be exposed on cellular surface (e.g. calreticulin) and might be passively (e.g. high mobility group box 1 (HMGB1) proteins) or actively (e.g. ATP) released [157]. DAMPs derived by the ICD of cancer cells activate, together with inflammatory cytokines, the dendritic cells (DCs) making them effective antigen presenting cells (APCs) [158] and generating an efficient antitumor immune response [159]. Although ICD is triggered by radiotherapy, the overall effects are much more complex. Tumors evolved in order to escape the surveillance of the immune system, coupled with other intrinsic and extrinsic survival pressures such as hypoxia, acidosis and uncontrolled proliferation, allow to build a state of chronic inflammation and immune suppression [160-161]. In this context immunosuppressive cells as T_{reg} , TAM and myeloid-derived suppressor cells (MDSCs) are recruited in order to fuel the immunosuppressive status by secreting cytokines as IL-6, IL-10 and TGF- β [162-163]. After radiotherapy also a local increase of these immunosuppressive cells has been seen, being less sensitive to radiation than the other lymphocytes subsets [164-165]. The presence of such immunosuppressive cells may competitively inhibit T cells activation, since the activation of these cell requires several signals as the interaction between the T-cell receptor (TCR) and the appropriate antigen-loaded MHC of APC cells [153,166]. Besides awakening the immune system against cancer cells with ICD, the enhanced activity of surviving and recruiting immunosuppressive cells potentially constrains the anti-tumor immune response [167-168]. Overcoming these effects to promote the action of immune cells against cancer is a main topic of research [169]. Proteins

involved in the stimulation and activation of T cells as CTLA-4, PD-1 and OX40 may represent promising targets after radiation therapy treatment [170]. Specific monoclonal antibodies against these proteins are currently used in the treatment of some tumors and have demonstrated to improve survival of patients [170]. Combining radiotherapy with immunotherapies is an area of great interest but more in-depth investigations have to be done since the most recent results are still contrasting [171-173]. Beside the role of immune cells, other microenvironmental actors have to be taken into account after radiation treatment. Radiation alters vasculature, inducing endothelial cell dysfunctions, increasing vascular permeability, inflammation and fibrotic processes [174]. The effects on tumor vasculatures depend on the total dose and its fractionation and also on the type, location and stage of the tumor and on the vessel derivation [175-176]. Radiation may potentiate hypoxia, a key regulator of tumor growth and radioresistance [177-178]. In particular, the disruption of the microvasculature, which on one hand contribute to increase the lack of oxygen and on the other reduces the production of ROS. This, coupled with the presence of extensive hypoxic zones into the tumor mass, reduces radiation effects [153]. Hypoxia induces also the expression of HIF-1 α , which independently induce radioresistance promoting tumor revascularization via vascular-endothelial growth factor (VEGF) [179]. Restore oxygenation before and during radiotherapy, for example with hyperbaric oxygen (HBO) may have therapeutics benefits and improve radiation effects [180]. Finally, tumor cells are able to implement a series of protective mechanisms to escape cell death induced by radiation treatment [181]. Tumor cells, in particular cancer stem cells (CSCs), have altered DNA damage response and repair pathways. If in a normal tissue, stem cells are responsible for ensuring tissue maintenance and therefore have active error-free DNA repair pathways [182-183], in tumor something similar happens with CSC, which ensure tumor survival by restoring tumor populations [83]. In GBM, an enriched CSCs tumor, an enhanced activation of ATM, ataxia telangiectasia and Rad3-related protein (ATR) and their downstream effectors Chk1 and Chk2 are implicated in radioresistance [83,184-185]. These kinases regulate the DNA damage response activating the complex DNA repair mechanisms [83]. CSCs also have an increased expression of NBS1, a component the MRN complex involved in DSB sensing [186] and of proteins involved in homologous recombination (HR) as RAD51, BRCA1 and BRCA2 [187-188]. One of the reasons underlying this enhanced DNA damage response seems to be an adaptation to the increased replication stress and oxidative damage already present in the GCSs, leading to an increment in the activation of DNA damage response also after radiation [189-191]. Another additional mechanism of resistance to radiation treatment may be premature induction of quiescence and senescence in CSCs [192-193]. Stopping the cell cycle allows the tumor cells to repair the DNA and restart proliferation. Finally radiation may also activate in tumor cells pathways involved in

migration, invasion and epithelial–mesenchymal transition (EMT) [194]. Indeed ZEB1, Twist-1 and the TGF- β signaling are frequently upregulated in radioresistance cells [195-196].

3. Purinergic signaling in cancer

Purine and pyrimidine are the base constituents of nucleosides and nucleotides, essential elements in several biological functions as parts of the building blocks of nucleic acids, coenzymes, energy intermediates and intracellular and extracellular messengers [197]. The evidence of the role of nucleosides and nucleotides as extracellular signals is not very recent [198] but actually many data are available on their role in many cellular processes as migration, proliferation, differentiation, activation or inhibition of cell death and secretion of growth factors, extracellular vesicles and inflammatory mediators [199-203]. Indeed fundamental pathophysiological processes such as tissue homeostasis, neurodegeneration, immunity, inflammation and cancer are modulated by purinergic signaling [197]. In cancer purinergic signaling is mainly focused on adenosine nucleosides (adenosine) and nucleotides (ADP and ATP), since robust data on extracellular messenger role for pyrimidine nucleotides (UDP and UTP) are mainly focused on immune cells, epithelial cells and hematopoietic cells [204-206]. This is probably due to the fact that ADP and ATP might activate all the purinergic receptor repertoire, whilst UDP and UTP are agonists only for four P2Y receptor (P2YR) subtypes (P2Y2R, P2Y4R, P2Y6R and P2Y14R) [206]. Four types of P1 receptors for adenosine (A1, A2A, A2B and A3), eight subtypes of G protein-coupled, metabotropic receptors (P2Y1, P2Y2, P2Y4, P2Y6, P2Y11, P2Y12, P2Y13 and P2Y14) and seven subtypes of P2X ionotropic receptor (P2X1-7) have been identified [207]. In addition, the adenosine and ATP cellular communication system has actually been better investigated rather than pyrimidine nucleotide system and this has also contributed to the development of a wide range of techniques available for the measure of ATP (e.g. luciferase-based methods) making the measure of uridine nucleosides and nucleotides still difficult and laborious [197].

3.1 ATP is an important constituent of the TME

The TME cellular and biochemical composition, enriched in nucleosides and nucleotides, affects tumor progression and metastatic spread as well as response to therapy. Within this context the ATP and adenosine concentration in the tumor interstitium is much higher than in healthy tissues [208-209]; indeed ATP and adenosine levels in resting/healthy tissues is very low, in the nanomolar range, whereas in stimulated or diseased tissues it can reach hundreds of $\mu\text{mol/l}$ [210-211]. ATP is a

key energy currency as well as a ubiquitous extracellular messenger [198]. ATP meets several characteristics to be an optimal extracellular messenger: it is present at low concentration in the extracellular space (except for inflammatory environments), it is preserved at high concentration intracellularly by the cells (5 to 10 mmol/l), it is water soluble and quickly eliminated by extracellular nucleotidases activity. The demonstration that extracellular ATP concentration is altered in pathological conditions, especially in TME has been successfully demonstrated only in the recent years thanks to the development of genetically encoded probe (plasma membrane luciferase (pmeLUC)) able to measure ATP in the extracellular space in particular close to the cell surface or in the cell-to-cell contacts sites [212]. This probe has allowed to study the dynamic concentration changes of ATP in the extracellular space, easily traceable *in vivo* by total body luminometry [209]. ATP increase in TME is mainly due to its passive release after plasma membrane damage in stressed, injured or dying cells [213]. Besides passive release, it is now clear that all cells are able to actively release ATP [214]. For example hypoxia is a strong stimulus of ATP release even without cellular damages [215] as well as radiation treatment, which causes passive and active release of ATP [157]. ATP might accumulate into the lumen of intracellular vesicles and released constitutively or following stimulation into the extracellular space, with other inflammatory mediators, by exocytosis [214-216]. In other cell types ATP release might occur also through non exocytotic mechanisms associated to anion-selective channels, such as maxi-anion channels or volume-regulated anion channels (VRACs), or by non-selective pores formed at plasma membrane levels, by proteins such as connexins, pannexin 1 and P2X7R [213-214]. Released ATP acts as extracellular messenger but to avoid overstimulation and receptor desensitization, is degraded by the sequential activity of plasma membrane ectonucleotidases as CD39 [203] that belongs to the ectonucleoside triphosphate diphosphohydrolase (E-NTPDase) family. In turn, AMP, a product of ATP degradation, is degraded into adenosine by the ectonucleotidase CD73. The expression of these membrane ectonucleotidases increases in hypoxic conditions [217] and under TGF- β stimulation [218], in particular in immune cells with known suppressive phenotype as T_{reg} cells [219], T_h17 lymphocytes [220] and M2 macrophages [221]. A novel system of ATP removal from the TME is found in recent studies where traditional cancer cell lines are able to take up extracellular ATP with mechanisms of macropinocytosis, which confers cells resistance to chemotherapeutic treatment [222-223]. The role of ATP in tumor-stroma/host dynamics depends principally on two crucial factors: (i) the panel of P2 receptors expressed on the tumor and infiltrating inflammatory cells, and (ii) the level of expression of nucleotide-hydrolyzing enzymes (CD39 and CD73) [197]. Depending on the local concentration and on the purinergic P2 receptor subtype engaged, ATP can trigger many different cell responses, including cell death or

proliferation [224-227]. In addition it may act as an immunostimulant or an immunosuppressive agent [203], depending on the dose and the engaged P2 receptor. ATP represents also the main source of adenosine in the TME despite the presence of a membrane transporter for this nucleoside [228]. Adenosine was widely studied in cancer research for several years, affecting considerably both tumor and stromal components of the TME [229]. On the host side, adenosine is well known for its strong immunodepressive/anti-inflammatory activity [230]. Its effect on the tumor itself is less clear, as it depends on the specific adenosine receptors expressed by the tumor cells; both growth stimulation and inhibition have been described [231]. A1 receptor activation is related to breast cancer growth [232] but it is also slightly expressed in advanced prostate cancer [233]. A2A receptor has a controversial role in tumor biology; studies in literature support both its role in tumor proliferation [234] and in triggering tumor cell death [235]. Overexpression of A2B receptor is associated with poor survival in patients with triple negative breast cancer (TNBC), multiple myeloma, acute myeloid leukaemia (AML) and liposarcoma [236]. A2B receptor seems also involved in invasion and metastatic dissemination, controlling tumor cell adhesion [237]. A3 receptor, instead, is widely expressed in tumors, and it seems correlated with the disease progression [238]. A3 receptor is involved in cell cycle regulation and in both pro- and anti-apoptotic functions depending on the level of receptor activation [239-241]. Interesting results have also been obtained from a phase I/II clinical trial which aimed to test the efficacy of A3R agonists for the treatment of hepatocellular carcinoma [242].

3.2 P2 receptors in cancer

Almost all living organisms have developed an intricate signaling system for extracellular nucleotides. In mammalian, the nucleotide receptor family called P2 receptors are subdivided in two groups: P2Y and P2X [243]. To date the P2Y receptor (P2YR) family counts eight members while the P2X receptor (P2XR) family counts seven members [243]. P2YR are membrane-spanning G-protein coupled receptors [198, 244] while P2XR are ligand-gated cation-selective channels permeable to K^+ , Na^+ or Ca^{2+} [198, 244]. P2YRs are involved in increase of cytoplasmatic Ca^{2+} levels, activation of ERK/MAPK pathway, and modulation of cAMP [213]. They display a mixed ligand nucleotide selectivity, since only P2Y11R has ATP as preferred ligand [243], whilst ADP, UDP, UTP, UDP-glucose and UDP-galactose are preferred and more potent agonists for the other P2YRs [245]. Nucleotide affinity is at low micromolar level for these receptors, making them highly sensitive to even slight nucleotides concentration changes [245]. P2XRs are more selective receptors since ATP is the only known physiological ligand. P2XRs might be further subclassified in fast-desensitizing (P2X1R and P2X3R), slowly or non-desensitizing (P2X2R, P2X4R and

P2X7R) and is non-functional in native conditions (P2X5R and P2X6R) [246]. ATP affinity ranges from low micromolar levels for P2X1R, P2X2R, P2X3R and P2X4R to high activation levels (0.5-1 millimolar depending on cell type and experimental conditions) for P2X7R [213, 246]. The wide range of P2 receptor subtypes, together with the multiple pathways activated by these receptors and the different levels and type of nucleotide selectivities, make the P2 signaling a very plastic and dynamic cell-cell communication system [213]. All cells virtually express P2 receptors and in particular it was found that many cancer cells and many primary human tumors express these receptors [201]. P2Y1, P2Y2 and P2Y6 receptors support growth of several cancers increasing intracellular Ca^{2+} levels and activating ERK/MAPK and PI3K/AKT pathways [201]. P2Y2R is also associated to tumor metastasis and dissemination; in particular, secreted ATP from platelets activates P2Y2R on endothelial cells opening endothelial barrier and facilitating cancer cell extravasation [247-248]. Blockade of P2Y12R, a major player in platelet activation and aggregation, inhibits tumor growth and dissemination [249-250]. P2X3 and P2X5 receptors are actually under study in cancer. P2X3R overexpression in hepatocellular cancer is associated with increased proliferation of cancer cells [251]. P2X5R participates to homeostasis of epithelial cells and seems also involved in differentiation processes, suggesting its possible role in decreasing cancer cell growth [252]. Among the P2 receptors engaged by extracellular ATP, the P2X7 receptor is one of the most intriguing, due to its unique properties such as the significant lower affinity to ATP with respect to the other family members and the complete lack of desensitization [213, 243-244].

3.3 P2X7 receptor

The P2X7R gene located on chromosome 12 at 12q24.31 encoded for a protein of 595 amino acid (aa) characterized by a short intracellular N-terminal tail (26 aa), a big extracellular domain (282 aa), two transmembrane helices (24 aa each) and a long intracellular C-terminal tail (239 aa) [253], the most intriguing domain of the protein. The C-terminal domain contains several lipids and proteins binding sites as the SRC homology 3 (SH3) domain, a site for the tumor necrosis factor receptor 1 and sites that bound the cytoskeleton [254]. P2X7 subunits assemble forming an homotrimeric functional receptor. Each monomer tridimensionally has been compared to the shape of a dolphin [255] where the flanks are represented by the two transmembrane helices and the large extracellular loop constitutes the various section of the dolphin body [256]. The binding site for ATP is located on the interface of each pair of monomers and contains aa residues conserved across P2XR in human and mouse [257-258]. The absence of positively charged aa at the entrance of the ATP-binding pocket probably suggests the low affinity for ATP and for eventual negatively

charged drug compounds resulted to be active on other P2XRs [243]; infact functional P2X7R ligands are usually small and hydrophobic. When ATP bounds the receptor, a significant conformational rearrangement occurs, where the monomers change their orientation but not their conformation generating a channel [255, 259]. This allows the rapid flow of Na⁺ and Ca²⁺ ions into the cells and K⁺ ions efflux. Prolonged exposure to ATP might promote further permeability through the formation of a larger pore that allows the influx of large hydrophilic molecules [246, 260]. The formation of the so called 'P2X7R pore' is an intrinsic property of the P2X7R that depends mainly by the C-terminal tail of the receptor [259]. The C-terminal role in pore formation consists in stabilization of the 'cytoplasmic cap' and in supporting the movement of the transmembrane helices [259]. Another interesting feature displayed by P2X7R is its reversibility. Indeed if ATP is removed, plasma membrane is completely restored within few minutes [243].

3.3.1 P2X7R variants

Ten splicing variants of P2X7R are actually known in human (P2X7A-J) [261]. Among these variants, four are truncated at C-terminal tail level (P2X7B, C, E and G), P2X7C lacks exon 4, P2X7D exon 5, P2X7E exon 7 and 8 and P2X7F exon 4 and 8. Instead, P2X7G and H have an additional exon, called N3, that once inserted, causes the deletion of the first transmembrane region. P2X7I has point mutation at the first intron level, causing a null allele [262] while P2X7J is truncated after exon 7 and for this reason is not functional [243]. Among all these variants the P2X7B attracted the most interest since is highly expressed in several tissues. The P2X7B receptor retains channel activity promoting cell growth but lacks pore functionality [263]. The P2X7B monomers may heterotrimerize with P2X7A causing an enhanced response in comparison to P2X7A homotrimers maintaining the ability to form the pore [264]. Human P2X7R gene is highly polymorphic and several non-synonymous SNPs (> 150) have been found, principally in the extracellular domain and in the C-terminal tail [265-266]. Eight loss-of-functions have already been identified [267], where the E496A and the I568N are well characterized since it causes a reduced receptor activity [268]. The R307Q instead is located at ATP binding site level decreasing deeply affinity for the agonist [269]. Several SNPs have been associated to pathological conditions as bipolar disorders, macular degeneration and cardiovascular diseases but further investigation have to be done [270-271] to confirm such preliminary data.

3.3.2 P2X7R role in cancer

P2X7R is highly expressed by cancer cells [227] and by different immune cells (NK, MDSCs, Treg and M2 macrophages) [272-273] indicating its strong role in tumor behavior, shaping the TME

participating to both immunostimulatory and immunosuppressive responses. Depending on the level of activation and the cell type, P2X7R triggers cell death or alternatively supports growth [224, 274]. In particular, low and tonic stimulation of P2X7R promotes cell survival and proliferation [202], through increased mitochondrial potential and oxidative phosphorylation efficiency and stabilizing all the mitochondrial network [225]. From a metabolic point of view, P2X7R stimulation induces overexpression of glycolytic enzymes as Glut-1 transporter, glyceraldehyde 3-phosphate dehydrogenase, phosphofructokinase, pyruvate kinase M2 and pyruvate dehydrogenase kinase 1; participating to 'Warburg effects' through the production of lactic acid. In addition P2X7R activation reduces GSK-3 β , increasing glycogen storage [275-276]. These metabolic alteration supports intracellular ATP accumulation and cancer cell growth. In addition several other pathways and transcription factors are activated by P2X7R stimulation, including PI3K/AKT, ERK/MAPK, NFATc1 and HIF-1 α [226, 275-278]. In particular the activation of PI3K/AKT pathway is involved in P2X7-dependent tumor cell growth, invasion, migration and metastatic spreading activating a positive feedback cycle [279-280]. P2X7R confers growth advantages in many cancer models also *in vivo*; indeed several immunocompetent and immunodeficient mouse models have been used to show an effective anti-tumor activity when anti-P2X7R drugs are tested [276, 281-282]. Stimulation of P2X7R deeply affects tumor invasion and metastatic spreading in *in vitro* models of melanoma and breast cancer triggering the release of active cysteine cathepsins and metalloproteinase (MMPs), able to remodel ECM and promote tumor motility [283-284]. P2X7R activation drives also the expression of several genes involved in EMT, such as Snail, E-cadherin, Claudin-1, IL-8 and MMP-3, all involved in the development of a migrative phenotype [280]. P2X7R is also responsible for the activation of RHO GTPase and ROS generation, both involved in the generation of invadopodia and pseudopodia extensive ability [285-288]. From the TME point of view, P2X7R is an important stimulator of VEGF release and of VEGFR2 receptor expression [276, 281, 289]. This happens not only on cancer cells but also in endothelial cells of the TME where P2X7R-expressing endothelial cells growth highly depends on VEGF release and glycolytic metabolism activated by P2X7R [290-291]. P2X7R is one of the most potent stimuli that triggers release of exosomes and plasma membrane-derived vesicles [292-294]. The content of the released vesicles is composed by different kind of molecules as nucleic acids, proteases, inflammasome proteins as NLRP3, cytokines, growth factors and ATP itself, deeply affecting TME biochemical composition and tumor-host interaction [295-296]. Indeed the association of P2X7R with inflammation is long standing. P2X7R promotes the release of proinflammatory cytokines as IL-6, IL-1 β , TNF [297-300] and immunosuppressive cytokines as IL-10 and TFG- β [273, 301-302]. P2X7R is important in the activation of inflammasome through NLRP3. Active inflammasome induces caspase-1 cleavage and

maturation of IL-1 β by different types of immune cells as macrophages, microglial cells and DCs [303]. Recent studies on the role of P2X7R in host response against tumor have shown that, in mouse melanoma or colon carcinoma models, tumor grows and metastasizes more in P2X7R-deficient than in P2X7R-wild-type mice, showing a significant reduction in immune cells infiltration and IL-1 β levels [304-305]. Based on the isoforms expressed, on cell types and on ATP concentration levels P2X7R can also activate some cell death mechanisms as pyroptosis, apoptosis and necrosis opening the pore [201]. P2X7R-dependent apoptotic cell death is induced by a marked mitochondrial catastrophe, followed by cytochrome c release and caspase-3, -8 and -9 cleavages [306-307]. In mononuclear cells, another mechanism of death triggered by P2X7R is pyroptosis induced by caspase-1 and gasdermin-D [308-310]. Necrosis induced by P2X7R is well documented in cells undergoing karyolysis, organelles swelling and plasma membrane permanent damage [224]. For its role in cell death, P2X7R plays an interesting role in ICD. ATP accumulates in TME after chemo- and radiation treatment and is recognized as DAMP activating mechanisms associated to cell death or to antitumor immune inflammation [153]. DCs IL-1 β is a strong local stimulus of their maturation and induces the recruitment of CD4⁺ and CD8⁺ T lymphocytes [303]. Nevertheless many cancer cells express high levels of P2X7R, its activation in TME is not constitutive as it could get to cell death and tumor reduction [213]. Indeed cancer cells enact some mechanisms to avoid cell death induced by pore opening. Among them, high amount of cholesterol content in the plasma membrane, commonly found in cancer cells, leads to inhibition of the P2X7R pore opening, leading to pro-survival Ca²⁺ influx channel activity [311]. In addition P2X7R isoforms B that not retains pore activity is overexpressed in many tumor types [263].

3.3.3 P2X7 as therapeutic target

The above-described role of P2X7R in several inflammatory diseases including cancer has encouraged many pharmaceutical companies to develop drugs against this receptor [262, 312-313]. Many types of molecules have been designed to target P2X7R. Among them several antagonists have been tested as oxidized ATP (oATP), a covalent and irreversible antagonist that binds the lysine residues of the ATP binding site [314]; and A740003, a tetrazole derivative that has proven to be efficacious in *in vivo* models of melanoma and neuroblastoma [276, 304, 315]. Antagonists are small, not charged molecules able to interact with the ATP-binding sites of the receptor and competing with ATP itself [314]. Other developed small molecules are allosteric modulators whose binding sites are different from the ATP-binding one, resulting in profound modifications of the receptor conformation and alterations of the effects of endogenous ligand ATP [316-319]. More than 30 phase I and II clinical trials have been done to test the efficacy of anti-P2X7R in several

diseases as osteoarthritis, rheumatoid arthritis, chronic obstructive pulmonary disease and Crohn's diseases [320-323]. Several P2X7R inhibitors have been tested in preclinical animal models of cancer displaying a promising reduced tumor growth and spreading [314]. Furthermore, a phase I clinical trial using an antibody against non-functional isoforms of P2X7R in basal cell carcinoma patients has shown promising results with a reduction of tumor masses in 65% of the patients [324]. More efforts should be made in order to evaluate the clinical potential of P2X7R-targeting drugs.

Aims of the study

GBM is the most malignant and aggressive primary adult brain tumor. The current standard of care for GBM patients is surgical resection followed by radiotherapy and chemotherapy with temozolomide. Despite this treatment, the median survival for patients with GBM tumor is 12-18 months with the majority of these patients die within two years [12], making GBM still a lethal and incurable tumor. Radiotherapy remains the most important and effective therapy for these patients and understand the mechanisms underlying radiation resistance is essential to develop more effective therapeutic strategies. GBM expresses high levels of P2X7R but its role in tumor behavior and response to therapy is still unknown. Contrasting results on P2X7R pharmacological blockade in GBM have been published. Both GBM tumor growth and reduction is founded after P2X7 pharmacological blockade, making the role of this receptor in GBM biology still confusing. Only one study [325] evaluates the association between P2X7R and radiation treatment, without deeply investigates its role in radiation resistance mechanisms. In the present study the aim is to investigate the role of P2X7R in resistance to radiation treatment using GBM stem-like cells derived from patients tumors.

Materials and Methods

Cell culture

Use of human tissues was in accordance with local research ethics board approval and patients gave informed consent prior to surgery. Primary stem-like tumor-propagating cells were obtained directly from patient tumor specimens after surgical eradication. Briefly tumor tissues classified as GBM by pathologists were washed and then enzymatically dissociated. Cells were then plated in NeuroCult NS-A medium (StemCell Technologies, Vancouver, BC, Canada) supplemented with 20 ng/ml of epidermal- and 10 ng/ml of fibroblast-growth factor (Sigma-Aldrich), 1% penicillin/streptomycin (GE Healthcare, Milan, Italy) and 2% amphotericin B (Euroclone) and maintained under hypoxic conditions (1% O₂) in a humidified 37 °C, 5% CO₂ incubator. All the primary GBM cell lines were checked periodically for mycoplasma contamination using the MycoAlert™ Mycoplasma Detection Kit (Lonza, Basel, Switzerland). For cell population analysis, 2,5 x 10⁵ GB40 and GB48 cells were plated in a T25 cm² flask. When cells reached the 90% of confluency, they were collected, disassociated to a single-cell suspension and replated in culture medium. The total number of viable cells was assessed at each passage with trypan blue exclusion test.

Irradiation treatment

GB40 and GB48 cells were plated at a density of 70-80% and treated with 7.5 Gy dose using the linear acceleration Elekta Synergy Platform system (Elekta Oncology Systems, Stockholm, Sweden) and the irradiation system described by Tesei A, et al. [326].

RNA extraction and Real-time Quantitative Polymerase Chain Reaction

Total RNA was extracted from GBM cells using TRIzol® reagent according to the manufacturer's instructions (Invitrogen). RNA was quantified using the Nanodrop® ND-1000 spectrophotometer. Reverse transcription reactions were performed in 20 µl of volume containing 200 ng of total RNA using the iScript cDNA Synthesis kit (Bio-Rad Laboratories, Hercules, CA, USA). Real-Time PCR was run using 7500 Fast Real-Time PCR system (Applied Biosystems) and TaqMan assays to detect the expression of P2RX7A, P2RX7B, ENTPD1 and NT5E genes. Reactions were carried out in triplicate at a final volume of 20 µL containing 15 ng of cDNA template, TaqMan universal PCR Master Mix (2X), and selected TaqMan assays (20X). Samples were maintained at 50°C for 2 min, then at 95°C for 10 min followed by 40 amplification cycles at 95°C for 15 s, and at 60°C for 30 s. The amount of mRNA was normalized to the endogenous genes GAPDH and HPRT-1.

***In vitro* measure of extracellular ATP levels**

ATP levels were measured in the culture supernatants with ENLITEN rLuciferase/Luciferin reagent (Promega), according to manufacturer's instructions. Briefly, 1.5×10^5 GB40 and GB48 cells were plated in a six-well plates. After each time points (1D, 7D, 14D, 21D and 28D) the luminescence were measured immediately after the addition of 50 μ l of ENLITEN reagent to 50 μ l of cell supernatant using the GloMax® bioluminescent reader (Promega). Data were obtained as nanomoles of ATP interpolating from a calibration curve performed by adding known ATP amounts and normalized on the total amount of proteins. Fold change in amount of ATP released compared to untreated cells were shown.

Cytosolic free calcium concentration measurements

Cytosolic Ca^{2+} concentration was measured using the fluorescent Ca^{2+} indicator Fura-2-acetoxymethyl ester (Fura-2/AM) (Thermo Fisher Scientific). Briefly, 1×10^6 GB40 and GB48 cells were incubated with Fura-2/AM (4 μ M) for 20 minutes at 37°C in saline solution (125 mM NaCl, 5 mM KCl, 1 mM MgSO_4 , 1 mM NaH_2PO_4 , 20 mM HEPES, 5.5 mM glucose, 1 mM CaCl_2 at pH 7.4) supplemented with sulfinpyrazone (250 μ M). Ca^{2+} concentration was measured at the wavelength excitation 340/380 nm and emission 505 nm in a thermostat-controlled (37 °C) and magnetically-stirred Cary Eclipse Fluorescence Spectrophotometer (Agilent Technologies, Milano, Italy) after stimulation at different concentrations (100, 300 and 500 μ M) of BzATP (Sigma-Aldrich) alone or after a pre-treatment with AZ 10606120 dihydrochloride (1 μ M) (Tocris Bioscience, Bristol, UK).

Ethidium bromide uptake

Alterations in plasma membrane permeability were measured through Ethidium Bromide uptake. 1×10^6 GB40 and GB48 cells were kept at 37° C in a thermostat-controlled and magnetically stirred cuvette of a Cary Eclipse Fluorescence Spectrophotometer (Agilent Technologies) in the presence of 20 μ M ethidium bromide (Sigma-Aldrich). Cells are exposed to different concentrations (100, 300 and 500 μ M) of BzATP alone or after pre-treatment with AZ 10606120 dihydrochloride (1 μ M). Fluorescence changes were acquired at 360 nm and 580 nm excitation and emission wavelengths, respectively.

Soft agar assay

Cells (1×10^3 per well) were mixed with 0.4% Seaplaque agar in growth medium with antibiotics, plated on top of a solidified layer of 1% Agar Noble in HBSS medium supplemented with antibiotics in a 24-well plate. Six series of samples were prepared for each treatment dose. Freshly prepared growth medium, containing or not P2X7R modulators, was added every 2 days. Colonies with more than 50 cells were weekly quantified under inverted microscope (Olympus IX51 microscope, Olympus Corporation, Tokyo, Japan) by two independent observers.

Western Blot

Cells were detached and lysed in RIPA lysis buffer () for 1h at 4°C. Equal protein amounts were separated on Novex NuPage Bis-Tris 4–12% precast gel (Life Technologies, Milano, Italy) and transferred to nitrocellulose membranes (GE Healthcare-Life Sciences, Milano, Italy). After incubation with TBS–Tween-20 (0.1%) supplemented with 5% non-fat powdered milk for 1 h to saturate unspecific binding sites, membranes were incubated overnight with primary antibodies at 4 °C. The anti-BCL2 polyclonal antibody (dilution 1:200) (NeoMarkers, Fremont, CA), the anti-Bax antibody (Cell signaling technology) (dilution 1:1000) and the anti-p21 antibody (Cell signaling technology) (dilution 1:800) were incubated in TBS–Tween-20 (0.1%) supplemented with 5% non-fat powdered milk. The anti-myosin (Sigma-Aldrich, cat. N. A5060) was diluted 1:1000. The anti-P2X7R polyclonal antibody (Merck-Millipore, Milano, Italy, cat n. AB5246) was diluted 1:1000 and incubated in TBS–Tween-20 (0.1%) supplemented with 2% of BSA. Membranes were incubated with secondary goat anti-rabbit HRP-conjugated antibodies (Invitrogen-Thermo Fisher Scientific, Monza, Italy, cat n. 31460) at a 1:3,000 dilution for 1 h at room temperature. All the antibody were diluted in TBS–Tween-20 (0.1%) supplemented with 5% non-fat powdered milk.

β-Galactosidase assay

β-Galactosidase staining was performed with the Senescence β-Galactosidase Staining Kit (Cell Signaling, #9860) according to the manufacturer's instructions. Briefly, GB40 and GB48 cells were plated at 1.5×10^5 cells in a 6 well plate pre-coated with Matrigel diluted 1:50 in HBSS medium supplemented with antibiotics in order to force cells attachment at each time point (1 day, 7 days, 14 days, 21 days and 28 days). Cell were then fixed in 1X fixative solution for 10 minutes at room temperature and stained overnight at 37°C with the β-galactosidase staining solution at pH 6.0. Images were acquired with an inverted Olympus IX51 microscope (Olympus Corporation, Tokyo,

Japan) with the 10X objective, equipped with a Nikon Digital Sight DS-Vi1 camera (CCD vision sensor, square pixels of 4.4 μM side length, 1600 \times 1200 pixel resolution, 8-bit grey level) (Nikon Instruments, Spa. Florence, Italy). Percentage of β -Galactosidase positive cells were obtained counting 5 different image fields.

***In vitro* measure of lactate dehydrogenase (LDH) release**

LDH release was measured in the culture supernatants with LDH-Glo™ Cytotoxicity Assay (Promega), according to manufacturer's instructions. Briefly, 1.5×10^5 GB40 and GB48 cells were plated in a six-well plates. After each time point (1 day, 7 days, 14 days, 21 days and 28 days), cell supernatants diluted 1:25 in LDH storage buffer (200mM Tris-HCl (pH 7.3), 10% Glycerol, 1% BSA in deionized water) was added to LDH detection reagent at ratio 1:1 and incubated at room temperature for 60 minutes. Luminescence were then measured using the GloMax® bioluminescent reader (Promega). LDH release (%), was calculated by using the following formula: LDH release (%) = [(experimental LDH release value) – (background value)]/[(LDH release value in 10% Triton X-100-treated samples) – (background value)] \times 100 and normalized on total amount of proteins.

Total cholesterol assay

Total cellular cholesterol was quantified using an Amplex Red cholesterol assay kit according to the manufacturer's instructions (Invitrogen, Grand Island, NY, USA). Briefly, 2.5×10^5 GB40 and GB48 cells were collected after each time point (1 day, 7 days, 14 days, 21 days and 28 days), snap freezing in liquid nitrogen and resuspended in 50 μl of 1X Reaction Buffer working solution. 1 μg of total protein was used in the assay for each sample. Fluorescence was measured in a Perkin Elmer Wallac Victor3 1420 system (Perkin Elmer, Wellesley, Massachusetts, USA) according to the manufacturer's instructions.

Data are expressed as micromolar concentration of cholesterol interpolating from a standard curve performed by adding known cholesterol amounts.

Inflammasome Caspase-1 activity assay

The Caspase1 activity was performed with Caspase-Glo 1 inflammasome assay kit (Promega, Milan, Italy) according to manufacturer's instructions. Prior to the assay, the Caspase-1 luminescent substrate solution was prepared and equilibrated to room temperature. After the respective incubation periods, 100 μL of the substrate solution was added to each well of the 96-well plate, the plates were mixed for 30 s and then incubated at room temperature for 1.5 hrs to allow the

luminescent signal to stabilize. Luminescence were then measured using the GloMax® bioluminescent reader (Promega).

Digital PCR

dPCR was used to determine the expression level of P2X7A and P2X7B in seven GBM primary cells. All dPCR experiments were carried out using the chip-based QuantStudio™ 3D Digital PCR system (Applied Biosystems, Foster City, CA, USA). P2X7A and P2X7B were run in singleplex using 10 ng cDNA. Reaction mixes containing either cDNA or water (no-template controls) were first prepared by adding 2X QuantStudio 3D™ Digital PCR Master Mix v2 (Applied Biosystems) and 20X gene specific assay in a total volume of 15.5 µl. Chips were run using GeneAmp PCR System 9700 (Applied Biosystems) by applying the following conditions: hold at 96°C for 10 min; 45 cycles of 60°C for 2 min and 98°C for 30 sec; hold at 60°C for 2 min. At the end of the reaction, chips were processed using the QuantStudio™ 3D Digital PCR system (Applied Biosystems) and analyzed with QuantStudio™ 3D Analysis Suite™ software (version 3.0.3).

Cell cycle distribution

After radiation treatment, GB40 and GB48 cells were fixed in 70% ethanol at each time point (day1, day 7, day 14, day 21 and day 28). Cells were then stained with propidium iodide (10 mg/ml, MP Biomedicals, Verona, Italy), RNase (10 kunits/ ml, Sigma-Aldrich) and NP40 (0.01%, Sigma Aldrich) overnight at 37C° in the dark, and analyzed by FACS Canto flow cytometer (Becton Dickinson, San Diego, CA, USA) equipped with 488 nm (blue) and 633 (red) lasers. 10000 events for each sample were acquired. Data acquisition and analysis were performed using FACSDiva (Becton Dickinson) and ModFit 2.0 (DNA Modelling System, Verity Software House, Inc., Topsham, ME, USA). Data were expressed as fractions of cells in the different cycle phases.

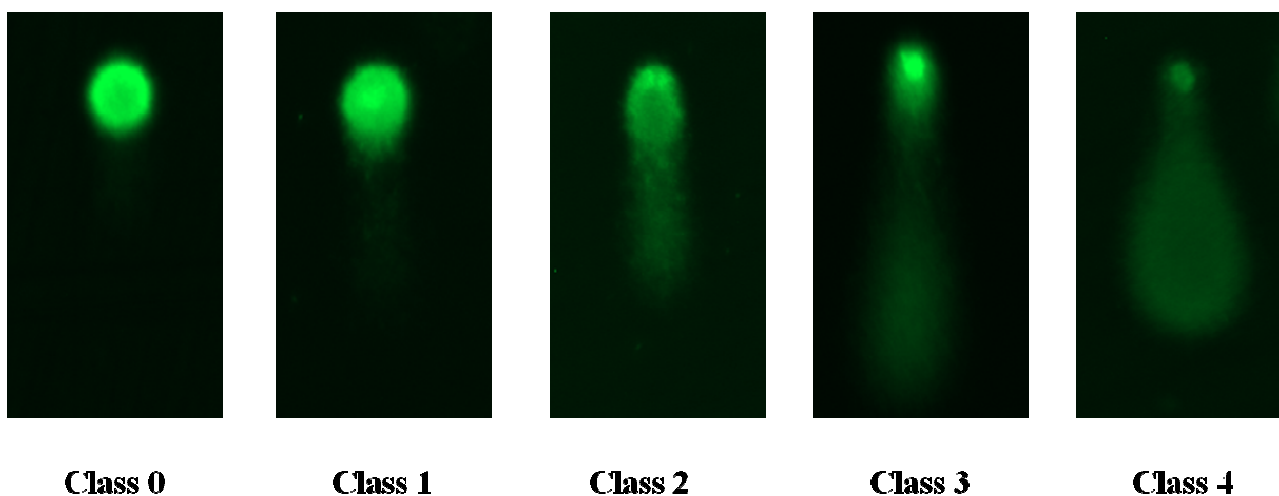
Immunophenotypic analysis

GB40 and GB48 cells were collected, washed twice with PBS 1x and stained with APC-conjugated anti-CD44 antibody (dilution 1:50) (Becton Dickinson, BD Pharmigen) and PE-conjugated anti-Eph2A antibody (dilution 1:20) (Biolegend) for 30-45 minutes at 4°C. APC-conjugated anti-CD133 antibody (dilution 1:20) (miltenyi biotec) was used for single staining of GBM cells.

After three washes, cells were acquired using a FACS Canto flow cytometer (Becton Dickinson, San Diego, CA, USA) equipped with 488 nm (blue) and 633 (red) lasers. Appropriate isotype control was included for each sample.

Alkalyne comet assay

The alkalyne comet assay was performed according to the manufacturer's protocol (Comet assay, Trevigen, Gaithersburg, MD). Briefly, 3000 cells were suspended in LMAgarose (at 37°C) at a ratio of 1:10 (v/v), and 35 µl were immediately transferred onto the comet slide and left at 4°C for gelling time. The slides were then immersed for 1 hr at 4°C in a prechilled lysis solution, washed in the dark for 1 hr 4°C in alkaline unwinding solution, then electrophoresed for 30 min at 21V. Slides were immersed twice in dH2O for 5 minutes each, then dipped in 70% ethanol and stained with 20 µl of diluted SYBR® Green Master Mix (BioRad). At least one hundred comets spanning from category 0 to category 4 (see also Figure VII) were evaluated by EVOS Cell Imaging Systems 10x, Thermo Fisher Scientific – US. DNA damage was quantified by computing, in each comet, the displacement between the genetic material contained in the nucleus, typically representing the 'comet head', and the genetic material in the surrounding part, considered as the 'comet tail'. Percentage of DNA in tail for different categories of comets was expressed, as previously described by Garcia O, et al. [327]. In order to obtain reproducible and reliable data, we developed an easy-to-use tool named CometAnalyser.



Comet Analyser Software

CometAnalyser is a semi-automatic tool developed with the goal to be extremely user friendly. It has been developed in MatLab (The MathWorks, Inc., Natick, MA, USA) and the current version (CometAnalyser v0.9) requires MatLab R2017b and the MatLab Image Processing Toolbox 10.1, or a later version. CometAnalyser works with silver staining and fluorescent images. The working procedure can be briefly summarized in three main steps. (a) First of all, the user has to draw with the mouse a region surrounding the comet of interest. The tool then automatically segments comet

heads and nuclei. By default, the Otsu thresholding segmentation method is used [328], but other algorithms are available and several parameters can be then modified to adjust the segmentation. (b) Once the comets have been segmented, Tail Moment and all the other features listed by Gyori BM, et al. are automatically computed and saved as Excel file [329]. (c) Snapshots of all the segmented comets are stored in different folders according to a classification manually performed by the user. Finally, the project with all the labels can be saved and loaded back for future modifications.

Results

4.1 P2X7R is expressed in patients-derived GBM-stem like cells

Digital PCR and western blot were used to evaluate P2X7R transcript isoforms expression and protein levels in GBM stem-like cells derived from patients tissue samples. Both P2X7R isoforms are expressed by GBM cells with a significant higher prevalence of P2X7RB transcript than P2X7RA transcript in all the GBM cells tested (n=7) (43.34 ± 21.90 vs 1.41 ± 0.50 copies/ μ l) (Figure 1A). P2X7R protein, evaluated by western blot, showed different expression levels in the GBM cells tested (Figure 1B). GB40 cells express the highest P2X7R protein levels while GB48 the lowest. HEK293 wild-type cells and HEK293 cells transfected to express human full-length P2X7R were used as negative and positive control, respectively. Whole exome analysis was performed in GB40 and GB48 cells and no mutations in exons were observed for P2X7R gene. GB40 and GB48 cells, expressing different levels of P2X7R protein, were selected for the experiments described below. GBM is notoriously highly heterogeneous and enriched in cancer stem cells. Concerning the morphological features of our cells, GB40 cells grew as single cells or small aggregates both in suspension and in adhesion (Figure 1C), while GB48 grew preferentially as small neurospheres with different degree of compactness (Figure 1D). In order to demonstrate the stem-like nature of the GBM cells isolated, immunophenotyping with stemness markers CD44, EphA2 and CD133 was performed (Figure 1E-F). Coupled immunophenotyping of CD44 and EphA2 was performed, showing in GB40 a prevalent population that expresses only CD44 (98.9% of cells), whilst only the 0.8% of cells expresses both markers and the 0.3% of cells do not express any of these two markers (Figure 1E, upper pie chart). On the contrary, in GB48 the majority of the cells co-express both markers (97.0%), whilst only the 2.8% of the entire population expresses only CD44 (Figure 1E, bottom pie chart). CD133 positive population is similar in both GB40 and GB48 (57.80% vs 58.80% of the entire population) (Figure 1F). Finally rates of expansion of both cells were evaluated during time in culture showing that GB48 have a faster rate of expansion than GB40 (Figure 1G). GBM cells were considered stabilized cell lines after an exponential expansion and after reaching 10 passages. This analysis reflects the typical high heterogeneity of this tumor, confirming that our cells are a representative model to study GBM biology.

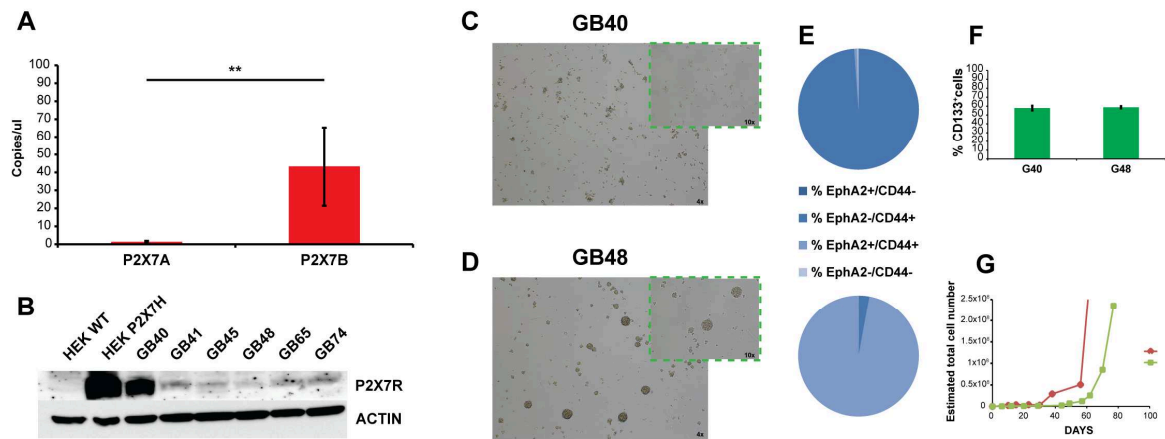


Figure 1. P2X7R is expressed in patient derived GBM-stem like cells. **A.** Digital PCR was used to measure P2X7RA and P2X7RB absolute expression levels in 7 patients-derived GBM-stem like cells. The data are expressed as mean \pm SD number of copies of the transcripts for each μ l. **B.** Western blot analysis was used to evaluate P2X7R full length expression in GBM stem-like cells. **C.** Brightfield representative images of GB40 and **D.** GB48 stem-like cells derived from human specimens. Magnification 4x and 10x. **E.** Representative analysis of the immunophenotype for CD44 and EphA2 and their co-expression in GB40 and GB48 using flow cytometry expressed in % of positive cells for each combination of the two markers analyzed. **F.** CD133 expression analysis in GB40 and GB48 cells using flow cytometry. **G.** Rates of expansion of both GB40 and GB48 cells. Cells counts were plotted into the y-axis while the days on the x-axis. Data were analyzed by Student T-test (* $p < 0.05$; ** $p < 0.01$; *** $p < 0.001$).

4.2 P2X7R is functional in GBM stem-like cells

To investigate the role of P2X7R in our GBM stem-like cells we treated cells with ATP at different concentrations (1, 3 and 5 mM) for 24 hours. Cytotoxicity was evaluated by LDH release. GB40 cells are sensitive to ATP *in vitro*, as a significant increase in the % of released LDH after the exposure to 3 mM (40.81 ± 0.26 % vs 11.18 ± 0.38 %) ($p = 0.0001$) and 5 mM (43.45 ± 0.93 % vs 11.18 ± 0.38 %) ($p = 0.0023$) of ATP was observed compared to untreated cells, showing ATP-induced cell death (Figure 2A, upper graph). On the contrary, ATP exposure on GB48 did not induce cell death but a significant slight reduction of the % released LDH in treated cells (Figure 2A, bottom graph) rather than untreated cells, suggesting a different function of P2X7R in the two GBM cells. From the morphological point of view, after ATP exposure GB40 cells showed an

increased irregular shape characterized by membrane ruffles and presence of debris, compatible with dying cells; only few cells retained cellular integrity and morphology similar to the untreated cells (Figure 2A, upper right images). GB48 cells displayed a significant change in morphology too, with a progressive loss of neurospheres replaced with single cells accumulation at the higher doses of ATP (Figure 2A, bottom right images).

To better understand how P2X7R affects tumor growth, we treated GBM cells with two antagonists, having two different binding sites. The AZ10606120 dihydrochloride antagonist acts as a negative allosteric modulator, binding to a different site than the ATP-binding site, whilst the A740003 antagonist interacts with the ATP-binding site. LDH release is slightly reduced after 24h of treatment with both antagonists at different concentrations (Figure 2B, upper graphs) in GB40 cells suggesting that cytotoxicity is not induced in such short period of time. Same effect was seen for GB48, in particular after treatment with A740003 antagonist (Figure 2B, bottom graphs). Taken together, these data suggest that short term treatment with P2X7R antagonists does not affect viability of GBM cells. To evaluate the long term effects of P2X7R antagonists treatments, a soft-agar colony forming assay was used. A slight reduction in survival fraction (0.82 ± 0.01) of GB40 cells was seen after 28 days of treatment with 10 μM AZ10606120. Treatment with 20 μM A740003 induced in GB40 a significant reduction in survival fraction (0.59 ± 0.003) ($p=0.001$) than the one observed in cells treated with AZ10606120 (Figure 2C, upper graph). Long term treatment with AZ10606120 in GB48 impacts more on cell survival than in GB40 (0.67 ± 0.01) (Figure 2C, bottom graph) but treatment with A740003 is less effective (0.81 ± 0.003) in GB48 cells rather than what observed in GB40 cells.

To further investigate the functional role of P2X7R in our GBM cells we evaluated fluctuations of Ca^{2+} intracellular levels after stimulation with BzATP, a selective P2X7R agonist. In GB40, stimulation with a range of concentrations of BzATP (100, 300 and 500 μM) triggered a progressive raise of intracellular Ca^{2+} (Figure 2D, upper graph), suggesting an activation of the P2X7R cation-channel. To support this hypothesis, that is the Ca^{2+} increase depends on P2X7R stimulation, GB40 cells were pre-treated with AZ10606120 at 1 μM , showing a complete blockade of Ca^{2+} uptake even after stimulation with the highest concentration of BzATP (Figure 2D, upper graph, violet line in the graph). GB48 has a functional P2X7R as well, even if the P2X7R-dependent Ca^{2+} increase was lower compared to the one observed in GB40 (Figure 2D, bottom graph).

Finally, to evaluate if prolonged stimulation of P2X7R induces the formation of the large pore in our GBM cells we performed ethidium bromide uptake experiments. In GB40 cells P2X7R stimulation with BzATP at the different concentrations slowly induced the uptake of the ethidium

bromide (Figure 2E, upper graph). To confirm that ethidium bromide uptake is P2X7R-dependent, cells were again pre-treated with AZ10606120 at 1 μ M displaying a complete blockade in ethidium bromide uptake (Figure 2E, upper graph, pink curve in the graph). Instead, in GB48 cells, none of concentrations of BzATP used to stimulate P2X7R triggered ethidium bromide uptake (Figure 2E, bottom graph). These data suggested that both GBM cells have functional P2X7R in terms of cation channel but only in GB40 the receptor retains the large pore activity usually associated to cell death.

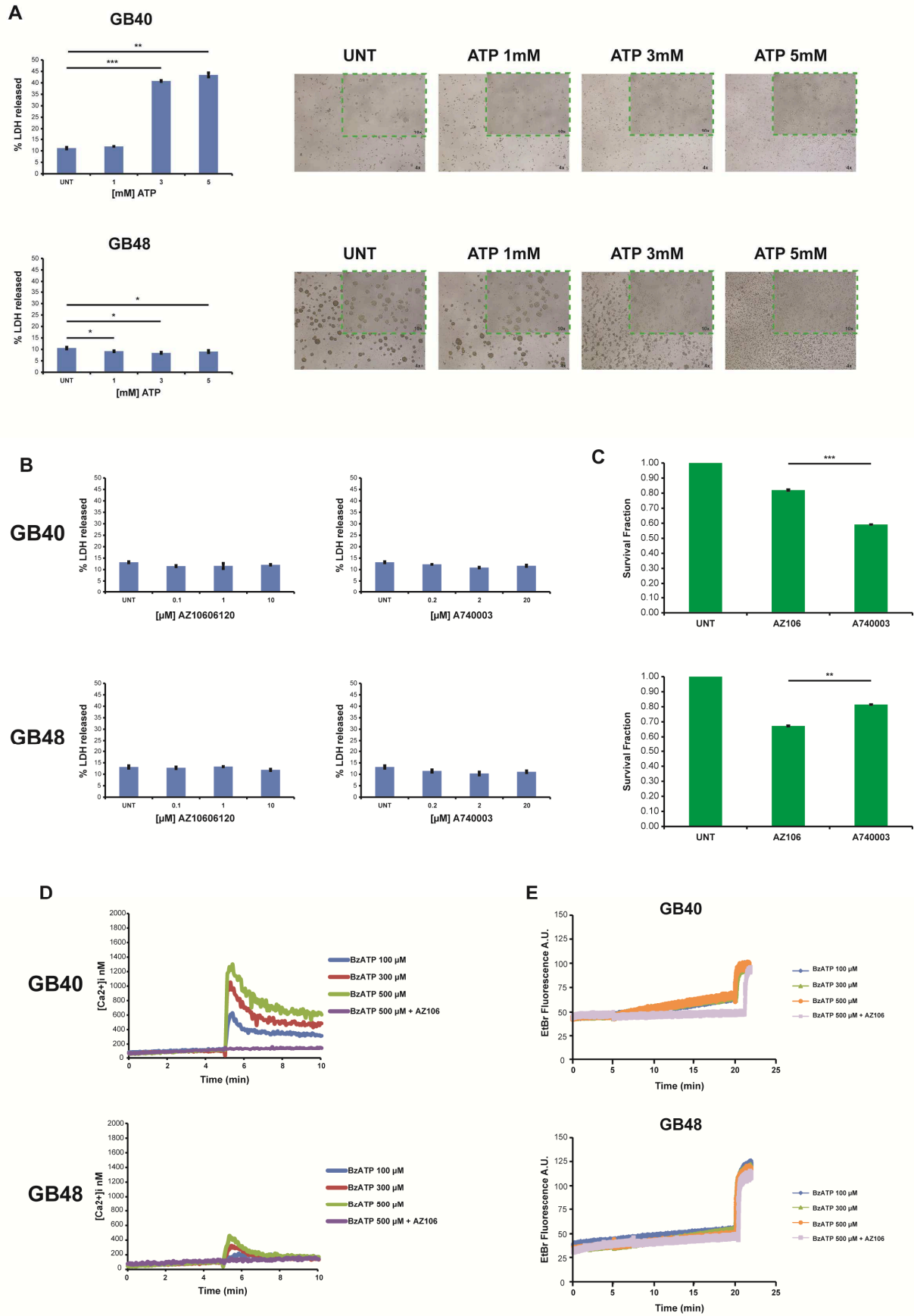


Figure 2. P2X7R showed different functional behavior in patient-derived GBM stem-like cells.

A. GB40 and GB48 were treated with 3 different concentration of ATP (1, 3 and 5 mM) for 24h. Cytotoxicity induced by ATP in GBM cells was measured in terms of % of released LDH. Data are represented as the mean \pm SD. Brightfield representative images of GB40 and GB48 cells after 24h of treatment with ATP. Magnification 4x and 10x. **B.** GBM cells were treated with two different P2X7R antagonists for 24h: AZ10606120 (0.1, 1 and 10 μ M) and A740003 (0.2, 2 and 20 μ M). Cytotoxicity induced by both antagonists in GBM cells was measured in terms of % of released LDH. Data are represented as the mean \pm SD. **C.** Soft-agar assay was used to evaluate long term effects of anti-P2X7R treatment in GBM cells. Data are represented as the mean \pm SD. **D.** Representative traces showing intracellular Ca^{2+} increase following stimulation with BzATP (100, 300 and 500 μ M) in GB40 and GB48 cells. **E.** Representative traces showing ethidium bromide uptake following stimulation with BzATP (100, 300 and 500 μ M) in GB40 and GB48 cells. Data were analyzed by Student T-test (* $p < 0.05$; ** $p < 0.01$; *** $p < 0.001$).

4.3 Radiation induces cell death and ATP release during time in patient-derived GBM stem-like cells

GB40 and GB48 cells were treated with 7.5 Gy doses of radiation, in order to mimick an hypofractionated treatment *in vitro*. Since it is widely known that radiation has mainly long term effects of cancer cell viability, to evaluate these effects on our GBM cells, the soft-agar colony forming assay was used. Radiation treatment toxicity was evaluated after 28 days, where a significant reduction in the survival fraction of both GB40 and GB48 cells (0.19 ± 0.005 and 0.21 ± 0.005) was obtained (Figure 3A). In order to monitor the time-dependent response to radiation treatment, five time points have been choosen (day 1, day 7, day 14, day 21 and day 28) and for each one radiation-induced cytotoxicity effects were evaluated in GBM cells by LDH release. Radiation affected cell viability starting from day 1 in GB40, whilst no significant effects were observed in GB48 at the same time point (20.80 ± 0.29 % vs 8.71 ± 1.52 %) compared to the respective untreated cells (Figure 3C-E). Radiation treatment highly impacted on cell viability of both cell lines at day 7 (47.07 ± 2.06 % in GB40 vs 47.82 ± 0.72 % in GB48); even from morphological point of view, alterations such as shrinkage of the cell bodies and ruffling membranes probably associated to dying cells are observed. Interestingly, besides dying cells, a population of cells with increased dimensions and volume, in particular in GB40, seemed survived (Figure 3B). Same population is observed in GB48 neurospheres, the latter appeared smaller and

less compact than the untreated ones (Figure 3D). At day 14 the cells keep dying (51.16 ± 1.94 % in GB40 vs 41.09 ± 2.58 % in GB48) with a lot of debris and dying cells clearly present. However the population of cells with increased dimension are still observed in both GB40 and GB48 (Figure 3B-D). At day 21 irradiated GB40 cells started the recovery (13.83 ± 0.06 % in irradiated cells vs 8.50 ± 0.17 % in untreated cells), in addition they partially restore their original morphology with only few cells retaining the increased dimension phenotype (Figure 3B). GB48 seemed to be slower in recovery, with just a small portion of cells those were dying (22.16 ± 0.98 %) compared to the untreated cells (8.54 ± 0.08 %) (Figure 3E). From the morphological point of view, a lot of debris are present, indicating that cell death is still occurring in GB48 (Figure 3D). At the last time point (day 28) GB40 cells completely restored the original morphology but a higher amount of aggregates were observed than untreated cells (Figure 3B). Cell death was comparable to the untreated cells (17.55 ± 0.34 % vs 16.49 ± 0.94 % respectively) at this time point (Figure 3C). Also GB48 cells restore their neurosphere morphology (Figure 3D) even if a few cells were still dying compared to the untreated cells (21.60 ± 0.19 % vs 15.53 ± 0.17 % respectively) (Figure 3E). ATP release in culture medium was also measured at each time point. In irradiated GB40 cell medium a constant but slight release of ATP was seen compared to untreated cells (Figure 3F, left graph). In GB48, instead, the amount of ATP in culture medium of irradiated cells is significantly increased 2.73 ± 0.10 time ($p=0.01$) starting from day 14 compared to untreated cells (Figure 3F, right graph).

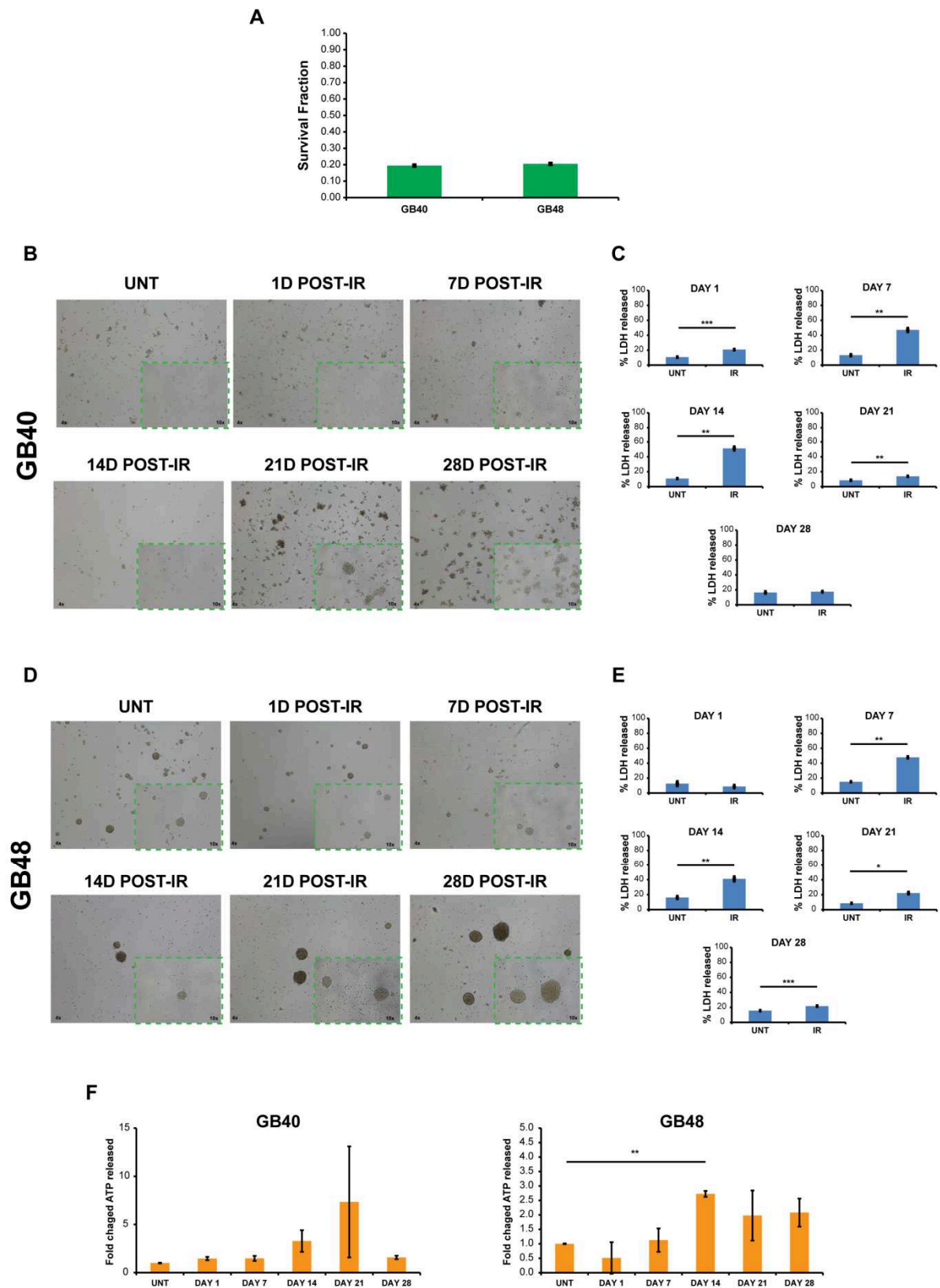


Figure 3. Radiation induces cell death and ATP release during time in GBM cells. **A.** Soft-agar assay was used to evaluate long term effects of radiation treatment in GBM cells. Data are represented as the mean \pm SD. **B-D.** Representative brightfield images of untreated and irradiated GB40 and GB48 cells at each time point, respectively. Magnification 4x and 10x. **C-E.**

Cytotoxicity, expressed as % of released LDH, was calculated for each time point. Data are represented as the mean \pm SD. **F.** Fold change in terms of amount of released ATP by irradiated cells normalized to untreated cells at each time point. Data are represented as the mean \pm SD. Data were analyzed by Student T-test (* $p < 0.05$; ** $p < 0.01$; *** $p < 0.001$).

Since the data obtained so far suggest that GBM cells have the ability to recover after radiation treatment, we performed an alkaline comet assay, to quantify DNA damage and to evaluate its repair along the 28 days after radiation dose. All the analysed comets have been categorized into a comet class, spanning from 0 =no damage, to 4 =total DNA fragmentation.

Figure 4A-B shows the analysis report of GB40. On the top, pie charts showing the comet classes distribution at each time-point are given, highlighting class 1 as the most representative comet class, which initially plays a major role in DNA damage, covering more than half of total comets percentage (74.19 % at Day 1). Then, at day 7 and day 14, a substantial sector of the pie charts are covered by class 4 comets (50.00 % and 37.61%, respectively), suggesting how radiation dose highly impacted on DNA damage, reaching a climax at day 7. Finally, at day 21 and day 28, a progressive recovery of cells is visible, according to a growing prevalence of low grade classes. The same result is resumed in the bar chart reported on the bottom (Figure 4B), where the x-axis shows each time condition, while the y-axis reports the weighted calculated mean of the % DNA in the comet's tail.

Turning to GB48 (Figure 4C-D), the distribution of comet classes, visible in the pie charts representation, is considerably different (Figure 4C). Excluding day 1, where class 1 damage is highly represented (53.21 %), in a similar way with respect to GB40, it is remarkable how day 7 and day 14 are characterized by the presence of a homogenous distribution of each comet class, without the prevalence of high grade comet classes seen for GB40. Consistently, at day 21 and day 28, lower grade comet classes progressively set in, peaking at day 28, where no damage class play the leading role, covering 79.10 % of all comets analyzed. Again, the bottom of the figure (Figure 4D) shows the bar chart of the % of DNA in comet's tail, reported as weighted arithmetic mean. Even if the overall trend observed in GB40 is applicable also for GB48 and the most conspicuous peak is reached at day 7, lower % (7.32 ± 0.96 % vs 10.85 ± 1.00 %) are reached with respect to GB40, suggesting a putative lower sensitivity of GB48 to radiation treatment.

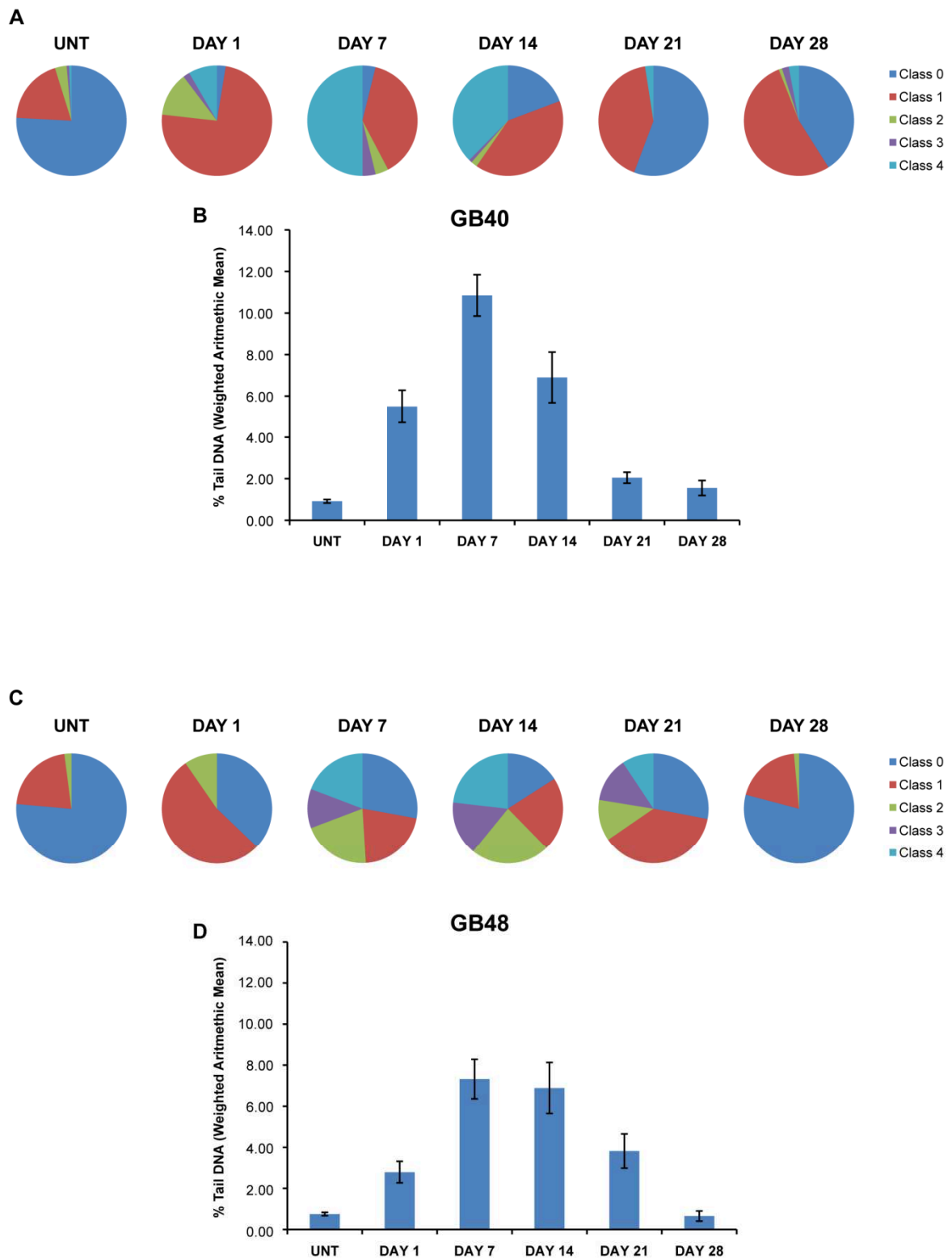


Figure 4. GBM cells are able to recover from radiation induced DNA damage. A-C. Pie charts representative of comet classes distribution in each experimental time point for GB40 and GB48 respectively. **B-D.** % of DNA in the comet's tail (calculated by (Mean % of tail DNA for each

class)* (% comets of that class/total)), was extrapolated for each experimental time point for GB40 and GB48 respectively. Data are represented as the mean \pm SEM.

4.4 Radiation resistant GBM cells display a senescent phenotype

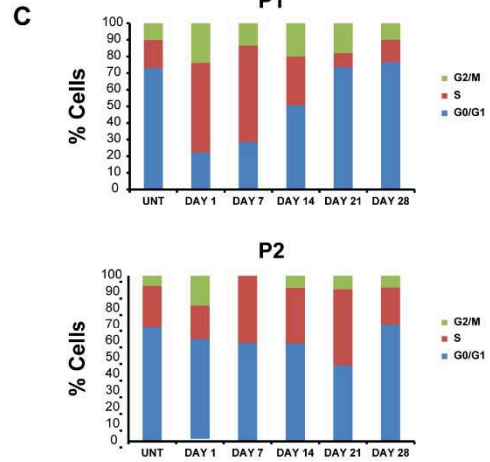
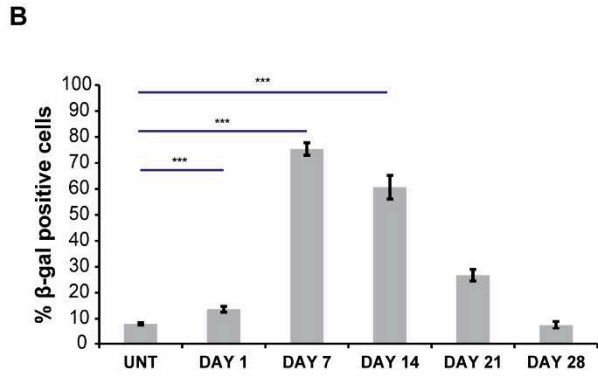
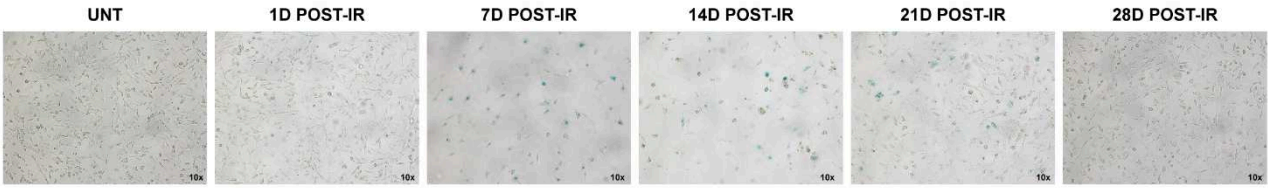
Since at day 28 both GBM cells recovered from the radiation treatment, our subsequent efforts have been done in order to understand some of the mechanisms underlying resistance to radiation treatment. We previously noticed that cells those seemed survive displayed an unusual phenotype characterized by increased volume and dimensions (Figure 3B-D). For this reason, to verify if GBM cells underwent a senescent state after radiation treatment, the β -galactosidase assay was performed at each time point (Figure 5A-B-D-E). A significant increase in the percentage of β -galactosidase positive GB40 cells was observed starting from day 1 (13.62 ± 1.12 %) compared to untreated cells (8.04 ± 0.45 %) ($p=0.0001$), reaching a maximum at day 7 (75.37 ± 2.42 %). From day 14 the amount of β -galactosidase positive cells progressively decreased, reaching comparable percentage of untreated cells at day 28 (7.52 ± 1.39 %) (Figure 5A-B). In GB48 β -galactosidase positive cells increases immediately at 1 day (33.65 ± 2.04 %), peaking at day 14 (64.37 ± 3.20 %). A progressive reduction of β -galactosidase positive cells is also appreciated in GB48 cells after day 14, reaching almost the same levels of the untreated cells at day 28 (12.52 ± 1.62 % vs 10.03 ± 0.87 % respectively) (Figure 5D-E).

To confirm that GBM cells underwent a senescent state after radiation treatment, cell cycle analysis have been performed at each time point (Figure 5C-F). In both our GBM cells we found two sub-populations each, those retain different contents of DNA. These data are consistent with the high heterogeneity of GBM tumors and its typical genetic instability, confirming that our patient-derived cells represent a quite good representative model to study GBM. For this reason the cell cycle data for each time point and for each GBM cell types were provided for both the population (P1 and P2) found (Figure 5C-F). ModFit 2.0 software was used to calculate cell cycle distribution. Irradiated GB40 cells seemed to accumulate in phase S starting from day 1 (Figure 5C) reaching 54.11% in the P1 population. Cell cycle of irradiated cells progressively returns similar to untreated cells at day 21 and day 28 in both P1 and P2 GB40 populations (Figure 5C). An accumulation in phase S and G2/M is observed in GB48 irradiated cells starting from day 1 and peaking at day 14 for both populations P1 and P2 (Figure 5F). At day 28 the irradiated cells completely recover and the cell cycle distribution shows the same pattern of untreated cells. These data have to be confirmed with further investigation in order to understand the contribution of each population in the response to radiation treatment. Cell cycle alterations was deeper investigated by evaluation of the expression of

the cell cycle regulator p21 protein. An increased expression of p21 protein in both GBM senescent cells is observed after radiation treatment confirming that both GB40 and GB48 triggered cell cycle arrest (Figure 5G-H). In particular in GB40 irradiated cells the highest expression of p21 was observed at 7 and 14 days after radiation treatment (Figure 5G). In GB48 irradiated cells, p21 protein levels increases drastically at day 7, and subsequently a slight decrease is observed in the subsequent time points (Figure 5H).

Finally, we investigate the role of Bcl-2 proteins as potential mechanism of resistance adopted by GBM senescent cells. Pro- and anti-apoptotic proteins Bax and Bcl-2 expression levels were then evaluated by western blot at each time point. In GB40 irradiated cells Bax level increases at day 7 suggesting an activation of the apoptotic signaling (Figure 5G, bottom left panel). At day 14, 21 e 28 Bax levels remains higher with respect to untreated cells, but slightly reduced than day 7. In addition, GB40 cells triggered the expression of the Bcl-2 protein (Figure 5G, middle left panel) in particular starting from day 14 suggesting that a population of GB40 cells activates an anti-apoptotic signaling. Bax expression in GB48 irradiated cells increased starting from day 1 and decreases at day 14 and 21 (Figure 5H, bottom right panel). GB48 cells already expresses the Bcl-2 protein in untreated cells, however it slightly increased after radiation treatment (Figure 5H, middle right panel). These data together suggested that a population of GBM senescent cells is able to activate a pro-survival signal in contrast to the apoptotic signal triggered by Bax protein.

A **GB40**



D **GB48**

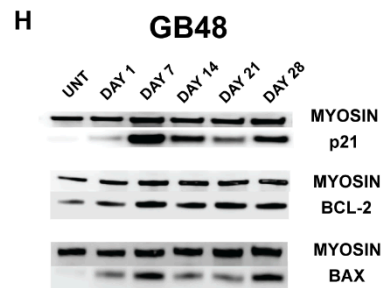
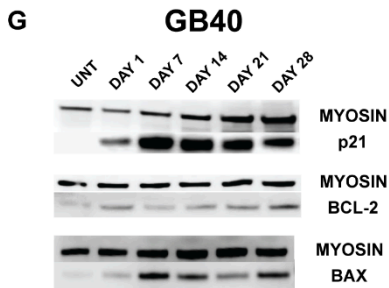
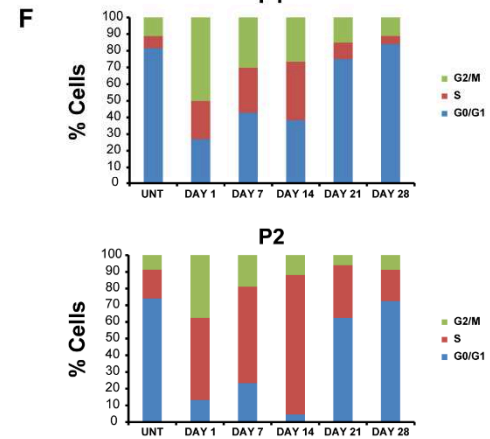
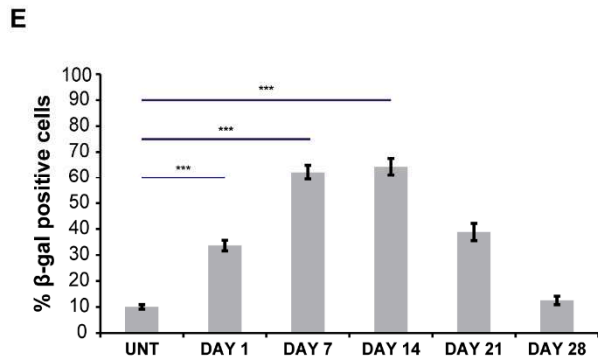
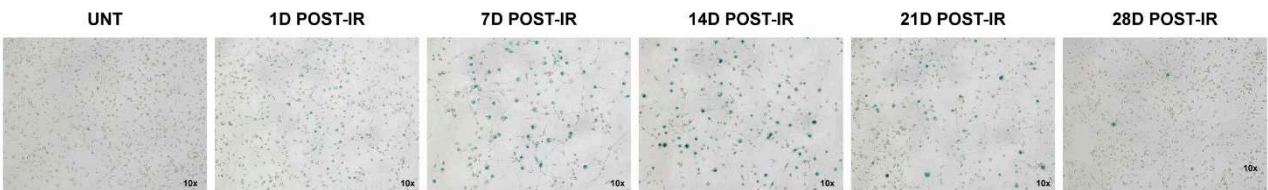


Figure 5. Radiation resistant GBM cells display a senescence phenotype. A-D. Representative brightfield images of untreated and irradiated GB40 and GB48 cells stained for β -galactosidase respectively. Magnification 4x and 10x. **B-E.** % of β -galactosidase positive cells expressed as the mean \pm SD for GB40 and GB48 cells respectively, at each time point. Data are represented as the mean \pm SD. **C-F.** Cell cycle distribution at each time point after radiation treatment of the two populations observed in both GB40 and GB48 cells were represented as percentage of cells in each phases of the cell cycle. **G-H.** Western blot analysis was used to evaluate p21, Bax and Bcl-2 protein levels in GB40 and GB48 cells respectively at each time point after radiation treatment. Myosin was used as housekeeping. Data were analyzed by Student T-test (* $p < 0.05$; ** $p < 0.01$; *** $p < 0.001$).

4.5 Radiation dynamically modifies P2X7R signaling in GBM cells during recovery from treatment

To further investigate the resistance mechanisms triggered by our GBM cells after radiation treatment, in particular regarding P2X7R signaling, expression levels of P2X7A and P2X7B isoforms were evaluated by Real-time PCR. P2X7B isoforms levels are significantly increased in GB40 and GB48 cells after radiation treatment compared to untreated cells ($p = 0.02$ and $p = 0.016$) respectively) at day 14 (Figure 6A), suggesting that radiation might both select clones those express P2X7B and/or induce the expression of this isoform in our GBM cells. In addition, P2X7A isoform expression in GB40 is downregulated starting from day 7 in irradiated cells (Figure 6A, left graph). In GB48 P2X7A expression is downregulated starting from day 14, and its expression returns comparable with untreated cells at day 28 (Figure 6A, right graph). P2X7B expression reach the maximum at day 14 in both GB40 and GB48. Expression levels of ENTPD1 and NT5E were also performed for each time point to investigate if GBM cells activate the ectonucleotidases CD39 and CD73 as an additional mechanism of resistance to radiation-released ATP (Figure 6A). A slight downregulation of both ENTPD1 and NT5E was observed in irradiated GB40 cells (Figure 6A). On the contrary, a slight upregulation of ENTPD1 is observed in GB48 cells till day 14 (Figure 6A, right graph). No significant modulation in NT5E gene was found in GB48 cells. Taken together these data suggested that our GBM cells did not significantly modulate their ectonucleotidases status.

Cholesterol is also important in regulation of P2X7R functionality. Indeed, in addition to increased P2X7B expression, a significant increase in the amount of cholesterol is measured in both cells. In particular in GB40 cells cholesterol concentration significantly grows till day 14, where irradiated

GB40 cells owned an higher amount of cholesterol than untreated cells ($0.35 \pm 0.06 \mu\text{M}$ vs $0.02 \pm 0.006 \mu\text{M}$) ($p=0.04$) (Figure 6B, left graph). The amount of cholesterol of irradiated GB40 cells returned comparable to untreated cells at day 28 ($0.08 \pm 0.03 \mu\text{M}$ vs $0.02 \pm 0.006 \mu\text{M}$). A significant increase in the total amount of cholesterol was also measured in GB48 cells, peaking at day 7, compared to untreated cells ($0.22 \pm 0.01 \mu\text{M}$ vs $0.05 \pm 0.01 \mu\text{M}$) ($p=0.007$) (Figure 6B, right graph). A slow decrease is observed after day 14, reaching at day 28 almost the level measured in untreated cells ($0.07 \pm 0.001 \mu\text{M}$ vs $0.05 \pm 0.01 \mu\text{M}$) (Figure 6B).

Since in both GBM cells day 7 and day 14 seemed to be crucial in the response to radiation treatment, we checked alterations in inflammasome caspase-1 activity, one of the main pathways activated by P2X7R. Activity of caspase-1 enzyme significantly increased in irradiated GB40 cells at day 7 and 14 compared to the untreated cells ($p=0.009$ and $p=0.008$ respectively) (Figure 6C, left graph). In GB48 caspase-1 seemed more active than in GB40 (Figure 6C). A significant increment in caspase-1 activity was observed both at day 7 and day 14 in GB48 irradiated cells compared to untreated cells ($p=0.05$ and $p=0.007$ respectively) (Figure 6C, right graph). These data seem to suggest that inflammasome activity might be involved in radiation-induced cell death of both our GBM cells. Further investigations has to be done in order to confirm this hypothesis.

Finally to confirm that P2X7R signaling is an important mechanism of resistance to radiation treatment, GBM cells were treated in combination with radiation and anti-P2X7R antagonists. A significant reduction of the survival fraction of GB40 cells was observed in cells treated with AZ10606120 ($10 \mu\text{M}$) and radiation (7.5 Gy) compared to radiation alone (0.10 ± 0.004 vs 0.19 ± 0.005) ($p=0.002$) (Figure 6D, left graph). Combination treatment with A740003 ($20 \mu\text{M}$) resulted even more effective (0.07 ± 0.001 vs 0.19 ± 0.005) ($p=0.006$). In GB48 cells the concomitant treatment with AZ10606120 ($10 \mu\text{M}$) and radiation seemed more effective than what observed in GB40 cells with a significant reduction of the survival fraction to 0.09 ± 0.002 compared to radiation alone (Figure 6D, right graph). The treatment in combination with A740003 ($20 \mu\text{M}$) have also significantly reduced the survival fraction of GB48 cells compared to radiation treatment alone (0.08 ± 0.003 vs 0.21 ± 0.005) ($p=0.002$).

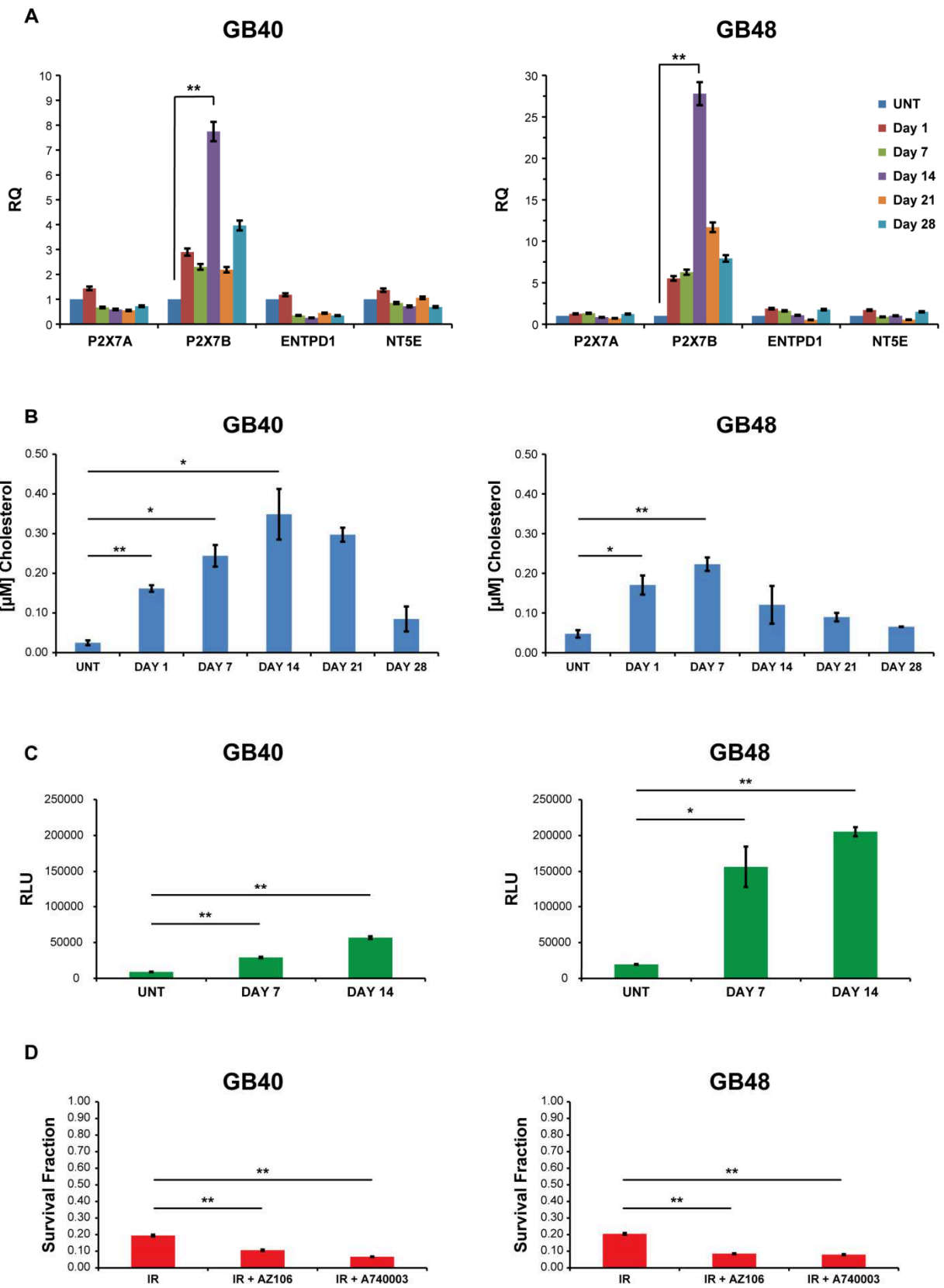


Figure 6. Radiation dynamically modifies P2X7R signaling in GBM cells during recovery from treatment. **A.** mRNA expression levels of P2X7A, P2X7B, ENTPD1 and NT5E genes in GB40 and GB48 cells at each time point respect to untreated cells and normalized to HPRT-1 and GAPDH housekeeping. **B.** Total amount of cholesterol expressed in μM concentration in GB40 and GB48 cells at each time point compared to untreated cells. **C.** Caspase-1 enzyme activity expresses in RLU in GB40 and GB48 cells at day 7 and day 14 after radiation treatment compared to untreated cells. **D.** Soft-agar assay was used to evaluate long term effects of radiation treatment combined with anti-P2X7R antagonists in GBM cells. Data are represented as Mean \pm SD. Data were analyzed by Student T-test (* $p < 0.05$; ** $p < 0.01$; *** $p < 0.001$).

Discussion

The current gold standard treatment for GBM is surgery followed by radiotherapy and chemotherapy with TMZ [57] but unfortunately this approach is largely ineffective, showing poor success in patient survival [12]. Indeed GBM remains a lethal and incurable tumor, as the median survival for patients is 12-18 months and the majority of them dies within two years [12]. Discovery of new potential therapeutic targets as well as the development of more effective strategies in the standard clinical practice is urgently needed to improve survival of GBM patients and to increase their quality of life. Recently the role of P2X7R in cancer has attracted great interest for its role both in tumor growth and in shaping stromal-immune response in TME [213]. ATP, the physiological ligand of P2X7R, is released in TME by cancer cells and stromal cells and its concentration further increases in response to cellular stresses like hypoxia or chemo- and radiation treatments, reaching several hundreds of $\mu\text{mol/l}$ [210-211]. Once engaged by ATP, P2X7R can trigger cell death or promote growth, depending on its levels of activation and on the cell type considered [234, 274]. The role of P2X7R in GBM is still under debate since contrasting data are reported in literature. Recent studies have reported that stimulation of P2X7R in glioma cells is associated with increased proliferation, migration and release of proinflammatory and neoangiogenic factors *in vitro* [330-332]. In addition the treatment with anti-P2X7R has inhibited tumor growth in C6 glioma model *in vivo* [333]. On the contrary it was also reported that silencing or pharmacologically inhibiting P2X7R increased *in vitro* and *in vivo* tumor growth in GL261 glioma cells and C6 glioma model, respectively [334-335]. In our study we showed that patient-derived GBM cells express different levels and isoforms of P2X7R with high prevalence of the P2X7B isoform, that lack of the large pore function. In our study we further demonstrate that GBM cells derived from different patients owned P2X7R with different functionality, based on the amount and on the isoform expressed. This results in a differential response to P2X7R stimulation observed in GB40 and GB48, as GB40 displays both cation-channel and large pore activity while GB48 retains only cation-channel functionality and thus less sensitivity to receptor stimulation. To strengthen and support our hypothesis we observed that exposure to ATP induces acute cell death in GB40 cells but not in GB48 cells. These data together are in line with the nature of GBM tumors those are highly heterogeneous and for this reason the expression levels of P2X7R and its function can greatly vary among different patients. In addition, our data might also be helpful to explain the opposite results reported in literature, those describe the role of P2X7R as controversial, probably due to the differences in isoforms and levels of P2X7R expressed in the different cellular or mice models used. Furthermore our data suggest that treatment with anti-P2X7R antagonists alone do not

deeply affect GBM tumor growth, acting principally in slowing GBM cells proliferation and, again, the response seems dependent on the amount and isoforms of P2X7R expressed. Previous similar data are reported in literature where no significant effects were observed on U251 cells or human glioblastoma stem cells exposed to selective P2X7R antagonists or to apyrase *in vitro* [336]. Taken together our data highlighted the importance of P2X7R in GBM biology affecting cell proliferation and eventually activating cell death, therefore a more accurate analysis of its functional activity has to be done for each individual case when such heterogeneous and plastic tumors are investigated. However, the main issue remains the treatment of GBM patients. Despite many tumors respond to standard treatment at the beginning, almost all patients with GBM recur; indeed the median time to progression is 6.9 months [57]. Resistance to standard therapy of GBM cells is a major clinical issue, limiting the success of the treatment. In particular, resistance to radiation treatment is a crucial point of interest, as it represents, together with surgery, the most important and effective therapy for these patients. Thus, unravelling the mechanisms underlying radiation resistance is essential to develop more effective therapeutic strategies. It is well known that many different pathways are significantly altered after radiotherapy [337]. In the past years, several studies aimed to understand the molecular and genetic basis involved in tumor radiosensitivity [325]. DNA variants as well as activation of several DNA repair systems might contribute to radioresistance, for this reason targeting these pathways may be used to increase the tumors sensitivity to radiation. In this study, we aimed to understand how radiation therapy affects GBM cells, focusing on P2X7R signaling alterations. We demonstrated that radiation treatment induce massive cell death in our GBM cells those express functional P2X7R, killing almost the 80% of cells in both our models. Radiation-induced GBM cell death is time-dependent, reaching the maximum after 7 and 14 days from the treatment and it is associated to the release of ATP in cell culture medium, with concomitant activation of the pro-apoptotic protein Bax. These findings are in tandem with a reduction in P2X7RA isoform expression in GBM cells after radiation treatment suggesting that GBM clones those express high levels of P2X7RA are more sensitive to radiation and are preferentially killed by this treatment, partially by the accumulation of ATP released in culture. These data are consistent with previous data published in literature where P2X7R gene is considered as a radiation-responsive gene, showing that an high and full functional expression of P2X7R in GBM cells is associated to a successful response to radiotherapy [325]. The main clinical issue remains the relapse after treatment in these patients and what happens in the period of time between the end of the radiation treatment and tumor recurrence. In order to address this question we followed GBM cells for almost one month after radiation treatment with the objective to understand how the P2X7R-dependent mechanisms are altered in response to radiation treatment.

We observed that GBM cells underwent to a transient senescent phenotype that became predominant after 7 and 14 days from the treatment. Senescent cells express high levels of p21 protein, a potent cyclin-dependent kinase inhibitor that binds and inhibits the activity of several cyclin-CDK complexes, functioning as a regulator of cell cycle progression [338]. Its activation contributes to accumulation of irradiated GBM cells in phase S/G2. Cells in this temporary senescent state are able to recover from radiation-induced DNA damage, restoring completely DNA integrity and leaving the senescent state at day 28. Surviving cells activate also the anti-apoptotic Bcl-2 protein in contrast to the pro-apoptotic signals triggered by Bax. Caspase-1 activity is also significantly increased at day 7 and 14 in both GBM cells, suggesting the activation of inflammasome. P2X7R is a major driver of inflammasome activation, but its association to radiation treatment response in our GBM cells remains to be fully investigated. It may act inducing the secretion of pro-inflammatory cytokines by GBM senescent cells or activating cell death by pyroptosis. P2X7RB isoform became predominant in GBM resistant senescent cells especially at day 7 and 14, the critical time points in radiation response in our models. GBM resistant senescent cells those express P2X7RB are probably protected from the high amount of ATP released after radiation treatment, eventually taking advantage for recovery. Coupled with increased P2X7RB expression, GBM resistant senescent cells increased the amount of membrane cholesterol, strongly affecting receptor functionality through the interaction with the transmembrane helix [311]. Such alterations of P2X7R functionality and expression seemed to be highly and dynamically regulated, highlighting the high plasticity of GBM cells in escaping radiation-induced death. Indeed P2X7RB and cholesterol levels decreased when GBM cells are completely recovered. Since several antagonists against P2X7R are currently available, we also tried a combination with radiation treatment to prove that P2X7R signaling is important for radio-resistant GBM cells. Indeed we demonstrated that combination treatment significantly affects survival of both GBM cells tested compared to radiation alone. These data suggest that coupling P2X7R antagonists to radiation might be important to eradicate GBM senescent resistant cells those modify P2X7R functionality to survive. Taken together these data have highlighted a new mechanism of resistance to radiation triggered by GBM cells to escape the radiation-induced cell death mediated by P2X7R, opening also a new possible application of anti-P2X7R treatment in combination with radiotherapy for such tumors.

Further experiments have to be performed, in order to strikingly prove that senescent GBM cells alter their P2X7R signaling to escape cell death. New approach of single cell analysis might be helpful to discriminate the populations of sensitive and resistant GBM cells and how they shape the P2X7R signaling to survive. Nonetheless, *in vivo* experiments are necessary to validate the

suggested resistance mechanisms. In such a more complex scenario, the role of P2X7R in both stromal and tumor cells have to be elucidated in response to radiation treatment, considering how deeply TME affects tumor behavior.

Bibliography

1. Louis DN, Ohgaki H, Wiestler OD, Cavenee WK. The 2016 WHO classification of tumors of the central nervous system. Lyon, France: IARC Press, 2016.
2. Ostrom QT, Gittleman H, Liao P, Vecchione-Koval T, Wolinsky Y, Kruchko C, Barnholtz-Sloan JS. CBTRUS Statistical Report: Primary brain and other central nervous system tumors diagnosed in the United States in 2010-2014. *Neuro Oncol.* 2017 Nov 6;19(suppl_5):v1-v88.
3. Nakada M, Kita D, Watanabe T, Hayashi Y, Teng L, Pyko IV, Hamada J. Aberrant signaling pathways in glioma. *Cancers (Basel).* 2011 Aug 10;3(3):3242-78.
4. Chakrabarti I, Cockburn M, Cozen W, Wang YP, Preston-Martin S. A population-based description of glioblastoma multiforme in Los Angeles County, 1974-1999. *Cancer.* 2005 Dec 15;104(12):2798-806.
5. Kleihues P, Louis DN, Scheithauer BW, Rorke LB, Reifenberger G, Burger PC, Cavenee WK. The WHO classification of tumors of the nervous system. *J Neuropathol Exp Neurol.* 2002 Mar;61(3):215-25; discussion 226-9.
6. Engelhard HH, Villano JL, Porter KR, Stewart AK, Barua M, Barker FG, Newton HB. Clinical presentation, histology, and treatment in 430 patients with primary tumors of the spinal cord, spinal meninges, or cauda equina. *J Neurosurg Spine.* 2010 Jul;13(1):67-77.
7. Babu R, Sharma R, Karikari IO, Owens TR, Friedman AH, Adamson C. Outcome and prognostic factors in adult cerebellar glioblastoma. *J Clin Neurosci.* 2013 Aug;20(8):1117-21.
8. Utsuki S, Oka H, Miyajima Y, Kijima C, Yasui Y, Fujii K. Adult cerebellar glioblastoma cases have different characteristics from supratentorial glioblastoma. *Brain Tumor Pathol.* 2012 Apr;29(2):87-95.
9. Weber DC, Miller RC, Villà S, Hanssens P, Baumert BG, Castadot P, Varlet P, Abacioglu U, Igdem S, Szutowicz E, Nishioka H, Hofer S, Rutz HP, Ozsahin M, Taghian A, Mirimanoff RO. Outcome and prognostic factors in cerebellar glioblastoma multiforme in adults: a retrospective study from the Rare Cancer Network. *Int J Radiat Oncol Biol Phys.* 2006 Sep 1;66(1):179-86.
10. Zito JL, Siva A, Smith TW, Leeds M, Davidson R. Glioblastoma of the cerebellum. Computed tomographic and pathologic considerations. *Surg Neurol.* 1983 Apr;19(4):373-8.
11. Konar SK, Maiti TK, Bir SC, Kalakoti P, Bollam P, Nanda A. Predictive Factors Determining the Overall Outcome of Primary Spinal Glioblastoma Multiforme: An Integrative Survival Analysis. *World Neurosurg.* 2016 Feb;86:341-8.e1-3.

12. Wen PY, Kesari S. Malignant gliomas in adults. *N Engl J Med*. 2008 Jul 31;359(5):492-507.
13. Fisher JL, Schwartzbaum JA, Wrensch M, Wiemels JL. Epidemiology of brain tumors. *Neurol Clin*. 2007 Nov;25(4):867-90, vii.
14. Farrell CJ, Plotkin SR. Genetic causes of brain tumors: neurofibromatosis, tuberous sclerosis, von Hippel-Lindau, and other syndromes. *Neurol Clin*. 2007 Nov;25(4):925-46, viii.
15. Ohgaki H, Kleihues P. Genetic pathways to primary and secondary glioblastoma. *Am J Pathol*. 2007 May;170(5):1445-53.
16. Sturm D, Bender S, Jones DT, Lichter P, Grill J, Becher O, Hawkins C, Majewski J, Jones C, Costello JF, Iavarone A, Aldape K, Brennan CW, Jabadó N, Pfister SM. Paediatric and adult glioblastoma: multiform (epi)genomic culprits emerge. *Nat Rev Cancer*. 2014 Feb;14(2):92-107.
17. Ohgaki H, Dessen P, Jourde B, Horstmann S, Nishikawa T, Di Patre PL, Burkhard C, Schüler D, Probst-Hensch NM, Maiorka PC, Baeza N, Pisani P, Yonekawa Y, Yasargil MG, Lütolf UM, Kleihues P. Genetic pathways to glioblastoma: a population-based study. *Cancer Res*. 2004 Oct 1;64(19):6892-9.
18. Ohgaki H, Kleihues P. Population-based studies on incidence, survival rates, and genetic alterations in astrocytic and oligodendroglial gliomas. *J Neuropathol Exp Neurol*. 2005 Jun;64(6):479-89.
19. DeAngelis LM. Brain tumors. *N Engl J Med*. 2001 Jan 11;344(2):114-23.
20. Vecht CJ, Kerkhof M, Duran-Pena A. Seizure prognosis in brain tumors: new insights and evidence-based management. *Oncologist*. 2014 Jul;19(7):751-9. doi: 10.1634/theoncologist.2014-0060.
21. Eoli M, Menghi F, Bruzzone MG, De Simone T, Valletta L, Pollo B, Bissola L, Silvani A, Bianchessi D, D'Incerti L, Filippini G, Broggi G, Boiardi A, Finocchiaro G. Methylation of O6-methylguanine DNA methyltransferase and loss of heterozygosity on 19q and/or 17p are overlapping features of secondary glioblastomas with prolonged survival. *Clin Cancer Res*. 2007 May 1;13(9):2606-13.
22. Lai A, Kharbanda S, Pope WB, Tran A, Solis OE, Peale F, Forrest WF, Pujara K, Carrillo JA, Pandita A, Ellingson BM, Bowers CW, Soriano RH, Schmidt NO, Mohan S, Yong WH, Seshagiri S, Modrusan Z, Jiang Z, Aldape KD, Mischel PS, Liau LM, Escovedo CJ, Chen W, Nghiemphu PL, James CD, Prados MD, Westphal M, Lamszus K, Cloughesy T, Phillips HS. Evidence for sequenced molecular evolution of IDH1 mutant glioblastoma from a

- distinct cell of origin. *J Clin Oncol*. 2011 Dec 1;29(34):4482-90. doi: 10.1200/JCO.2010.33.8715.
23. Burger PC, Kleihues P. Cytologic composition of the untreated glioblastoma with implications for evaluation of needle biopsies. *Cancer*. 1989 May 15;63(10):2014-23.
 24. Verhaak RG, Hoadley KA, Purdom E, Wang V, Qi Y, Wilkerson MD, Miller CR, Ding L, Golub T, Mesirov JP, Alexe G, Lawrence M, O'Kelly M, Tamayo P, Weir BA, Gabriel S, Winckler W, Gupta S, Jakkula L, Feiler HS, Hodgson JG, James CD, Sarkaria JN, Brennan C, Kahn A, Spellman PT, Wilson RK, Speed TP, Gray JW, Meyerson M, Getz G, Perou CM, Hayes DN; Cancer Genome Atlas Research Network. Integrated genomic analysis identifies clinically relevant subtypes of glioblastoma characterized by abnormalities in PDGFRA, IDH1, EGFR, and NF1. *Cancer Cell*. 2010 Jan 19;17(1):98-110. doi: 10.1016/j.ccr.2009.12.020.
 25. Fuller GN, Bigner SH. Amplified cellular oncogenes in neoplasms of the human central nervous system. *Mutat Res*. 1992 May;276(3):299-306.
 26. Francis JM, Zhang CZ, Maire CL, Jung J, Manzo VE, Adalsteinsson VA, Homer H, Haidar S, Blumenstiel B, Peadamallu CS, Ligon AH, Love JC, Meyerson M, Ligon KL. EGFR variant heterogeneity in glioblastoma resolved through single-nucleus sequencing. *Cancer Discov*. 2014 Aug;4(8):956-71. doi: 10.1158/2159-8290.CD-13-0879.
 27. Brennan CW, Verhaak RG, McKenna A, Campos B, Nounshmehr H, Salama SR, Zheng S, Chakravarty D, Sanborn JZ, Berman SH, Beroukheim R, Bernard B, Wu CJ, Genovese G, Shmulevich I, Barnholtz-Sloan J, Zou L, Vegesna R, Shukla SA, Ciriello G, Yung WK, Zhang W, Sougnez C, Mikkelsen T, Aldape K, Bigner DD, Van Meir EG, Prados M, Sloan A, Black KL, Eschbacher J, Finocchiaro G, Friedman W, Andrews DW, Guha A, Iacocca M, O'Neill BP, Foltz G, Myers J, Weisenberger DJ, Penny R, Kucherlapati R, Perou CM, Hayes DN, Gibbs R, Marra M, Mills GB, Lander E, Spellman P, Wilson R, Sander C, Weinstein J, Meyerson M, Gabriel S, Laird PW, Haussler D, Getz G, Chin L; TCGA Research Network. The somatic genomic landscape of glioblastoma. *Cell*. 2013 Oct 10;155(2):462-77. doi: 10.1016/j.cell.2013.09.034.
 28. Ciardiello F, Tortora G. A novel approach in the treatment of cancer: targeting the epidermal growth factor receptor. *Clin Cancer Res*. 2001 Oct;7(10):2958-70.
 29. Mizoguchi M, Nutt CL, Mohapatra G, Louis DN. Genetic alterations of phosphoinositide 3-kinase subunit genes in human glioblastomas. *Brain Pathol*. 2004 Oct;14(4):372-7.
 30. Mueller W, Mizoguchi M, Silen E, D'Amore K, Nutt CL, Louis DN. Mutations of the PIK3CA gene are rare in human glioblastoma. *Acta Neuropathol*. 2005 Jun;109(6):654-5.

31. Tohma Y, Gratas C, Biernat W, Peraud A, Fukuda M, Yonekawa Y, Kleihues P, Ohgaki H. PTEN (MMAC1) mutations are frequent in primary glioblastomas (de novo) but not in secondary glioblastomas. *J Neuropathol Exp Neurol*. 1998 Jul;57(7):684-9.
32. Cancer Genome Atlas Research Network. Comprehensive genomic characterization defines human glioblastoma genes and core pathways. *Nature*. 2008 Oct 23;455(7216):1061-8. doi: 10.1038/nature07385.
33. Watanabe K, Tachibana O, Sata K, Yonekawa Y, Kleihues P, Ohgaki H. Overexpression of the EGF receptor and p53 mutations are mutually exclusive in the evolution of primary and secondary glioblastomas. *Brain Pathol*. 1996 Jul;6(3):217-23; discussion 23-4.
34. Biernat W, Kleihues P, Yonekawa Y, Ohgaki H. Amplification and overexpression of MDM2 in primary (de novo) glioblastomas. *J Neuropathol Exp Neurol*. 1997 Feb;56(2):180-5.
35. Biernat W, Tohma Y, Yonekawa Y, Kleihues P, Ohgaki H. Alterations of cell cycle regulatory genes in primary (de novo) and secondary glioblastomas. *Acta Neuropathol*. 1997 Oct;94(4):303-9.
36. Ueki K, Ono Y, Henson JW, Efird JT, von Deimling A, Louis DN. CDKN2/p16 or RB alterations occur in the majority of glioblastomas and are inversely correlated. *Cancer Res*. 1996 Jan 1;56(1):150-3.
37. Nakamura M, Watanabe T, Klangby U, Asker C, Wiman K, Yonekawa Y, Kleihues P, Ohgaki H. p14ARF deletion and methylation in genetic pathways to glioblastomas. *Brain Pathol*. 2001 Apr;11(2):159-68.
38. Nakamura M, Yonekawa Y, Kleihues P, Ohgaki H. Promoter hypermethylation of the RB1 gene in glioblastomas. *Lab Invest*. 2001 Jan;81(1):77-82.
39. Killela PJ, Reitman ZJ, Jiao Y, Bettegowda C, Agrawal N, Diaz LA Jr, Friedman AH, Friedman H, Gallia GL, Giovanella BC, Grollman AP, He TC, He Y, Hruban RH, Jallo GI, Mandahl N, Meeker AK, Mertens F, Netto GJ, Rasheed BA, Riggins GJ, Rosenquist TA, Schiffman M, Shih IeM, Theodorescu D, Torbenson MS, Velculescu VE, Wang TL, Wentzensen N, Wood LD, Zhang M, McLendon RE, Bigner DD, Kinzler KW, Vogelstein B, Papadopoulos N, Yan H. TERT promoter mutations occur frequently in gliomas and a subset of tumors derived from cells with low rates of self-renewal. *Proc Natl Acad Sci U S A*. 2013 Apr 9;110(15):6021-6. doi: 10.1073/pnas.1303607110.
40. Bell RJ, Rube HT, Kreig A, Mancini A, Fouse SD, Nagarajan RP, Choi S, Hong C, He D, Pekmezci M, Wiencke JK, Wrensch MR, Chang SM, Walsh KM, Myong S, Song JS, Costello JF. Cancer. The transcription factor GABP selectively binds and activates the

- mutant TERT promoter in cancer. *Science*. 2015 May 29;348(6238):1036-9. doi: 10.1126/science.aab0015.
41. Suvà ML, Riggi N, Bernstein BE. Epigenetic reprogramming in cancer. *Science*. 2013 Mar 29;339(6127):1567-70. doi: 10.1126/science.1230184.
 42. Suvà ML, Rheinbay E, Gillespie SM, Patel AP, Wakimoto H, Rabkin SD, Riggi N, Chi AS, Cahill DP, Nahed BV, Curry WT, Martuza RL, Rivera MN, Rossetti N, Kasif S, Beik S, Kadri S, Tirosh I, Wortman I, Shalek AK, Rozenblatt-Rosen O, Regev A, Louis DN, Bernstein BE. Reconstructing and reprogramming the tumor-propagating potential of glioblastoma stem-like cells. *Cell*. 2014 Apr 24;157(3):580-94. doi: 10.1016/j.cell.2014.02.030.
 43. de Vries NA, Hulsman D, Akhtar W, de Jong J, Miles DC, Blom M, van Tellingen O, Jonkers J, van Lohuizen M. Prolonged Ezh2 Depletion in Glioblastoma Causes a Robust Switch in Cell Fate Resulting in Tumor Progression. *Cell Rep*. 2015 Jan 20;10(3):383-397. doi: 10.1016/j.celrep.2014.12.028.
 44. Gerson SL. MGMT: its role in cancer aetiology and cancer therapeutics. *Nat Rev Cancer*. 2004 Apr;4(4):296-307.
 45. Hegi ME, Liu L, Herman JG, Stupp R, Wick W, Weller M, Mehta MP, Gilbert MR. Correlation of O6-methylguanine methyltransferase (MGMT) promoter methylation with clinical outcomes in glioblastoma and clinical strategies to modulate MGMT activity. *J Clin Oncol*. 2008 Sep 1;26(25):4189-99. doi: 10.1200/JCO.2007.11.5964.
 46. Sottoriva A, Spiteri I, Piccirillo SG, Touloumis A, Collins VP, Marioni JC, Curtis C, Watts C, Tavaré S. Intratumor heterogeneity in human glioblastoma reflects cancer evolutionary dynamics. *Proc Natl Acad Sci U S A*. 2013 Mar 5;110(10):4009-14. doi: 10.1073/pnas.1219747110.
 47. Patel AP, Tirosh I, Trombetta JJ, Shalek AK, Gillespie SM, Wakimoto H, Cahill DP, Nahed BV, Curry WT, Martuza RL, Louis DN, Rozenblatt-Rosen O, Suvà ML, Regev A, Bernstein BE. Single-cell RNA-seq highlights intratumoral heterogeneity in primary glioblastoma. *Science*. 2014 Jun 20;344(6190):1396-401. doi: 10.1126/science.1254257.
 48. Wang Q, Hu B, Hu X, Kim H, Squatrito M, Scarpace L, deCarvalho AC, Lyu S, Li P, Li Y, Barthel F, Cho HJ, Lin YH, Satani N, Martinez-Ledesma E, Zheng S, Chang E, Sauv e CG, Olar A, Lan ZD, Finocchiaro G, Phillips JJ, Berger MS, Gabrusiewicz KR, Wang G, Eskilsson E, Hu J, Mikkelsen T, DePinho RA, Muller F, Heimberger AB, Sulman EP, Nam DH, Verhaak RGW. Tumor Evolution of Glioma-Intrinsic Gene Expression Subtypes

- Associates with Immunological Changes in the Microenvironment. *Cancer Cell*. 2017 Jul 10;32(1):42-56.e6. doi: 10.1016/j.ccell.2017.06.003.
49. Neftel C, Laffy J, Filbin MG, Hara T, Shore ME, Rahme GJ, Richman AR, Silverbush D, Shaw ML, Hebert CM, Dewitt J, Gritsch S, Perez EM, Gonzalez Castro LN, Lan X, Druck N, Rodman C, Dionne D, Kaplan A, Bertalan MS, Small J, Pelton K, Becker S, Bonal D, Nguyen QD, Servis RL, Fung JM, Mylvaganam R, Mayr L, Gojo J, Haberler C, Geyeregger R, Czech T, Slavic I, Nahed BV, Curry WT, Carter BS, Wakimoto H, Brastianos PK, Batchelor TT, Stemmer-Rachamimov A, Martinez-Lage M, Frosch MP, Stamenkovic I, Riggi N, Rheinbay E, Monje M, Rozenblatt-Rosen O, Cahill DP, Patel AP, Hunter T, Verma IM, Ligon KL, Louis DN, Regev A, Bernstein BE, Tirosh I, Suvà ML. An Integrative Model of Cellular States, Plasticity, and Genetics for Glioblastoma. *Cell*. 2019 Aug 8;178(4):835-849.e21. doi: 10.1016/j.cell.2019.06.024.
50. Stupp R, Brada M, van den Bent MJ, Tonn JC, Pentheroudakis G; ESMO Guidelines Working Group. High-grade glioma: ESMO Clinical Practice Guidelines for diagnosis, treatment and follow-up. *Ann Oncol*. 2014 Sep;25 Suppl 3:iii93-101. doi: 10.1093/annonc/mdu050.
51. Lacroix M, Abi-Said D, Fourney DR, Gokaslan ZL, Shi W, DeMonte F, Lang FF, McCutcheon IE, Hassenbusch SJ, Holland E, Hess K, Michael C, Miller D, Sawaya R. A multivariate analysis of 416 patients with glioblastoma multiforme: prognosis, extent of resection, and survival. *J Neurosurg*. 2001 Aug;95(2):190-8.
52. Weller M, Stupp R, Reifenberger G, Brandes AA, van den Bent MJ, Wick W, Hegi ME. MGMT promoter methylation in malignant gliomas: ready for personalized medicine? *Nat Rev Neurol*. 2010 Jan;6(1):39-51. doi: 10.1038/nrneurol.2009.197.
53. Stummer W, Pichlmeier U, Meinel T, Wiestler OD, Zanella F, Reulen HJ; ALA-Glioma Study Group. Fluorescence-guided surgery with 5-aminolevulinic acid for resection of malignant glioma: a randomised controlled multicentre phase III trial. *Lancet Oncol*. 2006 May;7(5):392-401.
54. Walker MD, Green SB, Byar DP, Alexander E Jr, Batzdorf U, Brooks WH, Hunt WE, MacCarty CS, Mahaley MS Jr, Mealey J Jr, Owens G, Ransohoff J 2nd, Robertson JT, Shapiro WR, Smith KR Jr, Wilson CB, Strike TA. Randomized comparisons of radiotherapy and nitrosoureas for the treatment of malignant glioma after surgery. *N Engl J Med*. 1980 Dec 4;303(23):1323-9.

55. Liao G, Zhao Z, Yang H, Li X. Efficacy and Safety of Hypofractionated Radiotherapy for the Treatment of Newly Diagnosed Glioblastoma Multiforme: A Systematic Review and Meta-Analysis. *Front Oncol.* 2019 Oct 14;9:1017. doi: 10.3389/fonc.2019.01017.
56. Reddy K, Damek D, Gaspar LE, Ney D, Waziri A, Lillehei K, Stuhr K, Kavanagh BD, Chen C. Phase II trial of hypofractionated IMRT with temozolomide for patients with newly diagnosed glioblastoma multiforme. *Int J Radiat Oncol Biol Phys.* 2012 Nov 1;84(3):655-60. doi: 10.1016/j.ijrobp.2012.01.035.
57. Stupp R, Mason WP, van den Bent MJ, Weller M, Fisher B, Taphoorn MJ, Belanger K, Brandes AA, Marosi C, Bogdahn U, Curschmann J, Janzer RC, Ludwin SK, Gorlia T, Allgeier A, Lacombe D, Cairncross JG, Eisenhauer E, Mirimanoff RO; European Organisation for Research and Treatment of Cancer Brain Tumor and Radiotherapy Groups; National Cancer Institute of Canada Clinical Trials Group. Radiotherapy plus concomitant and adjuvant temozolomide for glioblastoma. *N Engl J Med.* 2005 Mar 10;352(10):987-96.
58. Stupp R, Hegi ME, Mason WP, van den Bent MJ, Taphoorn MJ, Janzer RC, Ludwin SK, Allgeier A, Fisher B, Belanger K, Hau P, Brandes AA, Gijtenbeek J, Marosi C, Vecht CJ, Mokhtari K, Wesseling P, Villa S, Eisenhauer E, Gorlia T, Weller M, Lacombe D, Cairncross JG, Mirimanoff RO; European Organisation for Research and Treatment of Cancer Brain Tumour and Radiation Oncology Groups; National Cancer Institute of Canada Clinical Trials Group. Effects of radiotherapy with concomitant and adjuvant temozolomide versus radiotherapy alone on survival in glioblastoma in a randomised phase III study: 5-year analysis of the EORTC-NCIC trial. *Lancet Oncol.* 2009 May;10(5):459-66. doi: 10.1016/S1470-2045(09)70025-7.
59. Zhang J, Stevens MF, Bradshaw TD. Temozolomide: mechanisms of action, repair and resistance. *Curr Mol Pharmacol.* 2012 Jan;5(1):102-14.
60. Wheelhouse RT, Stevens MFG. Decomposition of the antitumour drug Temozolomide in deuterated phosphate buffer: Methyl group transfer is accompanied by deuterium exchange. *J. Chem. Soc. Chem. Commun.* 1993;1993:1177. doi: 10.1039/c39930001177.
61. Hegi ME, Diserens AC, Gorlia T, Hamou MF, de Tribolet N, Weller M, Kros JM, Hainfellner JA, Mason W, Mariani L, Bromberg JE, Hau P, Mirimanoff RO, Cairncross JG, Janzer RC, Stupp R. MGMT gene silencing and benefit from temozolomide in glioblastoma. *N Engl J Med.* 2005 Mar 10;352(10):997-1003.
62. Weller M, Stupp R, Wick W. Epilepsy meets cancer: when, why, and what to do about it? *Lancet Oncol.* 2012 Sep;13(9):e375-82. doi: 10.1016/S1470-2045(12)70266-8.

63. Osuka S, Van Meir EG. Overcoming therapeutic resistance in glioblastoma: the way forward. *J Clin Invest*. 2017 Feb 1;127(2):415-426. doi: 10.1172/JCI89587.
64. Smith DR, Hardman JM, Earle KM. Contiguous glioblastoma multiforme and fibrosarcoma with extracranial metastasis. *Cancer*. 1969 Aug;24(2):270-6.
65. Sullivan JP, Nahed BV, Madden MW, Oliveira SM, Springer S, Bhore D, Chi AS, Wakimoto H, Rothenberg SM, Sequist LV, Kapur R, Shah K, Iafrate AJ, Curry WT, Loeffler JS, Batchelor TT, Louis DN, Toner M, Maheswaran S, Haber DA. Brain tumor cells in circulation are enriched for mesenchymal gene expression. *Cancer Discov*. 2014 Nov;4(11):1299-309. doi: 10.1158/2159-8290.CD-14-0471.
66. Alcantara Llaguno SR, Wang Z, Sun D, Chen J, Xu J, Kim E, Hatanpaa KJ, Raisanen JM, Burns DK, Johnson JE, Parada LF. Adult Lineage-Restricted CNS Progenitors Specify Distinct Glioblastoma Subtypes. *Cancer Cell*. 2015 Oct 12;28(4):429-440. doi: 10.1016/j.ccell.2015.09.007.
67. Jacques TS, Swales A, Brzozowski MJ, Henriquez NV, Linehan JM, Mirzadeh Z, O' Malley C, Naumann H, Alvarez-Buylla A, Brandner S. Combinations of genetic mutations in the adult neural stem cell compartment determine brain tumour phenotypes. *EMBO J*. 2010 Jan 6;29(1):222-35. doi: 10.1038/emboj.2009.327.
68. Chen J, Li Y, Yu TS, McKay RM, Burns DK, Kernie SG, Parada LF. A restricted cell population propagates glioblastoma growth after chemotherapy. *Nature*. 2012 Aug 23;488(7412):522-6. doi: 10.1038/nature11287.
69. Friedmann-Morvinski D, Bushong EA, Ke E, Soda Y, Marumoto T, Singer O, Ellisman MH, Verma IM. Dedifferentiation of neurons and astrocytes by oncogenes can induce gliomas in mice. *Science*. 2012 Nov 23;338(6110):1080-4. doi: 10.1126/science.1226929.
70. Bachoo RM, Maher EA, Ligon KL, Sharpless NE, Chan SS, You MJ, Tang Y, DeFrances J, Stover E, Weissleder R, Rowitch DH, Louis DN, DePinho RA. Epidermal growth factor receptor and Ink4a/Arf: convergent mechanisms governing terminal differentiation and transformation along the neural stem cell to astrocyte axis. *Cancer Cell*. 2002 Apr;1(3):269-77.
71. Lathia JD, Mack SC, Mulkearns-Hubert EE, Valentim CL, Rich JN. Cancer stem cells in glioblastoma. *Genes Dev*. 2015 Jun 15;29(12):1203-17. doi: 10.1101/gad.261982.115.
72. Osuka S, Sampetean O, Shimizu T, Saga I, Onishi N, Sugihara E, Okubo J, Fujita S, Takano S, Matsumura A, Saya H. IGF1 receptor signaling regulates adaptive radioprotection in glioma stem cells. *Stem Cells*. 2013 Apr;31(4):627-40. doi: 10.1002/stem.1328.

73. Kim Y, Kim KH, Lee J, Lee YA, Kim M, Lee SJ, Park K, Yang H, Jin J, Joo KM, Lee J, Nam DH. Wnt activation is implicated in glioblastoma radioresistance. *Lab Invest.* 2012 Mar;92(3):466-73. doi: 10.1038/labinvest.2011.161.
74. Zhang N, Wei P, Gong A, Chiu WT, Lee HT, Colman H, Huang H, Xue J, Liu M, Wang Y, Sawaya R, Xie K, Yung WK, Medema RH, He X, Huang S. FoxM1 promotes β -catenin nuclear localization and controls Wnt target-gene expression and glioma tumorigenesis. *Cancer Cell.* 2011 Oct 18;20(4):427-42. doi: 10.1016/j.ccr.2011.08.016.
75. Wang J, Wakeman TP, Lathia JD, Hjelmeland AB, Wang XF, White RR, Rich JN, Sullenger BA. Notch promotes radioresistance of glioma stem cells. *Stem Cells.* 2010 Jan;28(1):17-28. doi: 10.1002/stem.261.
76. Kim SH, Ezhilarasan R, Phillips E, Gallego-Perez D, Sparks A, Taylor D, Ladner K, Furuta T, Sabit H, Chhipa R, Cho JH, Mohyeldin A, Beck S, Kurozumi K, Kuroiwa T, Iwata R, Asai A, Kim J, Sulman EP, Cheng SY, Lee LJ, Nakada M, Guttridge D, DasGupta B, Goidts V, Bhat KP, Nakano I. Serine/Threonine Kinase MLK4 Determines Mesenchymal Identity in Glioma Stem Cells in an NF- κ B-dependent Manner. *Cancer Cell.* 2016 Feb 8;29(2):201-13. doi: 10.1016/j.ccell.2016.01.005.
77. Cao Y, Lathia JD, Eyler CE, Wu Q, Li Z, Wang H, McLendon RE, Hjelmeland AB, Rich JN. Erythropoietin Receptor Signaling Through STAT3 Is Required For Glioma Stem Cell Maintenance. *Genes Cancer.* 2010 Jan 1;1(1):50-61.
78. Ligon KL, Huillard E, Mehta S, Kesari S, Liu H, Alberta JA, Bachoo RM, Kane M, Louis DN, Depinho RA, Anderson DJ, Stiles CD, Rowitch DH. Olig2-regulated lineage-restricted pathway controls replication competence in neural stem cells and malignant glioma. *Neuron.* 2007 Feb 15;53(4):503-17.
79. Zbinden M, Duquet A, Lorente-Trigos A, Ngwabyt SN, Borges I, Ruiz i Altaba A. NANOG regulates glioma stem cells and is essential in vivo acting in a cross-functional network with GLI1 and p53. *EMBO J.* 2010 Aug 4;29(15):2659-74. doi: 10.1038/emboj.2010.137.
80. Ikushima H, Todo T, Ino Y, Takahashi M, Saito N, Miyazawa K, Miyazono K. Glioma-initiating cells retain their tumorigenicity through integration of the Sox axis and Oct4 protein. *J Biol Chem.* 2011 Dec 2;286(48):41434-41. doi: 10.1074/jbc.M111.300863.
81. Ikushima H, Todo T, Ino Y, Takahashi M, Miyazawa K, Miyazono K. Autocrine TGF-beta signaling maintains tumorigenicity of glioma-initiating cells through Sry-related HMG-box factors. *Cell Stem Cell.* 2009 Nov 6;5(5):504-14. doi: 10.1016/j.stem.2009.08.018.
82. Anido J, Sáez-Borderías A, González-Juncà A, Rodón L, Folch G, Carmona MA, Prieto-Sánchez RM, Barba I, Martínez-Sáez E, Prudkin L, Cuartas I, Raventós C, Martínez-Ricarte

- F, Poca MA, García-Dorado D, Lahn MM, Yingling JM, Rodón J, Sahuquillo J, Baselga J, Seoane J. TGF- β Receptor Inhibitors Target the CD44(high)/Id1(high) Glioma-Initiating Cell Population in Human Glioblastoma. *Cancer Cell*. 2010 Dec 14;18(6):655-68. doi: 10.1016/j.ccr.2010.10.023.
83. Bao S, Wu Q, McLendon RE, Hao Y, Shi Q, Hjelmeland AB, Dewhirst MW, Bigner DD, Rich JN. Glioma stem cells promote radioresistance by preferential activation of the DNA damage response. *Nature*. 2006 Dec 7;444(7120):756-60.
84. Jackson S, Meeks C, Vézina A, Robey RW, Tanner K, Gottesman MM. Model systems for studying the blood-brain barrier: Applications and challenges. *Biomaterials*. 2019 Sep;214:119217. doi: 10.1016/j.biomaterials.2019.05.028.
85. van Tellingen O1, Yetkin-Arik B, de Gooijer MC, Wesseling P, Wurdinger T, de Vries HE. Overcoming the blood-brain tumor barrier for effective glioblastoma treatment. *Drug Resist Updat*. 2015 Mar;19:1-12. doi: 10.1016/j.drug.2015.02.002.
86. Obermeier B, Daneman R, Ransohoff RM. Development, maintenance and disruption of the blood-brain barrier. *Nat Med*. 2013 Dec;19(12):1584-96. doi: 10.1038/nm.3407.
87. Abbott NJ, Rönnbäck L, Hansson E. Astrocyte-endothelial interactions at the blood-brain barrier. *Nat Rev Neurosci*. 2006 Jan;7(1):41-53.
88. Basseville A, Hall MD, Chau CH, Robey RW, Gottesman MM, Figg WD, Bates SE. The ABCG2 multidrug transporter M.A. George (Ed.), *ABC Transporters - 40 Years on*, Springer International Publishing, Cham (2016), pp. 195-226.
89. Banks WA. Characteristics of compounds that cross the blood-brain barrier. *BMC Neurol*. 2009 Jun 12;9 Suppl 1:S3. doi: 10.1186/1471-2377-9-S1-S3.
90. Harder BG, Blomquist MR, Wang J, Kim AJ, Woodworth GF, Winkles JA, Loftus JC, Tran NL. Developments in Blood-Brain Barrier Penetration and Drug Repurposing for Improved Treatment of Glioblastoma. *Front Oncol*. 2018 Oct 23;8:462. doi: 10.3389/fonc.2018.00462.
91. Iloff JJ, Wang M, Liao Y, Plogg BA, Peng W, Gundersen GA, Benveniste H, Vates GE, Deane R, Goldman SA, Nagelhus EA, Nedergaard M. A paravascular pathway facilitates CSF flow through the brain parenchyma and the clearance of interstitial solutes, including amyloid β . *Sci Transl Med*. 2012 Aug 15;4(147):147ra111. doi: 10.1126/scitranslmed.3003748.
92. Healy AT, Vogelbaum MA. Convection-enhanced drug delivery for gliomas. *Surg Neurol Int*. 2015 Feb 13;6(Suppl 1):S59-67. doi: 10.4103/2152-7806.151337.

93. Etame AB, Diaz RJ, Smith CA, Mainprize TG, Hynynen K, Rutka JT. Focused ultrasound disruption of the blood-brain barrier: a new frontier for therapeutic delivery in molecular neurooncology. *Neurosurg Focus*. 2012 Jan;32(1):E3. doi: 10.3171/2011.10.FOCUS11252.
94. Emerich DF, Snodgrass P, Dean R, Agostino M, Hasler B, Pink M, Xiong H, Kim BS, Bartus RT. Enhanced delivery of carboplatin into brain tumours with intravenous Cereport (RMP-7): dramatic differences and insight gained from dosing parameters. *Br J Cancer*. 1999 Jun;80(7):964-70.
95. Prados MD, Schold SC Jr, Fine HA, Jaeckle K, Hochberg F, Mechtler L, Fetell MR, Phuphanich S, Feun L, Janus TJ, Ford K, Graney W. A randomized, double-blind, placebo-controlled, phase 2 study of RMP-7 in combination with carboplatin administered intravenously for the treatment of recurrent malignant glioma. *Neuro Oncol*. 2003 Apr;5(2):96-103. doi: 10.1093/neuonc/5.2.96.
96. Alyautdin R, Khalin I, Nafeeza MI, Haron MH, Kuznetsov D. Nanoscale drug delivery systems and the blood-brain barrier. *Int J Nanomedicine*. 2014 Feb 7;9:795-811. doi: 10.2147/IJN.S52236.
97. Li Y, Wu M, Zhang N, Tang C, Jiang P, Liu X, Yan F, Zheng H. Mechanisms of enhanced antiglioma efficacy of polysorbate 80-modified paclitaxel-loaded PLGA nanoparticles by focused ultrasound. *J Cell Mol Med*. 2018 Sep;22(9):4171-4182. doi: 10.1111/jcmm.13695.
98. Cheng Y, Dai Q, Morshed RA, Fan X, Wegscheid ML, Wainwright DA, Han Y, Zhang L, Auffinger B, Tobias AL, Rincón E, Thaci B, Ahmed AU, Warnke PC, He C, Lesniak MS. Blood-brain barrier permeable gold nanoparticles: an efficient delivery platform for enhanced malignant glioma therapy and imaging. *Small*. 2014 Dec 29;10(24):5137-50. doi: 10.1002/smll.201400654.
99. Yang T, Martin P, Fogarty B, Brown A, Schurman K, Phipps R, Yin VP, Lockman P, Bai S. Exosome delivered anticancer drugs across the blood-brain barrier for brain cancer therapy in *Danio rerio*. *Pharm Res*. 2015 Jun;32(6):2003-14. doi: 10.1007/s11095-014-1593-y.
100. Drappatz J, Brenner A, Wong ET, Eichler A, Schiff D, Groves MD, Mikkelsen T, Rosenfeld S, Sarantopoulos J, Meyers CA, Fielding RM, Elian K, Wang X, Lawrence B, Shing M, Kelsey S, Castaigne JP, Wen PY. Phase I study of GRN1005 in recurrent malignant glioma. *Clin Cancer Res*. 2013 Mar 15;19(6):1567-76. doi: 10.1158/1078-0432.CCR-12-2481.
101. Quail DF, Joyce JA. The Microenvironmental Landscape of Brain Tumors. *Cancer Cell*. 2017 Mar 13;31(3):326-341. doi: 10.1016/j.ccell.2017.02.009.

102. Henrik Heiland D, Ravi VM, Behringer SP, Frenking JH, Wurm J, Joseph K, Garrelfs NWC, Strähle J, Heynckes S, Grauvogel J, Franco P, Mader I, Schneider M, Potthoff AL, Delev D, Hofmann UG, Fung C, Beck J, Sankowski R, Prinz M, Schnell O. Tumor-associated reactive astrocytes aid the evolution of immunosuppressive environment in glioblastoma. *Nat Commun.* 2019 Jun 11;10(1):2541. doi: 10.1038/s41467-019-10493-6.
103. Quail DF, Bowman RL, Akkari L, Quick ML, Schuhmacher AJ, Huse JT, Holland EC, Sutton JC, Joyce JA. The tumor microenvironment underlies acquired resistance to CSF-1R inhibition in gliomas. *Science.* 2016 May 20;352(6288):aad3018. doi: 10.1126/science.aad3018.
104. Matias D, Balça-Silva J, da Graça GC, Wanjiru CM, Macharia LW, Nascimento CP, Roque NR, Coelho-Aguiar JM, Pereira CM, Dos Santos MF, Pessoa LS, Lima FRS, Schanaider A, Ferrer VP; Tania Cristina Leite de Sampaio e Spohr, Moura-Neto V. Microglia/Astrocytes-Glioblastoma Crosstalk: Crucial Molecular Mechanisms and Microenvironmental Factors. *Front Cell Neurosci.* 2018 Aug 3;12:235. doi: 10.3389/fncel.2018.00235.
105. Meacham CE, Morrison SJ. Tumour heterogeneity and cancer cell plasticity. *Nature.* 2013 Sep 19;501(7467):328-37. doi: 10.1038/nature12624.
106. Mathew LK, Skuli N, Mucaj V, Lee SS, Zinn PO, Sathyan P, Imtiyaz HZ, Zhang Z, Davuluri RV, Rao S, Venneti S, Lal P, Lathia JD, Rich JN, Keith B, Minn AJ, Simon MC. miR-218 opposes a critical RTK-HIF pathway in mesenchymal glioblastoma. *Proc Natl Acad Sci U S A.* 2014 Jan 7;111(1):291-6. doi: 10.1073/pnas.1314341111.
107. Oushy S, Hellwinkel JE, Wang M, Nguyen GJ, Gunaydin D, Harland TA, Anchordoquy TJ, Graner MW. Glioblastoma multiforme-derived extracellular vesicles drive normal astrocytes towards a tumour-enhancing phenotype. *Philos Trans R Soc Lond B Biol Sci.* 2018 Jan 5;373(1737). pii: 20160477. doi: 10.1098/rstb.2016.0477.
108. Hambardzumyan D, Gutmann DH, Kettenmann H. The role of microglia and macrophages in glioma maintenance and progression. *Nat Neurosci.* 2016 Jan;19(1):20-7. doi: 10.1038/nn.4185.
109. Bowman RL, Klemm F, Akkari L, Pyonteck SM, Sevenich L, Quail DF, Dhara S, Simpson K, Gardner EE, Iacobuzio-Donahue CA, Brennan CW, Tabar V, Gutin PH, Joyce JA. Macrophage Ontogeny Underlies Differences in Tumor-Specific Education in Brain Malignancies. *Cell Rep.* 2016 Nov 22;17(9):2445-2459. doi: 10.1016/j.celrep.2016.10.052.
110. Bennett ML, Bennett FC, Liddel SA, Ajami B, Zamanian JL, Fernhoff NB, Mulinyawe SB, Bohlen CJ, Adil A, Tucker A, Weissman IL, Chang EF, Li G, Grant GA,

- Hayden Gephart MG, Barres BA. New tools for studying microglia in the mouse and human CNS. *Proc Natl Acad Sci U S A*. 2016 Mar 22;113(12):E1738-46. doi: 10.1073/pnas.1525528113.
111. Komohara Y, Ohnishi K, Kuratsu J, Takeya M. Possible involvement of the M2 anti-inflammatory macrophage phenotype in growth of human gliomas. *J Pathol*. 2008 Sep;216(1):15-24. doi: 10.1002/path.2370.
112. Coniglio SJ, Eugenin E, Dobrenis K, Stanley ER, West BL, Symons MH, Segall JE. Microglial stimulation of glioblastoma invasion involves epidermal growth factor receptor (EGFR) and colony stimulating factor 1 receptor (CSF-1R) signaling. *Mol Med*. 2012 May 9;18:519-27. doi: 10.2119/molmed.2011.00217.
113. Saederup N, Cardona AE, Croft K, Mizutani M, Cotleur AC, Tsou CL, Ransohoff RM, Charo IF. Selective chemokine receptor usage by central nervous system myeloid cells in CCR2-red fluorescent protein knock-in mice. *PLoS One*. 2010 Oct 27;5(10):e13693. doi: 10.1371/journal.pone.0013693.
114. Wesolowska A, Kwiatkowska A, Slomnicki L, Dembinski M, Master A, Sliwa M, Franciszkiewicz K, Chouaib S, Kaminska B. Microglia-derived TGF-beta as an important regulator of glioblastoma invasion--an inhibition of TGF-beta-dependent effects by shRNA against human TGF-beta type II receptor. *Oncogene*. 2008 Feb 7;27(7):918-30.
115. Lu-Emerson C, Snuderl M, Kirkpatrick ND, Goveia J, Davidson C, Huang Y, Riedemann L, Taylor J, Ivy P, Duda DG, Ancukiewicz M, Plotkin SR, Chi AS, Gerstner ER, Eichler AF, Dietrich J, Stemmer-Rachamimov AO, Batchelor TT, Jain RK. Increase in tumor-associated macrophages after antiangiogenic therapy is associated with poor survival among patients with recurrent glioblastoma. *Neuro Oncol*. 2013 Aug;15(8):1079-87. doi: 10.1093/neuonc/not082.
116. Piao Y, Liang J, Holmes L, Zurita AJ, Henry V, Heymach JV, de Groot JF. Glioblastoma resistance to anti-VEGF therapy is associated with myeloid cell infiltration, stem cell accumulation, and a mesenchymal phenotype. *Neuro Oncol*. 2012 Nov;14(11):1379-92. doi: 10.1093/neuonc/nos158.
117. Waziri A, Killory B, Ogden AT 3rd, Canoll P, Anderson RC, Kent SC, Anderson DE, Bruce JN. Preferential in situ CD4+CD56+ T cell activation and expansion within human glioblastoma. *J Immunol*. 2008 Jun 1;180(11):7673-80.
118. Mohme M, Neidert MC, Regli L, Weller M, Martin R. Immunological challenges for peptide-based immunotherapy in glioblastoma. *Cancer Treat Rev*. 2014 Mar;40(2):248-58. doi: 10.1016/j.ctrv.2013.08.008.

119. Wojtowicz-Praga S. Reversal of tumor-induced immunosuppression: a new approach to cancer therapy. *J Immunother.* 1997 May;20(3):165-77.
120. Zuber P, Kuppner MC, De Tribolet N. Transforming growth factor-beta 2 down-regulates HLA-DR antigen expression on human malignant glioma cells. *Eur J Immunol.* 1988 Oct;18(10):1623-6.
121. Smyth MJ, Strobl SL, Young HA, Ortaldo JR, Ochoa AC. Regulation of lymphokine-activated killer activity and pore-forming protein gene expression in human peripheral blood CD8+ T lymphocytes. Inhibition by transforming growth factor-beta. *J Immunol.* 1991 May 15;146(10):3289-97.
122. Fecci PE, Mitchell DA, Whitesides JF, Xie W, Friedman AH, Archer GE, Herndon JE 2nd, Bigner DD, Dranoff G, Sampson JH. Increased regulatory T-cell fraction amidst a diminished CD4 compartment explains cellular immune defects in patients with malignant glioma. *Cancer Res.* 2006 Mar 15;66(6):3294-302.
123. Charles NA, Holland EC, Gilbertson R, Glass R, Kettenmann H. The brain tumor microenvironment. *Glia.* 2011 Aug;59(8):1169-80. doi: 10.1002/glia.21136.
124. Le DM, Besson A, Fogg DK, Choi KS, Waisman DM, Goodyer CG, Rewcastle B, Yong VW. Exploitation of astrocytes by glioma cells to facilitate invasiveness: a mechanism involving matrix metalloproteinase-2 and the urokinase-type plasminogen activator-plasmin cascade. *J Neurosci.* 2003 May 15;23(10):4034-43.
125. Brandao M, Simon T, Critchley G, Giamas G. Astrocytes, the rising stars of the glioblastoma microenvironment. *Glia.* 2019 May;67(5):779-790. doi: 10.1002/glia.23520.
126. Chen W, Wang D, Du X, He Y, Chen S, Shao Q, Ma C, Huang B, Chen A, Zhao P, Qu X, Li X. Glioma cells escaped from cytotoxicity of temozolomide and vincristine by communicating with human astrocytes. *Med Oncol.* 2015 Mar;32(3):43. doi: 10.1007/s12032-015-0487-0.
127. Chen Q, Boire A, Jin X, Valiente M, Er EE, Lopez-Soto A, Jacob L, Patwa R, Shah H, Xu K, Cross JR, Massagué J. Carcinoma-astrocyte gap junctions promote brain metastasis by cGAMP transfer. *Nature.* 2016 May 26;533(7604):493-498. doi: 10.1038/nature18268.
128. Minchinton AI, Tannock IF. Drug penetration in solid tumours. *Nat Rev Cancer.* 2006 Aug;6(8):583-92.
129. Gerlinger M, Rowan AJ, Horswell S, Math M, Larkin J, Endesfelder D, Gronroos E, Martinez P, Matthews N, Stewart A, Tarpey P, Varela I, Phillimore B, Begum S, McDonald NQ, Butler A, Jones D, Raine K, Latimer C, Santos CR, Nohadani M, Eklund AC, Spencer-

- Dene B, Clark G, Pickering L, Stamp G, Gore M, Szallasi Z, Downward J, Futreal PA, Swanton C. Intratumor heterogeneity and branched evolution revealed by multiregion sequencing. *N Engl J Med*. 2012 Mar 8;366(10):883-892. doi: 10.1056/NEJMoa1113205.
130. Bellot G, Garcia-Medina R, Gounon P, Chiche J, Roux D, Pouysségur J, Mazure NM. Hypoxia-induced autophagy is mediated through hypoxia-inducible factor induction of BNIP3 and BNIP3L via their BH3 domains. *Mol Cell Biol*. 2009 May;29(10):2570-81. doi: 10.1128/MCB.00166-09.
131. Shi Q, Le X, Wang B, Abbruzzese JL, Xiong Q, He Y, Xie K. Regulation of vascular endothelial growth factor expression by acidosis in human cancer cells. *Oncogene*. 2001 Jun 21;20(28):3751-6.
132. Huber V, Camisaschi C, Berzi A, Ferro S, Lugini L, Triulzi T, Tuccitto A, Tagliabue E, Castelli C, Rivoltini L. Cancer acidity: An ultimate frontier of tumor immune escape and a novel target of immunomodulation. *Semin Cancer Biol*. 2017 Apr;43:74-89. doi: 10.1016/j.semcancer.2017.03.001.
133. Cowan DS, Tannock IF. Factors that influence the penetration of methotrexate through solid tissue. *Int J Cancer*. 2001 Jan 1;91(1):120-5.
134. Harrington KJ, Billingham LJ, Brunner TB, Burnet NG, Chan CS, Hoskin P, Mackay RI, Maughan TS, Macdougall J, McKenna WG, Nutting CM, Oliver A, Plummer R, Stratford IJ, Illidge T. Guidelines for preclinical and early phase clinical assessment of novel radiosensitisers. *Br J Cancer*. 2011 Aug 23;105(5):628-39. doi: 10.1038/bjc.2011.240.
135. Baskar R, Lee KA, Yeo R, Yeoh KW. Cancer and radiation therapy: current advances and future directions. *Int J Med Sci*. 2012;9(3):193-9. doi: 10.7150/ijms.3635.
136. International Commission on Radiation Units. Prescribing, recording and reporting photon beam therapy. Supplement to ICRU Report 50. Bethesda: International Commission on Radiation Units and Measurement. MD: ICRU; 1999.
137. Elith C, Dempsey SE, Findlay N, Warren-Forward HM. An Introduction to the Intensity-modulated Radiation Therapy (IMRT) Techniques, Tomotherapy, and VMAT. *J Med Imaging Radiat Sci*. 2011 Mar;42(1):37-43. doi: 10.1016/j.jmir.2010.11.005.
138. Ellis F. Dose, time and fractionation: a clinical hypothesis. *Clin Radiol*. 1969 Jan;20(1):1-7.
139. van Leeuwen CM, Oei AL, Crezee J, Bel A, Franken NAP, Stalpers LJA, Kok HP. The alfa and beta of tumours: a review of parameters of the linear-quadratic model, derived from clinical radiotherapy studies. *Radiat Oncol*. 2018 May 16;13(1):96. doi: 10.1186/s13014-018-1040-z.

140. Santivasi WL, Xia F. Ionizing radiation-induced DNA damage, response, and repair. *Antioxid Redox Signal*. 2014 Jul 10;21(2):251-9. doi: 10.1089/ars.2013.5668.
141. Zhao W, Robbins ME. Inflammation and chronic oxidative stress in radiation-induced late normal tissue injury: therapeutic implications. *Curr Med Chem*. 2009;16(2):130-43.
142. Zanoni M, Cortesi M, Zamagni A, Tesei A. The Role of Mesenchymal Stem Cells in Radiation-Induced Lung Fibrosis. *Int J Mol Sci*. 2019 Aug 8;20(16). pii: E3876. doi: 10.3390/ijms20163876.
143. Shiloh Y, Ziv Y. The ATM protein kinase: regulating the cellular response to genotoxic stress, and more. *Nat Rev Mol Cell Biol*. 2013 Apr;14(4):197-210. doi: 10.1038/nrm3546.
144. Maier P, Hartmann L, Wenz F, Herskind C. Cellular Pathways in Response to Ionizing Radiation and Their Targetability for Tumor Radiosensitization. *Int J Mol Sci*. 2016 Jan 14;17(1). pii: E102. doi: 10.3390/ijms17010102.
145. Degtrev A, Yuan J. Expansion and evolution of cell death programmes. *Nat Rev Mol Cell Biol*. 2008 May;9(5):378-90. doi: 10.1038/nrm2393.
146. Cain K, Brown DG, Langlais C, Cohen GM. Caspase activation involves the formation of the aposome, a large (approximately 700 kDa) caspase-activating complex. *J Biol Chem*. 1999 Aug 6;274(32):22686-92.
147. Roninson IB. Tumor cell senescence in cancer treatment. *Cancer Res*. 2003 Jun 1;63(11):2705-15.
148. Quick QA, Gewirtz DA. An accelerated senescence response to radiation in wild-type p53 glioblastoma multiforme cells. *J Neurosurg*. 2006 Jul;105(1):111-8.
149. Faget DV, Ren Q, Stewart SA. Unmasking senescence: context-dependent effects of SASP in cancer. *Nat Rev Cancer*. 2019 Aug;19(8):439-453. doi: 10.1038/s41568-019-0156-2.
150. Gewirtz DA. Autophagy, senescence and tumor dormancy in cancer therapy. *Autophagy*. 2009 Nov;5(8):1232-4.
151. Yang L, Fang J, Chen J. Tumor cell senescence response produces aggressive variants. *Cell Death Discov*. 2017 Aug 21;3:17049. doi: 10.1038/cddiscovery.2017.49.
152. Vitale I, Galluzzi L, Castedo M, Kroemer G. Mitotic catastrophe: a mechanism for avoiding genomic instability. *Nat Rev Mol Cell Biol*. 2011 Jun;12(6):385-92. doi: 10.1038/nrm3115.

153. Barker HE, Paget JT, Khan AA, Harrington KJ. The tumour microenvironment after radiotherapy: mechanisms of resistance and recurrence. *Nat Rev Cancer*. 2015 Jul;15(7):409-25. doi: 10.1038/nrc3958.
154. Munn DH, Bronte V. Immune suppressive mechanisms in the tumor microenvironment. *Curr Opin Immunol*. 2016 Apr;39:1-6. doi: 10.1016/j.coi.2015.10.009.
155. Burnette BC, Liang H, Lee Y, Chlewicki L, Khodarev NN, Weichselbaum RR, Fu YX, Auh SL. The efficacy of radiotherapy relies upon induction of type I interferon-dependent innate and adaptive immunity. *Cancer Res*. 2011 Apr 1;71(7):2488-96. doi: 10.1158/0008-5472.CAN-10-2820.
156. Schae D, McBride WH. Links between innate immunity and normal tissue radiobiology. *Radiat Res*. 2010 Apr;173(4):406-17. doi: 10.1667/RR1931.1.
157. Krysko DV, Garg AD, Kaczmarek A, Krysko O, Agostinis P, Vandenabeele P. Immunogenic cell death and DAMPs in cancer therapy. *Nat Rev Cancer*. 2012 Dec;12(12):860-75. doi: 10.1038/nrc3380.
158. Apetoh L, Ghiringhelli F, Tesniere A, Obeid M, Ortiz C, Criollo A, Mignot G, Maiuri MC, Ullrich E, Saulnier P, Yang H, Amigorena S, Ryffel B, Barrat FJ, Saftig P, Levi F, Lidereau R, Nogues C, Mira JP, Chompret A, Joulin V, Clavel-Chapelon F, Bourhis J, André F, Delaloge S, Tursz T, Kroemer G, Zitvogel L. Toll-like receptor 4-dependent contribution of the immune system to anticancer chemotherapy and radiotherapy. *Nat Med*. 2007 Sep;13(9):1050-9.
159. Galluzzi L, Vacchelli E, Bravo-San Pedro JM, Buqué A, Senovilla L, Baracco EE, Bloy N, Castoldi F, Abastado JP, Agostinis P, Apte RN, Aranda F, Ayyoub M, Beckhove P, Blay JY, Bracci L, Caignard A, Castelli C, Cavallo F, Celis E, Cerundolo V, Clayton A, Colombo MP, Coussens L, Dhodapkar MV, Eggermont AM, Fearon DT, Fridman WH, Fučíková J, Gabilovich DI, Galon J, Garg A, Ghiringhelli F, Giaccone G, Gilboa E, Gnjatic S, Hoos A, Hosmalin A, Jäger D, Kalinski P, Kärre K, Kepp O, Kiessling R, Kirkwood JM, Klein E, Knuth A, Lewis CE, Liblau R, Lotze MT, Lugli E, Mach JP, Mattei F, Mavilio D, Melero I, Melief CJ, Mittendorf EA, Moretta L, Odunsi A, Okada H, Palucka AK, Peter ME, Pienta KJ, Porgador A, Prendergast GC, Rabinovich GA, Restifo NP, Rizvi N, Sautès-Fridman C, Schreiber H, Seliger B, Shiku H, Silva-Santos B, Smyth MJ, Speiser DE, Spisek R, Srivastava PK, Talmadge JE, Tartour E, Van Der Burg SH, Van Den Eynde BJ, Vile R, Wagner H, Weber JS, Whiteside TL, Wolchok JD, Zitvogel L, Zou W, Kroemer G. Classification of current anticancer immunotherapies. *Oncotarget*. 2014 Dec 30;5(24):12472-508.

160. Philip M, Rowley DA, Schreiber H. Inflammation as a tumor promoter in cancer induction. *Semin Cancer Biol.* 2004 Dec;14(6):433-9.
161. Lin WW, Karin M. A cytokine-mediated link between innate immunity, inflammation, and cancer. *J Clin Invest.* 2007 May;117(5):1175-83.
162. Harris TJ, Hipkiss EL, Borzillary S, Wada S, Grosso JF, Yen HR, Getnet D, Bruno TC, Goldberg MV, Pardoll DM, DeWeese TL, Drake CG. Radiotherapy augments the immune response to prostate cancer in a time-dependent manner. *Prostate.* 2008 Sep 1;68(12):1319-29. doi: 10.1002/pros.20794.
163. Laoui D, Van Overmeire E, De Baetselier P, Van Ginderachter JA, Raes G. Functional Relationship between Tumor-Associated Macrophages and Macrophage Colony-Stimulating Factor as Contributors to Cancer Progression. *Front Immunol.* 2014 Oct 7;5:489. doi: 10.3389/fimmu.2014.00489.
164. Kachikwu EL, Iwamoto KS, Liao YP, DeMarco JJ, Agazaryan N, Economou JS, McBride WH, Schaeue D. Radiation enhances regulatory T cell representation. *Int J Radiat Oncol Biol Phys.* 2011 Nov 15;81(4):1128-35. doi: 10.1016/j.ijrobp.2010.09.034.
165. Qu Y, Jin S, Zhang A, Zhang B, Shi X, Wang J, Zhao Y. Gamma-ray resistance of regulatory CD4⁺CD25⁺Foxp3⁺ T cells in mice. *Radiat Res.* 2010 Feb;173(2):148-57. doi: 10.1667/RR0978.1.
166. Qureshi OS, Zheng Y, Nakamura K, Attridge K, Manzotti C, Schmidt EM, Baker J, Jeffery LE, Kaur S, Briggs Z, Hou TZ, Futter CE, Anderson G, Walker LS, Sansom DM. Trans-endocytosis of CD80 and CD86: a molecular basis for the cell-extrinsic function of CTLA-4. *Science.* 2011 Apr 29;332(6029):600-3. doi: 10.1126/science.1202947.
167. Mantovani A, Romero P, Palucka AK, Marincola FM. Tumour immunity: effector response to tumour and role of the microenvironment. *Lancet.* 2008 Mar 1;371(9614):771-83. doi: 10.1016/S0140-6736(08)60241-X.
168. Finkelstein SE, Iclozan C, Bui MM, Cotter MJ, Ramakrishnan R, Ahmed J, Noyes DR, Cheong D, Gonzalez RJ, Heysek RV, Berman C, Lenox BC, Janssen W, Zager JS, Sondak VK, Letson GD, Antonia SJ, Gaborilovich DI. Combination of external beam radiotherapy (EBRT) with intratumoral injection of dendritic cells as neo-adjuvant treatment of high-risk soft tissue sarcoma patients. *Int J Radiat Oncol Biol Phys.* 2012 Feb 1;82(2):924-32. doi: 10.1016/j.ijrobp.2010.12.068.
169. de la Cruz-Merino L, Illescas-Vacas A, Grueso-López A, Barco-Sánchez A, Míguez-Sánchez C; Cancer Immunotherapies Spanish Group (GETICA). Radiation for Awakening

- the Dormant Immune System, a Promising Challenge to be Explored. *Front Immunol.* 2014 Mar 14;5:102. doi: 10.3389/fimmu.2014.00102.
170. Kruger S, Ilmer M, Kobold S, Cadilha BL, Endres S, Ormanns S, Schuebbe G, Renz BW, D'Haese JG, Schloesser H, Heinemann V, Subklewe M, Boeck S, Werner J, von Bergwelt-Baildon M. Advances in cancer immunotherapy 2019 - latest trends. *J Exp Clin Cancer Res.* 2019 Jun 19;38(1):268. doi: 10.1186/s13046-019-1266-0.
171. Hammerich L1,2, Marron TU1,2, Upadhyay R1,2, Svensson-Arvelund J1,2, Dhainaut M2,3, Hussein S4, Zhan Y4, Ostrowski D1, Yellin M5, Marsh H5, Salazar AM6, Rahman AH2, Brown BD2,3, Merad M2,7, Brody JD8,9. Systemic clinical tumor regressions and potentiation of PD1 blockade with in situ vaccination. *Nat Med.* 2019 May;25(5):814-824. doi: 10.1038/s41591-019-0410-x.
172. Antonia SJ, Villegas A, Daniel D, Vicente D, Murakami S, Hui R, Yokoi T, Chiappori A, Lee KH, de Wit M, Cho BC, Bourhaba M, Quantin X, Tokito T, Mekhail T, Planchard D, Kim YC, Karapetis CS, Hirt S, Ostoros G, Kubota K, Gray JE, Paz-Ares L, de Castro Carpeño J, Wadsworth C, Melillo G, Jiang H, Huang Y, Dennis PA, Özgüroğlu M; PACIFIC Investigators. Durvalumab after Chemoradiotherapy in Stage III Non-Small-Cell Lung Cancer. *N Engl J Med.* 2017 Nov 16;377(20):1919-1929. doi: 10.1056/NEJMoa1709937.
173. McBride SM, Sherman EJ, Tsai CJ, Baxi SS, Aghalar J, Eng J, et al. A phase II randomized trial of nivolumab with stereotactic body radiotherapy (SBRT) versus nivolumab alone in metastatic (M1) head and neck squamous cell carcinoma (HNSCC). *J Clin Oncol.* 2018;36(15_suppl):6009.
174. Wynn TA. Cellular and molecular mechanisms of fibrosis. *J Pathol.* 2008 Jan;214(2):199-210.
175. Park HJ, Griffin RJ, Hui S, Levitt SH, Song CW. Radiation-induced vascular damage in tumors: implications of vascular damage in ablative hypofractionated radiotherapy (SBRT and SRS). *Radiat Res.* 2012 Mar;177(3):311-27.
176. Jain RK. Molecular regulation of vessel maturation. *Nat Med.* 2003 Jun;9(6):685-93.
177. Harris AL. Hypoxia--a key regulatory factor in tumour growth. *Nat Rev Cancer.* 2002 Jan;2(1):38-47.
178. Overgaard J. Hypoxic modification of radiotherapy in squamous cell carcinoma of the head and neck--a systematic review and meta-analysis. *Radiother Oncol.* 2011 Jul;100(1):22-32. doi: 10.1016/j.radonc.2011.03.004.

179. Semenza GL. Intratumoral hypoxia, radiation resistance, and HIF-1. *Cancer Cell*. 2004 May;5(5):405-6.
180. Yoshimura M, Itasaka S, Harada H, Hiraoka M. Microenvironment and radiation therapy. *Biomed Res Int*. 2013;2013:685308. doi: 10.1155/2013/685308.
181. Schulz A, Meyer F, Dubrovskaja A, Borgmann K. Cancer Stem Cells and Radioresistance: DNA Repair and Beyond. *Cancers (Basel)*. 2019 Jun 21;11(6). pii: E862. doi: 10.3390/cancers11060862.
182. Mandal PK, Blanpain C, Rossi DJ. DNA damage response in adult stem cells: pathways and consequences. *Nat Rev Mol Cell Biol*. 2011 Mar;12(3):198-202. doi: 10.1038/nrm3060.
183. Vitale I, Manic G, De Maria R, Kroemer G, Galluzzi L. DNA Damage in Stem Cells. *Mol Cell*. 2017 May 4;66(3):306-319. doi: 10.1016/j.molcel.2017.04.006.
184. Ahmed SU, Carruthers R, Gilmour L, Yildirim S, Watts C, Chalmers AJ. Selective Inhibition of Parallel DNA Damage Response Pathways Optimizes Radiosensitization of Glioblastoma Stem-like Cells. *Cancer Res*. 2015 Oct 15;75(20):4416-28. doi: 10.1158/0008-5472.CAN-14-3790.
185. Carruthers R, Ahmed SU, Strathdee K, Gomez-Roman N, Amoah-Buahin E, Watts C, Chalmers AJ. Abrogation of radioresistance in glioblastoma stem-like cells by inhibition of ATM kinase. *Mol Oncol*. 2015 Jan;9(1):192-203. doi: 10.1016/j.molonc.2014.08.003.
186. Cheng L, Wu Q, Huang Z, Guryanova OA, Huang Q, Shou W, Rich JN, Bao S. L1CAM regulates DNA damage checkpoint response of glioblastoma stem cells through NBS1. *EMBO J*. 2011 Mar 2;30(5):800-13. doi: 10.1038/emboj.2011.10.
187. King HO, Brend T, Payne HL, Wright A, Ward TA, Patel K, Egnuni T, Stead LF, Patel A, Wurdak H, Short SC. RAD51 Is a Selective DNA Repair Target to Radiosensitize Glioma Stem Cells. *Stem Cell Reports*. 2017 Jan 10;8(1):125-139. doi: 10.1016/j.stemcr.2016.12.005.
188. Lim YC, Roberts TL, Day BW, Harding A, Kozlov S, Kijas AW, Ensbey KS, Walker DG, Lavin MF. A role for homologous recombination and abnormal cell-cycle progression in radioresistance of glioma-initiating cells. *Mol Cancer Ther*. 2012 Sep;11(9):1863-72. doi: 10.1158/1535-7163.MCT-11-1044.
189. Carruthers RD, Ahmed SU, Ramachandran S, Strathdee K, Kurian KM, Hedley A, Gomez-Roman N, Kalna G, Neilson M, Gilmour L, Stevenson KH, Hammond EM, Chalmers AJ. Replication Stress Drives Constitutive Activation of the DNA Damage

- Response and Radioresistance in Glioblastoma Stem-like Cells. *Cancer Res.* 2018 Sep 1;78(17):5060-5071. doi: 10.1158/0008-5472.CAN-18-0569.
190. Diehn M, Cho RW, Lobo NA, Kalisky T, Dorie MJ, Kulp AN, Qian D, Lam JS, Ailles LE, Wong M, Joshua B, Kaplan MJ, Wapnir I, Dirbas FM, Somlo G, Garberoglio C, Paz B, Shen J, Lau SK, Quake SR, Brown JM, Weissman IL, Clarke MF. Association of reactive oxygen species levels and radioresistance in cancer stem cells. *Nature.* 2009 Apr 9;458(7239):780-3. doi: 10.1038/nature07733.
191. Bartkova J, Hamerlik P, Stockhausen MT, Ehrmann J, Hlobilkova A, Laursen H, Kalita O, Kolar Z, Poulsen HS, Broholm H, Lukas J, Bartek J. Replication stress and oxidative damage contribute to aberrant constitutive activation of DNA damage signalling in human gliomas. *Oncogene.* 2010 Sep 9;29(36):5095-102. doi: 10.1038/onc.2010.249.
192. Chen Y, Li D, Wang D, Liu X, Yin N, Song Y, Lu SH, Ju Z, Zhan Q. Quiescence and attenuated DNA damage response promote survival of esophageal cancer stem cells. *J Cell Biochem.* 2012 Dec;113(12):3643-52. doi: 10.1002/jcb.24228.
193. Yang L, Fang J, Chen J. Tumor cell senescence response produces aggressive variants. *Cell Death Discov.* 2017 Aug 21;3:17049. doi: 10.1038/cddiscovery.2017.49.
194. Mahabir R, Tanino M, Elmansuri A, Wang L, Kimura T, Itoh T, Ohba Y, Nishihara H, Shirato H, Tsuda M, Tanaka S. Sustained elevation of Snail promotes glial-mesenchymal transition after irradiation in malignant glioma. *Neuro Oncol.* 2014 May;16(5):671-85. doi: 10.1093/neuonc/not239.
195. Gouazé-Andersson V, Ghérardi MJ, Lemarié A, Gilhodes J, Lubrano V, Arnauduc F, Cohen-Jonathan Moyal E, Toulas C. FGFR1/FOXO1 pathway: a key regulator of glioblastoma stem cells radioresistance and a prognosis biomarker. *Oncotarget.* 2018 Aug 3;9(60):31637-31649. doi: 10.18632/oncotarget.25827.
196. Konge J, Leteurtre F, Goislard M, Biard D, Morel-Altmeier S, Vaurijoux A, Gruel G, Chevillard S, Lebeau J. Breast cancer stem cell-like cells generated during TGF β -induced EMT are radioresistant. *Oncotarget.* 2018 May 4;9(34):23519-23531. doi: 10.18632/oncotarget.25240.
197. Di Virgilio F, Adinolfi E. Extracellular purines, purinergic receptors and tumor growth. *Oncogene.* 2017 Jan 19;36(3):293-303. doi: 10.1038/onc.2016.206.
198. Burnstock G. Pathophysiology and therapeutic potential of purinergic signaling. *Pharmacol Rev.* 2006 Mar;58(1):58-86.
199. Idzko M, Ferrari D, Eltzschig HK. Nucleotide signalling during inflammation. *Nature.* 2014 May 15;509(7500):310-7. doi: 10.1038/nature13085.

200. Antonioli L, Blandizzi C, Pacher P, Haskó G. Immunity, inflammation and cancer: a leading role for adenosine. *Nat Rev Cancer*. 2013 Dec;13(12):842-57. doi: 10.1038/nrc3613.
201. Burnstock G, Di Virgilio F. Purinergic signalling and cancer. *Purinergic Signal*. 2013 Dec;9(4):491-540.
202. Di Virgilio F. Purines, purinergic receptors, and cancer. *Cancer Res*. 2012 Nov 1;72(21):5441-7. doi: 10.1158/0008-5472.CAN-12-1600.
203. Vijayan D, Young A, Teng MWL, Smyth MJ. Targeting immunosuppressive adenosine in cancer. *Nat Rev Cancer*. 2017 Dec;17(12):709-724. doi: 10.1038/nrc.2017.86.
204. Rossi L, Manfredini R, Bertolini F, Ferrari D, Fogli M, Zini R, Salati S, Salvestrini V, Gulinelli S, Adinolfi E, Ferrari S, Di Virgilio F, Baccarani M, Lemoli RM. The extracellular nucleotide UTP is a potent inducer of hematopoietic stem cell migration. *Blood*. 2007 Jan 15;109(2):533-42.
205. Koizumi S, Shigemoto-Mogami Y, Nasu-Tada K, Shinozaki Y, Ohsawa K, Tsuda M, Joshi BV, Jacobson KA, Kohsaka S, Inoue K. UDP acting at P2Y6 receptors is a mediator of microglial phagocytosis. *Nature*. 2007 Apr 26;446(7139):1091-5.
206. Lazarowski ER, Harden TK. UDP-Sugars as Extracellular Signaling Molecules: Cellular and Physiologic Consequences of P2Y14 Receptor Activation. *Mol Pharmacol*. 2015 Jul;88(1):151-60. doi: 10.1124/mol.115.098756.
207. Burnstock G. Purine and pyrimidine receptors. *Cell Mol Life Sci*. 2007 Jun;64(12):1471-83.
208. Ohta A, Gorelik E, Prasad SJ, Ronchese F, Lukashev D, Wong MK, Huang X, Caldwell S, Liu K, Smith P, Chen JF, Jackson EK, Apasov S, Abrams S, Sitkovsky M. A2A adenosine receptor protects tumors from antitumor T cells. *Proc Natl Acad Sci U S A*. 2006 Aug 29;103(35):13132-7.
209. Pellegatti P, Raffaghello L, Bianchi G, Piccardi F, Pistoia V, Di Virgilio F. Increased level of extracellular ATP at tumor sites: in vivo imaging with plasma membrane luciferase. *PLoS One*. 2008 Jul 9;3(7):e2599. doi: 10.1371/journal.pone.0002599.
210. Falzoni S, Donvito G, Di Virgilio F. Detecting adenosine triphosphate in the pericellular space. *Interface Focus*. 2013 Jun 6;3(3):20120101. doi: 10.1098/rsfs.2012.0101.
211. Yegutkin GG. Enzymes involved in metabolism of extracellular nucleotides and nucleosides: functional implications and measurement of activities. *Crit Rev Biochem Mol Biol*. 2014 Nov-Dec;49(6):473-97. doi: 10.3109/10409238.2014.953627.

212. Pellegatti P, Falzoni S, Pinton P, Rizzuto R, Di Virgilio F. A novel recombinant plasma membrane-targeted luciferase reveals a new pathway for ATP secretion. *Mol Biol Cell*. 2005 Aug;16(8):3659-65.
213. Di Virgilio F, Sarti AC, Falzoni S, De Marchi E, Adinolfi E. Extracellular ATP and P2 purinergic signalling in the tumour microenvironment. *Nat Rev Cancer*. 2018 Oct;18(10):601-618. doi: 10.1038/s41568-018-0037-0.
214. Lazarowski ER. Vesicular and conductive mechanisms of nucleotide release. *Purinergic Signal*. 2012 Sep;8(3):359-73. doi: 10.1007/s11302-012-9304-9.
215. Hatfield SM, Kjaergaard J, Lukashev D, Schreiber TH, Belikoff B, Abbott R, Sethumadhavan S, Philbrook P, Ko K, Cannici R, Thayer M, Rodig S, Kutok JL, Jackson EK, Karger B, Podack ER, Ohta A, Sitkovsky MV. Immunological mechanisms of the antitumor effects of supplemental oxygenation. *Sci Transl Med*. 2015 Mar 4;7(277):277ra30. doi: 10.1126/scitranslmed.aaa1260.
216. Evans RJ, Derkach V, Surprenant A. ATP mediates fast synaptic transmission in mammalian neurons. *Nature*. 1992 Jun 11;357(6378):503-5.
217. Li J, Wang L, Chen X, Li L, Li Y, Ping Y, Huang L, Yue D, Zhang Z, Wang F, Li F, Yang L, Huang J, Yang S, Li H, Zhao X, Dong W, Yan Y, Zhao S, Huang B, Zhang B, Zhang Y. CD39/CD73 upregulation on myeloid-derived suppressor cells via TGF- β -mTOR-HIF-1 signaling in patients with non-small cell lung cancer. *Oncoimmunology*. 2017 Apr 21;6(6):e1320011. doi: 10.1080/2162402X.2017.1320011.
218. Ryzhov SV, Pickup MW, Chytil A, Gorska AE, Zhang Q, Owens P, Feoktistov I, Moses HL, Novitskiy SV. Role of TGF- β signaling in generation of CD39+CD73+ myeloid cells in tumors. *J Immunol*. 2014 Sep 15;193(6):3155-64. doi: 10.4049/jimmunol.1400578.
219. Bono MR, Fernández D, Flores-Santibáñez F, Roseblatt M, Sauma D. CD73 and CD39 ectonucleotidases in T cell differentiation: Beyond immunosuppression. *FEBS Lett*. 2015 Nov 14;589(22):3454-60. doi: 10.1016/j.febslet.2015.07.027.
220. Chalmin F, Mignot G, Bruchard M, Chevriaux A, Végran F, Hichami A, Ladoire S, Derangère V, Vincent J, Masson D, Robson SC, Eberl G, Pallandre JR, Borg C, Ryffel B, Apetoh L, Rébé C, Ghiringhelli F. Stat3 and Gfi-1 transcription factors control Th17 cell immunosuppressive activity via the regulation of ectonucleotidase expression. *Immunity*. 2012 Mar 23;36(3):362-73. doi: 10.1016/j.immuni.2011.12.019.
221. Montalbán Del Barrio I, Penski C, Schlahsa L, Stein RG, Diessner J, Wöckel A, Dietl J, Lutz MB, Mittelbronn M, Wischhusen J, Häusler SFM. Adenosine-generating ovarian cancer cells attract myeloid cells which differentiate into adenosine-generating

- tumor associated macrophages - a self-amplifying, CD39- and CD73-dependent mechanism for tumor immune escape. *J Immunother Cancer*. 2016 Aug 16;4:49. doi: 10.1186/s40425-016-0154-9.
222. Qian Y, Wang X, Liu Y, Li Y, Colvin RA, Tong L, Wu S, Chen X. Extracellular ATP is internalized by macropinocytosis and induces intracellular ATP increase and drug resistance in cancer cells. *Cancer Lett*. 2014 Sep 1;351(2):242-51. doi: 10.1016/j.canlet.2014.06.008.
223. Wang X, Li Y, Qian Y, Cao Y, Shriwas P, Zhang H, Chen X. Extracellular ATP, as an energy and phosphorylating molecule, induces different types of drug resistances in cancer cells through ATP internalization and intracellular ATP level increase. *Oncotarget*. 2017 Sep 23;8(50):87860-87877. doi: 10.18632/oncotarget.21231.
224. Di Virgilio F, Chiozzi P, Falzoni S, Ferrari D, Sanz JM, Venketaraman V, Baricordi OR. Cytolytic P2X purinoceptors. *Cell Death Differ*. 1998 Mar;5(3):191-9.
225. Adinolfi E, Callegari MG, Ferrari D, Bolognesi C, Minelli M, Wieckowski MR, Pinton P, Rizzuto R, Di Virgilio F. Basal activation of the P2X7 ATP receptor elevates mitochondrial calcium and potential, increases cellular ATP levels, and promotes serum-independent growth. *Mol Biol Cell*. 2005 Jul;16(7):3260-72.
226. Adinolfi E, Callegari MG, Cirillo M, Pinton P, Giorgi C, Cavagna D, Rizzuto R, Di Virgilio F. Expression of the P2X7 receptor increases the Ca²⁺ content of the endoplasmic reticulum, activates NFATc1, and protects from apoptosis. *J Biol Chem*. 2009 Apr 10;284(15):10120-8. doi: 10.1074/jbc.M805805200.
227. Di Virgilio F, Ferrari D, Adinolfi E. P2X(7): a growth-promoting receptor-implications for cancer. *Purinergic Signal*. 2009 Jun;5(2):251-6. doi: 10.1007/s11302-009-9145-3.
228. Young JD, Yao SY, Baldwin JM, Cass CE, Baldwin SA. The human concentrative and equilibrative nucleoside transporter families, SLC28 and SLC29. *Mol Aspects Med*. 2013 Apr-Jun;34(2-3):529-47. doi: 10.1016/j.mam.2012.05.007.
229. Stagg J, Smyth MJ. Extracellular adenosine triphosphate and adenosine in cancer. *Oncogene*. 2010 Sep 30;29(39):5346-58. doi: 10.1038/onc.2010.292.
230. Haskó G, Linden J, Cronstein B, Pacher P. Adenosine receptors: therapeutic aspects for inflammatory and immune diseases. *Nat Rev Drug Discov*. 2008 Sep;7(9):759-70. doi: 10.1038/nrd2638.

231. Gessi S, Merighi S, Sacchetto V, Simioni C, Borea PA. Adenosine receptors and cancer. *Biochim Biophys Acta*. 2011 May;1808(5):1400-12. doi: 10.1016/j.bbame.2010.09.020.
232. Lin Z, Yin P, Reierstad S, O'Halloran M, Coon VJ, Pearson EK, Mutlu GM, Bulun SE. Adenosine A1 receptor, a target and regulator of estrogen receptor α action, mediates the proliferative effects of estradiol in breast cancer. *Oncogene*. 2010 Feb 25;29(8):1114-22. doi: 10.1038/onc.2009.409.
233. Mousavi S, Panjehpour M, Izadpanahi MH, Aghaei M. Expression of adenosine receptor subclasses in malignant and adjacent normal human prostate tissues. *Prostate*. 2015 May;75(7):735-47. doi: 10.1002/pros.22955.
234. Etique N, Grillier-Vuissoz I, Lecomte J, Flament S. Crosstalk between adenosine receptor (A2A isoform) and ER α mediates ethanol action in MCF-7 breast cancer cells. *Oncol Rep*. 2009 Apr;21(4):977-81.
235. Merighi S, Mirandola P, Milani D, Varani K, Gessi S, Klotz KN, Leung E, Baraldi PG, Borea PA. Adenosine receptors as mediators of both cell proliferation and cell death of cultured human melanoma cells. *J Invest Dermatol*. 2002 Oct;119(4):923-33.
236. Mittal D, Sinha D, Barkauskas D, Young A, Kalimutho M, Stannard K, Caramia F, Haibe-Kains B, Stagg J, Khanna KK, Loi S, Smyth MJ. Adenosine 2B Receptor Expression on Cancer Cells Promotes Metastasis. *Cancer Res*. 2016 Aug 1;76(15):4372-82. doi: 10.1158/0008-5472.CAN-16-0544.
237. Ntantie E, Gonyo P, Lorimer EL, Hauser AD, Schuld N, McAllister D, Kalyanaraman B, Dwinell MB, Auchampach JA, Williams CL. An adenosine-mediated signaling pathway suppresses prenylation of the GTPase Rap1B and promotes cell scattering. *Sci Signal*. 2013 May 28;6(277):ra39. doi: 10.1126/scisignal.2003374.
238. Gessi S, Cattabriga E, Avitabile A, Gafa' R, Lanza G, Cavazzini L, Bianchi N, Gambari R, Feo C, Liboni A, Gullini S, Leung E, Mac-Lennan S, Borea PA. Elevated expression of A3 adenosine receptors in human colorectal cancer is reflected in peripheral blood cells. *Clin Cancer Res*. 2004 Sep 1;10(17):5895-901.
239. Yao Y, Sei Y, Abbracchio MP, Jiang JL, Kim YC, Jacobson KA. Adenosine A3 receptor agonists protect HL-60 and U-937 cells from apoptosis induced by A3 antagonists. *Biochem Biophys Res Commun*. 1997 Mar 17;232(2):317-22.
240. Gao Z, Li BS, Day YJ, Linden J. A3 adenosine receptor activation triggers phosphorylation of protein kinase B and protects rat basophilic leukemia 2H3 mast cells from apoptosis. *Mol Pharmacol*. 2001 Jan;59(1):76-82.

241. Merighi S, Benini A, Mirandola P, Gessi S, Varani K, Leung E, MacLennan S, Borea PA. A3 adenosine receptor activation inhibits cell proliferation via phosphatidylinositol 3-kinase/Akt-dependent inhibition of the extracellular signal-regulated kinase 1/2 phosphorylation in A375 human melanoma cells. *J Biol Chem.* 2005 May 20;280(20):19516-26.
242. Stemmer SM, Benjaminov O, Medalia G, Ciuraru NB, Silverman MH, Bar-Yehuda S, Fishman S, Harpaz Z, Farbstein M, Cohen S, Patoka R, Singer B, Kerns WD, Fishman P. CF102 for the treatment of hepatocellular carcinoma: a phase I/II, open-label, dose-escalation study. *Oncologist.* 2013;18(1):25-6. doi: 10.1634/theoncologist.2012-0211.
243. Di Virgilio F, Dal Ben D, Sarti AC, Giuliani AL, Falzoni S. The P2X7 Receptor in Infection and Inflammation. *Immunity.* 2017 Jul 18;47(1):15-31. doi: 10.1016/j.immuni.2017.06.020.
244. Di Virgilio F, Schmalzing G, Markwardt F. The Elusive P2X7 Macropore. *Trends Cell Biol.* 2018 May;28(5):392-404. doi: 10.1016/j.tcb.2018.01.005.
245. Jacobson KA, Müller CE. Medicinal chemistry of adenosine, P2Y and P2X receptors. *Neuropharmacology.* 2016 May;104:31-49. doi: 10.1016/j.neuropharm.2015.12.001.
246. North RA. Molecular physiology of P2X receptors. *Physiol Rev.* 2002 Oct;82(4):1013-67.
247. Stegner D, Dütting S, Nieswandt B. Mechanistic explanation for platelet contribution to cancer metastasis. *Thromb Res.* 2014 May;133 Suppl 2:S149-57. doi: 10.1016/S0049-3848(14)50025-4.
248. Reymond N, d'Água BB, Ridley AJ. Crossing the endothelial barrier during metastasis. *Nat Rev Cancer.* 2013 Dec;13(12):858-70. doi: 10.1038/nrc3628.
249. Gareau AJ, Brien C, Gebremeskel S, Liwski RS, Johnston B, Bezuhly M. Ticagrelor inhibits platelet-tumor cell interactions and metastasis in human and murine breast cancer. *Clin Exp Metastasis.* 2018 Feb;35(1-2):25-35. doi: 10.1007/s10585-018-9874-1.
250. Elaskalani O, Falasca M, Moran N, Berndt MC, Metharom P. The Role of Platelet-Derived ADP and ATP in Promoting Pancreatic Cancer Cell Survival and Gemcitabine Resistance. *Cancers (Basel).* 2017 Oct 24;9(10). pii: E142. doi: 10.3390/cancers9100142.
251. Maynard JP, Lee JS, Sohn BH, Yu X, Lopez-Terrada D, Finegold MJ, Goss JA, Thevananther S. P2X3 purinergic receptor overexpression is associated with poor recurrence-free survival in hepatocellular carcinoma patients. *Oncotarget.* 2015 Dec 1;6(38):41162-79. doi: 10.18632/oncotarget.6240.

252. Greig AV, Linge C, Healy V, Lim P, Clayton E, Rustin MH, McGrouther DA, Burnstock G. Expression of purinergic receptors in non-melanoma skin cancers and their functional roles in A431 cells. *J Invest Dermatol*. 2003 Aug;121(2):315-27.
253. Surprenant A, Rassendren F, Kawashima E, North RA, Buell G. The cytolytic P2Z receptor for extracellular ATP identified as a P2X receptor (P2X7). *Science*. 1996 May 3;272(5262):735-8.
254. Denlinger LC, Fisetto PL, Sommer JA, Watters JJ, Prabhu U, Dubyak GR, Proctor RA, Bertics PJ. Cutting edge: the nucleotide receptor P2X7 contains multiple protein- and lipid-interaction motifs including a potential binding site for bacterial lipopolysaccharide. *J Immunol*. 2001 Aug 15;167(4):1871-6.
255. Hattori M, Gouaux E. Molecular mechanism of ATP binding and ion channel activation in P2X receptors. *Nature*. 2012 May 10;485(7397):207-12. doi: 10.1038/nature11010.
256. Kaczmarek-Hájek K, Lörinczi E, Hausmann R, Nicke A. Molecular and functional properties of P2X receptors--recent progress and persisting challenges. *Purinergic Signal*. 2012 Sep;8(3):375-417. doi: 10.1007/s11302-012-9314-7.
257. Chataigneau T, Lemoine D, Grutter T. Exploring the ATP-binding site of P2X receptors. *Front Cell Neurosci*. 2013 Dec 30;7:273. doi: 10.3389/fncel.2013.00273.
258. Dal Ben D, Buccioni M, Lambertucci C, Marucci G, Thomas A, Volpini R. Purinergic P2X receptors: structural models and analysis of ligand-target interaction. *Eur J Med Chem*. 2015 Jan 7;89:561-80. doi: 10.1016/j.ejmech.2014.10.071.
259. Mansoor SE, Lü W, Oosterheert W, Shekhar M, Tajkhorshid E, Gouaux E. X-ray structures define human P2X(3) receptor gating cycle and antagonist action. *Nature*. 2016 Oct 6;538(7623):66-71. doi: 10.1038/nature19367.
260. Falzoni S, Munerati M, Ferrari D, Spisani S, Moretti S, Di Virgilio F. The purinergic P2Z receptor of human macrophage cells. Characterization and possible physiological role. *J Clin Invest*. 1995 Mar;95(3):1207-16.
261. Cheewatrakoolpong B, Gilchrest H, Anthes JC, Greenfeder S. Identification and characterization of splice variants of the human P2X7 ATP channel. *Biochem Biophys Res Commun*. 2005 Jun 24;332(1):17-27.
262. Sluyter R, Stokes L. Significance of P2X7 receptor variants to human health and disease. *Recent Pat DNA Gene Seq*. 2011 Apr;5(1):41-54.
263. Adinolfi E, Cirillo M, Woltersdorf R, Falzoni S, Chiozzi P, Pellegatti P, Callegari MG, Sandonà D, Markwardt F, Schmalzing G, Di Virgilio F. Trophic activity of a naturally

- occurring truncated isoform of the P2X7 receptor. *FASEB J.* 2010 Sep;24(9):3393-404. doi: 10.1096/fj.09-153601.
264. Liang X, Samways DS, Wolf K, Bowles EA, Richards JP, Bruno J, Dutertre S, DiPaolo RJ, Egan TM. Quantifying Ca²⁺ current and permeability in ATP-gated P2X7 receptors. *J Biol Chem.* 2015 Mar 20;290(12):7930-42. doi: 10.1074/jbc.M114.627810.
265. Wiley JS, Sluyter R, Gu BJ, Stokes L, Fuller SJ. The human P2X7 receptor and its role in innate immunity. *Tissue Antigens.* 2011 Nov;78(5):321-32. doi: 10.1111/j.1399-0039.2011.01780.x.
266. Bartlett R, Stokes L, Sluyter R. The P2X7 receptor channel: recent developments and the use of P2X7 antagonists in models of disease. *Pharmacol Rev.* 2014 Jul;66(3):638-75. doi: 10.1124/pr.113.008003.
267. Fuller SJ, Stokes L, Skarratt KK, Gu BJ, Wiley JS. Genetics of the P2X7 receptor and human disease. *Purinergic Signal.* 2009 Jun;5(2):257-62. doi: 10.1007/s11302-009-9136-4.
268. Gu BJ, Zhang W, Worthington RA, Sluyter R, Dao-Ung P, Petrou S, Barden JA, Wiley JS. A Glu-496 to Ala polymorphism leads to loss of function of the human P2X7 receptor. *J Biol Chem.* 2001 Apr 6;276(14):11135-42.
269. Gu BJ, Sluyter R, Skarratt KK, Shemon AN, Dao-Ung LP, Fuller SJ, Barden JA, Clarke AL, Petrou S, Wiley JS. An Arg307 to Gln polymorphism within the ATP-binding site causes loss of function of the human P2X7 receptor. *J Biol Chem.* 2004 Jul 23;279(30):31287-95.
270. Miller CM, Boulter NR, Fuller SJ, Zakrzewski AM, Lees MP, Saunders BM, Wiley JS, Smith NC. The role of the P2X₇ receptor in infectious diseases. *PLoS Pathog.* 2011 Nov;7(11):e1002212. doi: 10.1371/journal.ppat.1002212.
271. Jørgensen NR, Husted LB, Skarratt KK, Stokes L, Tofteng CL, Kvist T, Jensen JE, Eiken P, Brixen K, Fuller S, Clifton-Bligh R, Gartland A, Schwarz P, Langdahl BL, Wiley JS. Single-nucleotide polymorphisms in the P2X7 receptor gene are associated with post-menopausal bone loss and vertebral fractures. *Eur J Hum Genet.* 2012 Jun;20(6):675-81. doi: 10.1038/ejhg.2011.253.
272. Bergamin LS, Braganhol E, Figueiró F, Casali EA, Zanin RF, Sévigny J, Battastini AM. Involvement of purinergic system in the release of cytokines by macrophages exposed to glioma-conditioned medium. *J Cell Biochem.* 2015 May;116(5):721-9. doi: 10.1002/jcb.25018.

273. Bianchi G, Vuerich M, Pellegatti P, Marimpietri D, Emionite L, Marigo I, Bronte V, Di Virgilio F, Pistoia V, Raffaghello L. ATP/P2X7 axis modulates myeloid-derived suppressor cell functions in neuroblastoma microenvironment. *Cell Death Dis.* 2014 Mar 20;5:e1135. doi: 10.1038/cddis.2014.109.
274. Di Virgilio F, Bronte V, Collavo D, Zanovello P. Responses of mouse lymphocytes to extracellular adenosine 5'-triphosphate (ATP). Lymphocytes with cytotoxic activity are resistant to the permeabilizing effects of ATP. *J Immunol.* 1989 Sep 15;143(6):1955-60.
275. Amoroso F, Falzoni S, Adinolfi E, Ferrari D, Di Virgilio F. The P2X7 receptor is a key modulator of aerobic glycolysis. *Cell Death Dis.* 2012 Aug 16;3:e370. doi: 10.1038/cddis.2012.105.
276. Amoroso F, Capece M, Rotondo A, Cangelosi D, Ferracin M, Franceschini A, Raffaghello L, Pistoia V, Varesio L, Adinolfi E. The P2X7 receptor is a key modulator of the PI3K/GSK3 β /VEGF signaling network: evidence in experimental neuroblastoma. *Oncogene.* 2015 Oct 8;34(41):5240-51. doi: 10.1038/onc.2014.444.
277. Jacques-Silva MC, Rodnight R, Lenz G, Liao Z, Kong Q, Tran M, Kang Y, Gonzalez FA, Weisman GA, Neary JT. P2X7 receptors stimulate AKT phosphorylation in astrocytes. *Br J Pharmacol.* 2004 Apr;141(7):1106-17.
278. Tafani M, Schito L, Pellegrini L, Villanova L, Marfe G, Anwar T, Rosa R, Indelicato M, Fini M, Pucci B, Russo MA. Hypoxia-increased RAGE and P2X7R expression regulates tumor cell invasion through phosphorylation of Erk1/2 and Akt and nuclear translocation of NF- κ B. *Carcinogenesis.* 2011 Aug;32(8):1167-75. doi: 10.1093/carcin/bgr101.
279. Gómez-Villafuertes R, García-Huerta P, Díaz-Hernández JI, Miras-Portugal MT. PI3K/Akt signaling pathway triggers P2X7 receptor expression as a pro-survival factor of neuroblastoma cells under limiting growth conditions. *Sci Rep.* 2015 Dec 21;5:18417. doi: 10.1038/srep18417.
280. Qiu Y, Li WH, Zhang HQ, Liu Y, Tian XX, Fang WG. P2X7 mediates ATP-driven invasiveness in prostate cancer cells. *PLoS One.* 2014 Dec 8;9(12):e114371. doi: 10.1371/journal.pone.0114371.
281. Adinolfi E, Raffaghello L, Giuliani AL, Cavazzini L, Capece M, Chiozzi P, Bianchi G, Kroemer G, Pistoia V, Di Virgilio F. Expression of P2X7 receptor increases in vivo tumor growth. *Cancer Res.* 2012 Jun 15;72(12):2957-69. doi: 10.1158/0008-5472.CAN-11-1947.
282. Amoroso F, Salaro E, Falzoni S, Chiozzi P, Giuliani AL, Cavallesco G, Maniscalco P, Puozzo A, Bononi I, Martini F, Tognon M, Di Virgilio F. P2X7 targeting inhibits growth

- of human mesothelioma. *Oncotarget*. 2016 Aug 2;7(31):49664-49676. doi: 10.18632/oncotarget.10430.
283. Gu BJ, Wiley JS. Rapid ATP-induced release of matrix metalloproteinase 9 is mediated by the P2X7 receptor. *Blood*. 2006 Jun 15;107(12):4946-53.
284. Jelassi B, Chantôme A, Alcaraz-Pérez F, Baroja-Mazo A, Cayuela ML, Pelegrin P, Surprenant A, Roger S. P2X(7) receptor activation enhances SK3 channels- and cystein cathepsin-dependent cancer cells invasiveness. *Oncogene*. 2011 May 5;30(18):2108-22. doi: 10.1038/onc.2010.593.
285. Eddy RJ, Weidmann MD, Sharma VP, Condeelis JS. Tumor Cell Invadopodia: Invasive Protrusions that Orchestrate Metastasis. *Trends Cell Biol*. 2017 Aug;27(8):595-607. doi: 10.1016/j.tcb.2017.03.003.
286. Verhoef PA, Estacion M, Schilling W, Dubyak GR. P2X7 receptor-dependent blebbing and the activation of Rho-effector kinases, caspases, and IL-1 beta release. *J Immunol*. 2003 Jun 1;170(11):5728-38.
287. Morelli A, Chiozzi P, Chiesa A, Ferrari D, Sanz JM, Falzoni S, Pinton P, Rizzuto R, Olson MF, Di Virgilio F. Extracellular ATP causes ROCK I-dependent bleb formation in P2X7-transfected HEK293 cells. *Mol Biol Cell*. 2003 Jul;14(7):2655-64.
288. Mackenzie AB, Young MT, Adinolfi E, Surprenant A. Pseudoapoptosis induced by brief activation of ATP-gated P2X7 receptors. *J Biol Chem*. 2005 Oct 7;280(40):33968-76.
289. Hill LM, Gavala ML, Lenertz LY, Bertics PJ. Extracellular ATP may contribute to tissue repair by rapidly stimulating purinergic receptor X7-dependent vascular endothelial growth factor release from primary human monocytes. *J Immunol*. 2010 Sep 1;185(5):3028-34. doi: 10.4049/jimmunol.1001298.
290. Sluyter R. The P2X7 Receptor. *Adv Exp Med Biol*. 2017;1051:17-53. doi: 10.1007/5584_2017_59.
291. Draoui N, de Zeeuw P, Carmeliet P. Angiogenesis revisited from a metabolic perspective: role and therapeutic implications of endothelial cell metabolism. *Open Biol*. 2017 Dec;7(12). pii: 170219. doi: 10.1098/rsob.170219.
292. Pizzirani C, Ferrari D, Chiozzi P, Adinolfi E, Sandonà D, Savaglio E, Di Virgilio F. Stimulation of P2 receptors causes release of IL-1beta-loaded microvesicles from human dendritic cells. *Blood*. 2007 May 1;109(9):3856-64.
293. Kholia S, Jorfi S, Thompson PR, Causey CP, Nicholas AP, Inal JM, Lange S. A novel role for peptidylarginine deiminases in microvesicle release reveals therapeutic

- potential of PAD inhibition in sensitizing prostate cancer cells to chemotherapy. *J Extracell Vesicles*. 2015 Jun 19;4:26192. doi: 10.3402/jev.v4.26192.
294. Prada I, Furlan R, Matteoli M, Verderio C. Classical and unconventional pathways of vesicular release in microglia. *Glia*. 2013 Jul;61(7):1003-17. doi: 10.1002/glia.22497.
295. Baroni M, Pizzirani C, Pinotti M, Ferrari D, Adinolfi E, Calzavarini S, Caruso P, Bernardi F, Di Virgilio F. Stimulation of P2 (P2X7) receptors in human dendritic cells induces the release of tissue factor-bearing microparticles. *FASEB J*. 2007 Jun;21(8):1926-33.
296. Wendler F, Favicchio R, Simon T, Alifrangis C, Stebbing J, Giamas G. Extracellular vesicles swarm the cancer microenvironment: from tumor-stroma communication to drug intervention. *Oncogene*. 2017 Feb 16;36(7):877-884. doi: 10.1038/onc.2016.253.
297. Solini A, Chiozzi P, Morelli A, Fellin R, Di Virgilio F. Human primary fibroblasts in vitro express a purinergic P2X7 receptor coupled to ion fluxes, microvesicle formation and IL-6 release. *J Cell Sci*. 1999 Feb;112 (Pt 3):297-305.
298. Kurashima Y, Amiya T, Nochi T, Fujisawa K, Haraguchi T, Iba H, Tsutsui H, Sato S, Nakajima S, Iijima H, Kubo M, Kunisawa J, Kiyono H. Extracellular ATP mediates mast cell-dependent intestinal inflammation through P2X7 purinoceptors. *Nat Commun*. 2012;3:1034. doi: 10.1038/ncomms2023.
299. Shieh CH, Heinrich A, Serchov T, van Calker D, Biber K. P2X7-dependent, but differentially regulated release of IL-6, CCL2, and TNF- α in cultured mouse microglia. *Glia*. 2014 Apr;62(4):592-607. doi: 10.1002/glia.22628.
300. Ferrari D, La Sala A, Chiozzi P, Morelli A, Falzoni S, Girolomoni G, Idzko M, Dichmann S, Norgauer J, Di Virgilio F. The P2 purinergic receptors of human dendritic cells: identification and coupling to cytokine release. *FASEB J*. 2000 Dec;14(15):2466-76.
301. Chessell IP, Hatcher JP, Bountra C, Michel AD, Hughes JP, Green P, Egerton J, Murfin M, Richardson J, Peck WL, Grahames CB, Casula MA, Yiangou Y, Birch R, Anand P, Buell GN. Disruption of the P2X7 purinoceptor gene abolishes chronic inflammatory and neuropathic pain. *Pain*. 2005 Apr;114(3):386-96.
302. Monção-Ribeiro LC, Faffe DS, Santana PT, Vieira FS, da Graça CL, Marques-da-Silva C, Machado MN, Caruso-Neves C, Zin WA, Borojevic R, Takiya CM, Coutinho-Silva R. P2X7 receptor modulates inflammatory and functional pulmonary changes induced by silica. *PLoS One*. 2014 Oct 13;9(10):e110185. doi: 10.1371/journal.pone.0110185.
303. Ghiringhelli F, Apetoh L, Tesniere A, Aymeric L, Ma Y, Ortiz C, Vermaelen K, Panaretakis T, Mignot G, Ullrich E, Perfettini JL, Schlemmer F, Tasdemir E, Uhl M, Génin

- P, Civas A, Ryffel B, Kanellopoulos J, Tschopp J, André F, Lidereau R, McLaughlin NM, Haynes NM, Smyth MJ, Kroemer G, Zitvogel L. Activation of the NLRP3 inflammasome in dendritic cells induces IL-1beta-dependent adaptive immunity against tumors. *Nat Med.* 2009 Oct;15(10):1170-8. doi: 10.1038/nm.2028.
304. Adinolfi E, Capece M, Franceschini A, Falzoni S, Giuliani AL, Rotondo A, Sarti AC, Bonora M, Syberg S, Corigliano D, Pinton P, Jorgensen NR, Abelli L, Emionite L, Raffaghello L, Pistoia V, Di Virgilio F. Accelerated tumor progression in mice lacking the ATP receptor P2X7. *Cancer Res.* 2015 Feb 15;75(4):635-44. doi: 10.1158/0008-5472.CAN-14-1259.
305. Hofman P, Cherfils-Vicini J, Bazin M, Ilie M, Juhel T, Hébuterne X, Gilson E, Schmid-Alliana A, Boyer O, Adriouch S, Vouret-Craviari V. Genetic and pharmacological inactivation of the purinergic P2RX7 receptor dampens inflammation but increases tumor incidence in a mouse model of colitis-associated cancer. *Cancer Res.* 2015 Mar 1;75(5):835-45. doi: 10.1158/0008-5472.CAN-14-1778.
306. Raffaghello L, Chiozzi P, Falzoni S, Di Virgilio F, Pistoia V. The P2X7 receptor sustains the growth of human neuroblastoma cells through a substance P-dependent mechanism. *Cancer Res.* 2006 Jan 15;66(2):907-14.
307. Ferrari D, Los M, Bauer MK, Vandenabeele P, Wesselborg S, Schulze-Osthoff K. P2Z purinoreceptor ligation induces activation of caspases with distinct roles in apoptotic and necrotic alterations of cell death. *FEBS Lett.* 1999 Mar 19;447(1):71-5.
308. Yang D, He Y, Muñoz-Planillo R, Liu Q, Núñez G. Caspase-11 Requires the Pannexin-1 Channel and the Purinergic P2X7 Pore to Mediate Pyroptosis and Endotoxic Shock. *Immunity.* 2015 Nov 17;43(5):923-32. doi: 10.1016/j.immuni.2015.10.009.
309. Kayagaki N, Stowe IB, Lee BL, O'Rourke K, Anderson K, Warming S, Cuellar T, Haley B, Roose-Girma M, Phung QT, Liu PS, Lill JR, Li H, Wu J, Kummerfeld S, Zhang J, Lee WP, Snipas SJ, Salvesen GS, Morris LX, Fitzgerald L, Zhang Y, Bertram EM, Goodnow CC, Dixit VM. Caspase-11 cleaves gasdermin D for non-canonical inflammasome signalling. *Nature.* 2015 Oct 29;526(7575):666-71. doi: 10.1038/nature15541.
310. Shi J, Zhao Y, Wang K, Shi X, Wang Y, Huang H, Zhuang Y, Cai T, Wang F, Shao F. Cleavage of GSDMD by inflammatory caspases determines pyroptotic cell death. *Nature.* 2015 Oct 29;526(7575):660-5. doi: 10.1038/nature15514.
311. Karasawa A, Michalski K, Mikhelzon P, Kawate T. The P2X7 receptor forms a dye-permeable pore independent of its intracellular domain but dependent on membrane lipid composition. *Elife.* 2017 Sep 18;6. pii: e31186. doi: 10.7554/eLife.31186.

312. Gunosewoyo H, Kassiou M. P2X purinergic receptor ligands: recently patented compounds. *Expert Opin Ther Pat.* 2010 May;20(5):625-46. doi: 10.1517/13543771003702424.
313. Park JH, Kim YC. P2X7 receptor antagonists: a patent review (2010-2015). *Expert Opin Ther Pat.* 2017 Mar;27(3):257-267. doi: 10.1080/13543776.2017.1246538.
314. De Marchi E, Orioli E, Dal Ben D, Adinolfi E. P2X7 Receptor as a Therapeutic Target. *Adv Protein Chem Struct Biol.* 2016;104:39-79. doi: 10.1016/bs.apcsb.2015.11.004.
315. Perez-Medrano A, Donnelly-Roberts DL, Honore P, Hsieh GC, Namovic MT, Peddi S, Shuai Q, Wang Y, Faltynek CR, Jarvis MF, Carroll WA. Discovery and biological evaluation of novel cyanoguanidine P2X(7) antagonists with analgesic activity in a rat model of neuropathic pain. *J Med Chem.* 2009 May 28;52(10):3366-76. doi: 10.1021/jm8015848.
316. Coddou C, Stojilkovic SS, Huidobro-Toro JP. Allosteric modulation of ATP-gated P2X receptor channels. *Rev Neurosci.* 2011;22(3):335-54. doi: 10.1515/RNS.2011.014.
317. Coddou C, Yan Z, Obsil T, Huidobro-Toro JP, Stojilkovic SS. Activation and regulation of purinergic P2X receptor channels. *Pharmacol Rev.* 2011 Sep;63(3):641-83. doi: 10.1124/pr.110.003129.
318. Evans RJ. Orthosteric and allosteric binding sites of P2X receptors. *Eur Biophys J.* 2009 Mar;38(3):319-27. doi: 10.1007/s00249-008-0275-2.
319. Mehta N, Kaur M, Singh M, Chand S, Vyas B, Silakari P, Bahia MS, Silakari O. Purinergic receptor P2X₇: a novel target for anti-inflammatory therapy. *Bioorg Med Chem.* 2014 Jan 1;22(1):54-88. doi: 10.1016/j.bmc.2013.10.054.
320. Arulkumaran N, Unwin RJ, Tam FW. A potential therapeutic role for P2X7 receptor (P2X7R) antagonists in the treatment of inflammatory diseases. *Expert Opin Investig Drugs.* 2011 Jul;20(7):897-915. doi: 10.1517/13543784.2011.578068.
321. Stock TC, Bloom BJ, Wei N, Ishaq S, Park W, Wang X, Gupta P, Mebus CA. Efficacy and safety of CE-224,535, an antagonist of P2X7 receptor, in treatment of patients with rheumatoid arthritis inadequately controlled by methotrexate. *J Rheumatol.* 2012 Apr;39(4):720-7. doi: 10.3899/jrheum.110874.
322. Keystone EC, Wang MM, Layton M, Hollis S, McInnes IB; D1520C00001 Study Team. Clinical evaluation of the efficacy of the P2X7 purinergic receptor antagonist AZD9056 on the signs and symptoms of rheumatoid arthritis in patients with active disease despite treatment with methotrexate or sulphasalazine. *Ann Rheum Dis.* 2012 Oct;71(10):1630-5.

323. Eser A, Colombel JF, Rutgeerts P, Vermeire S, Vogelsang H, Braddock M, Persson T, Reinisch W. Safety and Efficacy of an Oral Inhibitor of the Purinergic Receptor P2X7 in Adult Patients with Moderately to Severely Active Crohn's Disease: A Randomized Placebo-controlled, Double-blind, Phase IIa Study. *Inflamm Bowel Dis*. 2015 Oct;21(10):2247-53. doi: 10.1097/MIB.0000000000000514.
324. US National Library of Medicine. ClinicalTrials.gov <https://clinicaltrials.gov/ct2/show/NCT02587819> (2016).
325. Gehring MP, Kipper F, Nicoletti NF, Sperotto ND, Zanin R, Tamajusuku AS, Flores DG, Meurer L, Roesler R, Filho AB, Lenz G, Campos MM, Morrone FB. P2X7 receptor as predictor gene for glioma radiosensitivity and median survival. *Int J Biochem Cell Biol*. 2015 Nov;68:92-100. doi: 10.1016/j.biocel.2015.09.001.
326. Tesei A, Sarnelli A, Arienti C, Menghi E, Medri L, Gabucci E, Pignatta S, Falconi M, Silvestrini R, Zoli W, D'Errico V, Romeo A, Parisi E, Polico R. In vitro irradiation system for radiobiological experiments. *Radiat Oncol*. 2013 Nov 1;8:257. doi: 10.1186/1748-717X-8-257.
327. Garcia O, Romero I, González JE, Mandina T. Measurements of DNA damage on silver stained comets using free Internet software. *Mutat Res*. 2007 Mar 5;627(2):186-90.
328. Otsu N. THRESHOLD SELECTION METHOD FROM GRAY-LEVEL HISTOGRAMS. *IEEE Trans Syst Man Cybern SMC-9*, 1979 62–66. doi:10.1109/tsmc.1979.4310076.
329. Gyori BM, Venkatachalam G, Thiagarajan PS, Hsu D, Clement MV. OpenComet: an automated tool for comet assay image analysis. *Redox Biol*. 2014 Jan 9;2:457-65. doi: 10.1016/j.redox.2013.12.020.
330. Wei W, Ryu JK, Choi HB, McLarnon JG. Expression and function of the P2X(7) receptor in rat C6 glioma cells. *Cancer Lett*. 2008 Feb 18;260(1-2):79-87.
331. Braganhol E, Kukulski F, Lévesque SA, Fausther M, Lavoie EG, Zanutto-Filho A, Bergamin LS, Pelletier J, Bahrami F, Ben Yebdri F, Fonseca Moreira JC, Battastini AM, Sévigny J. Nucleotide receptors control IL-8/CXCL8 and MCP-1/CCL2 secretions as well as proliferation in human glioma cells. *Biochim Biophys Acta*. 2015 Jan;1852(1):120-30. doi: 10.1016/j.bbadis.2014.10.014.
332. Ji Z, Xie Y, Guan Y, Zhang Y, Cho KS, Ji M, You Y. Involvement of P2X7 Receptor in Proliferation and Migration of Human Glioma Cells. *Biomed Res Int*. 2018 Jan 9;2018:8591397. doi: 10.1155/2018/8591397.

333. Ryu JK, Jantaratnotai N, Serrano-Perez MC, McGeer PL, McLarnon JG. Block of purinergic P2X7R inhibits tumor growth in a C6 glioma brain tumor animal model. *J Neuropathol Exp Neurol*. 2011 Jan;70(1):13-22. doi: 10.1097/NEN.0b013e318201d4d4.
334. Tamajusuku AS1, Villodre ES, Paulus R, Coutinho-Silva R, Battasstini AM, Wink MR, Lenz G. Characterization of ATP-induced cell death in the GL261 mouse glioma. *J Cell Biochem*. 2010 Apr 1;109(5):983-91. doi: 10.1002/jcb.22478.
335. Fang J, Chen X, Zhang L, Chen J, Liang Y, Li X, Xiang J, Wang L, Guo G, Zhang B, Zhang W. P2X7R suppression promotes glioma growth through epidermal growth factor receptor signal pathway. *Int J Biochem Cell Biol*. 2013 Jun;45(6):1109-20. doi: 10.1016/j.biocel.2013.03.005.
336. D'Alimonte I, Nargi E, Zuccarini M, Lanuti P, Di Iorio P, Giuliani P, Ricci-Vitiani L, Pallini R, Caciagli F, Ciccarelli R. Potentiation of temozolomide antitumor effect by purine receptor ligands able to restrain the in vitro growth of human glioblastoma stem cells. *Purinergic Signal*. 2015 Sep;11(3):331-46. doi: 10.1007/s11302-015-9454-7.
337. Lindgren T, Stigbrand T, Riklund K, Johansson L, Eriksson D. Gene expression profiling in MOLT-4 cells during gamma-radiation-induced apoptosis. *Tumour Biol*. 2012 Jun;33(3):689-700. doi: 10.1007/s13277-012-0329-z.
338. Abbas T, Dutta A. p21 in cancer: intricate networks and multiple activities. *Nat Rev Cancer*. 2009 Jun;9(6):400-14. doi: 10.1038/nrc2657.